1-1-2017

The In Vivo Effect Of Oil Palm Phenolics (opp) In Atherogenic Diet Induced Rats Model Of Alzheimer's Disease (ad)

Yan Wu
Wayne State University,

THE *in vivo* EFFECT OF OIL PALM PHENOLICS (OPP) IN ATHEROGENIC DIET INDUCED RATS MODEL OF ALZHEIMER'S DISEASE (AD)

by

YAN WU

DISSERTATION

Submitted to the Graduate School

of Wayne State University,

Detroit, Michigan

in partial fulfillment of the requirements

for the degree of

DOCTOR OF PHILOSOPHY

2017

MAJOR: NUTRITION AND FOOD SCIENCE

Approved By:

_____

Advisor   Date

_____

_____

_____

DEDICATION

To my family,

Especially my dad and mom; thank you dad for always supporting me

And mom I really missed you and you will be in my heart forever.

Yuhin Wu Mock, my cute son, I wish you will grow healthily and happily.

I will always love you.

TABLE OF CONTENTS

LIST OF TABLES

LIST OF FIGURES

LIST OF ABBREVIATIONS

ΔC_T Delta (normalized) cycle threshold value

^{1}H NMR   Proton nuclear magnetic resonance spectroscopy

Aβ Amyloid-β peptide

AD   Alzheimer's disease

ANOVA   Analysis of one way variance

APP   Amyloid precursor protein

BACE β secretase

BBB   Blood Brain Barrier

CSF   Cerebrospinal fluid

C_T Cycle threshold

H&E   Haematoxylin and eosin

IL-6   Interleukin 6

MRI   Magnetic resonance imaging

mRNA   Messenger ribonucleic acid

NF- κB   Nuclear factor kappa-light-chain-enhancer of activated ß cell

Notch1   Notch homolog 1

NTC   Non-template control

OPLS   Orthogonal projections to latent structures regression

OPLS-DA   Orthogonal partial least squares discriminant analysis

OPP   Oil palm phenolics

PCA   Principle component analysis

PLS-DA   Partial least square discriminant analysis

qRT-PCR	Quantitative real-time polymerase chain reaction
NFT	Neurofibrillary tangles
NMDR	N-methyl-D-aspartic acid receptor
RNA	Ribonucleic acid
RNS	Reactive nitrogen species
ROS	Reactive oxygen species

CHAPTER 1 INTRODUCTION

1.1 Alzheimer's Disease

Alzheimer's disease (AD) is characterized by degeneration of the brain tissue and the symptom of dementia [1]. It is named after Dr. Alois Alzheimer who first noticed the mental and behavior changes in a woman in1906, who eventually died after experiencing symptoms including memory loss, language problems and unpredictable behavior. After she died, he examined her brain tissues and found some pathological changes such as abnormal clumps (now called amyloid plaques) and tangled bundles of fibers (now called neurofibrillary, or tau, tangles). Now these symptoms are still being used as clinical evidence to diagnose AD, and the plaques and tangles found in the brain are considered some of its main features. According to the National Institute of Aging (NIA), AD is defined as "an irreversible, progressive brain disorder that slowly destroys memory and thinking skills, and eventually the ability to carry out the simplest tasks."[2] Although the symptoms and the effects of the disease are similar in patients, the age at which it occurs is used to differentiate it into two major types: the first of which is early-onset Alzheimer's, which occurs in people who are younger than age 65 and accounts for 5% of the cases; the second type is late-onset Alzheimer's, the most common form of the disease. People age 65 and older have a higher risk of showing the symptoms of late-onset AD. In addition to aging, conditions associated with chronic heart diseases have recently been discovered as risk factor of late onset AD [3]. Family history and genetic mutation are more frequently seen in the early-onset AD, which is also called familial Alzheimer's disease (FAD). The clinical features that help differentiate early-onset Alzheimer's include more pathological changes in brain than typically seen in late-onset patients, genetic mutations on chromosome 14, and symptoms of seizure and myoclonus (a form of muscle twitching and spasm) [4]. AD is now the sixth leading cause of death in the United States and the fifth leading cause of

death in Americans age ≥65 years. It was estimated that by 2016 about 5.2 million Americans of all ages already had Alzheimer's disease and this number will double to 10.2 million by 2050[5]. The total amount of money spent to date on health care, long-term care and hospice services for people age ≥65 years with dementia is estimated to be $236 billion, which places a substantial financial burden on families, community, and society [6].

1.2 Biological changes associated with Alzheimer's disease

The brain changes involved in the onset and progression of AD are complex and still require unraveling. Research has found that the brain tissue damage starts a decade or more before the memory and cognitive decline become apparent. During this preclinical stage when people seem to be symptom-free, neuropathological changes are taking place in the brain. As brain changes advance, synapses begin to malfunction and their numbers start to decline, leading to neuron death. The damage initially appears to take place in the hippocampus, the part of the brain essential in forming memories. As more neurons die, additional parts of the brain are affected, and the brain begins to shrink. At the final stage of Alzheimer's, there is widespread debris from dead and dying neurons in the brain, and a dramatic brain tissue shrinkage due to the cell loss [7]. Based on numerous studies of AD, the prevailing pathological mechanisms that have been proposed as causes include amyloid cascade hypothesis, tau protein hypothesis, genetic mutation, oxidative stress and inflammatory hypothesis and cholesterol hypothesis and cholinergic and other neurotransmitter hypothesis. Each of these hypotheses will be discussed in detail bellow.

1.2.1 Amyloid cascade hypothesis

The extracellular amyloid plaques formation is one of the hallmarks of AD. The amyloid cascade hypothesis states that the accumulation of amyloid is triggered by a chain of events that culminate in plaque formation in brain (Figure 1). Normally, an integral membrane protein known

amyloid precursor protein (APP) is expressed in the neurons, though its function is still not clear. It is hypothesized that APP might possess a natural neuroprotective effect to protect neurons from stress or injury by regulating the extra- and intra-cellular Ca^{2+} concentration[8]. It is thought that APP is then cleaved by the enzymes known as α-secretase at the cell surface and further by γ-secretase to form small size peptides that can be naturally digested and eliminated by the brain. However, under the pathological condition, i.e. overproduction of APP or the presence of β-secretase (BACE1) mutation, BACE1 activity competes with α-secretase to cleave APP at the endoplasmic reticulum and leaves a membrane bound C-terminal fragment, which is further cleaved by γ-secretase. This final cleavage generates the Aβ: 40 amino acid amyloid beta peptide (Aß40), the 42 amino acid amyloid beta peptide (Aß42), as well as an intracellular cytoplasmic fragment which can be rapidly digested. The majority of Aβ is 40 amino acids long (Aß40) (90%), but a small proportion (<10%) is slightly longer (Aβ42). Aß40 is produced in trans-Golgi network in which it is soluble and mostly innocuous, wheareas Aß42 are highly fibrillogenic and easily clumps together to form insoluble amyloid plaques (senile plaques) on the outside surface of neurons (amyloidosis). This is neurotoxic and ultimately leads to the killing of neurons [9, 10]. This hypothesis has been backed by an enormous amount of circumstantial evidence from multiple avenues of biological research [11-13] .
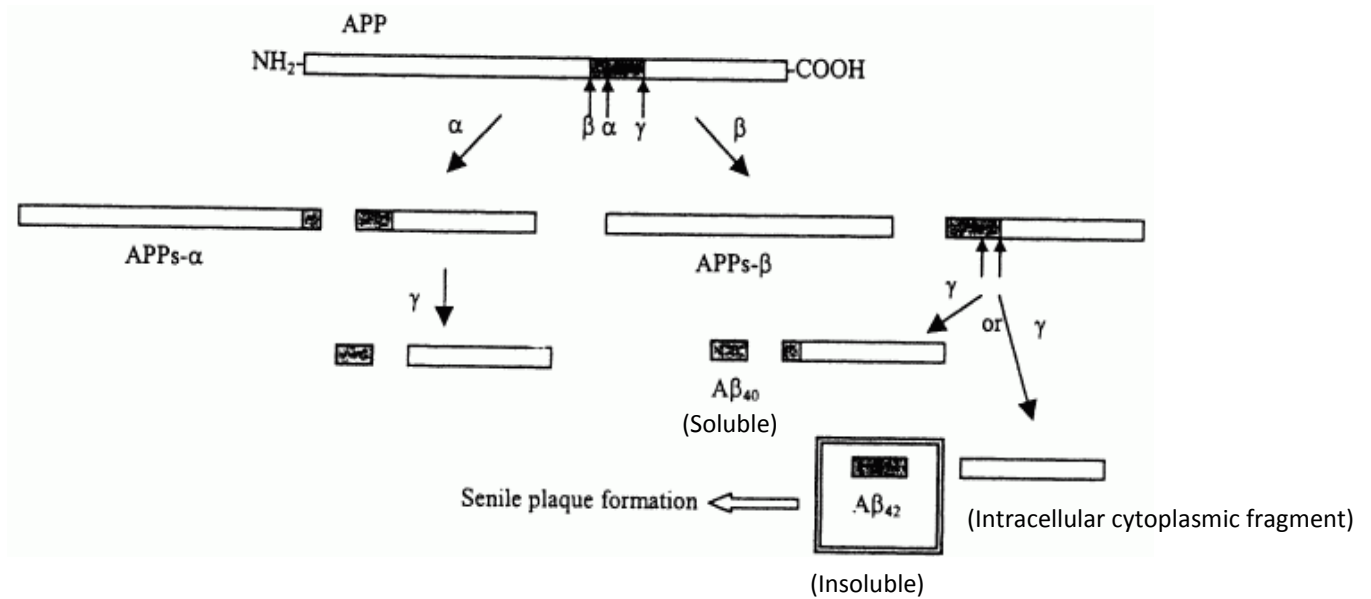
Figure 1. Amyloidogenic pathway: APP is sequentially cleaved by α-secratase (α), β-secratase(β) and γ–secratase(γ) that result in amyloid beta peptide 42 (Aβ42) accumulation and eventually plaque formation.

1.2.2 Tau hypothesis

Tau is a microtubule-associated protein abundant in neurons and its function is microtubule assembly and stabilization [14]. In healthy nerve cells, tau resides in a part of the nerve cell termed the axon, the long, slender part of the cell that carries electrical impulses away from the neuron's body. However, mutations can alter the function and isoform expression of tau with excessive or abnormal phosphorylation. Hyperphosphorylated tau disassembles microtubules and sequesters normal tau, MAP 1(microtubule associated protein1), MAP 2, and ubiquitin into neurofibrillary tangles (NFTs). These insoluble structures damage cytoplasmic functions and interferes with axonal transport, which can lead to cell death. NFTs are considered to be a follow-up event to amyloid plaque formation, and they cause the neuron death in AD brain. It has been suggested that amyloid plaques are very early event and that NFTs are a late event of an underlying process of

AD, meaning each event is independent. But a great deal evidence supports the view that Aß increases NFT formation[15]. Application of amyloid plaque to cultured neurons and injection of β-amyloid Aβ42 fibrils into the brains of P301L mutant tau transgenic mice caused fivefold increases in the numbers of NFTs [16]. Amyloid beta may facilitate Ca^{2+} influx into neurons, causing calcium-activated kinases to excessively phosphorylate tau protein leading to NFTs. Some researchers have found evidence that β-amyloid fibrils form pores in neurons leading to calcium influx and the neuron death associated with AD [17].

1.2.3 Genetic mutation

Ten percent of AD cases are known to have a genetic basis, especially for FADs. These abnormal changes in the sequence of chemical pairs occur in the genes for the amyloid precursor protein (APP) and the genes for the presenilin 1 and presenilin 2 proteins. It has been reported that those inheriting a mutation to the APP and presenilin 1 or presenilin 2 genes are guaranteed to develop earlier onset FAD[18]. Presinilin protein is one subunit of a complex called gamma- (γ-) secretase. The γ-secretase complex may be best known for its role in processing amyloid precursor protein (APP), which is made in the brain and other tissues. More than half of FAD cases are associated with the presenilin 1 gene located on chromosome 14, which encodes the enzyme that cleaves the γ-secretase site. The abnormal presinilin 1 and 2 significantly up-regulate the γ - secretase enzyme activities that result in more Aß42 peptide generation from the amyloid pathway. The mutation on chromosome 21 is presented in Amyloid Precursor Protein (APP) gene itself, which induces the over-production of the APP protein followed by higher activity of the amyloid cascade process [19].

Unlike inheriting the mutated genes above, inheriting the ε4 form of the APOE gene does not guarantee that an individual will develop Alzheimer's. The APOE gene provides the blueprint for

a protein that transports cholesterol in the bloodstream and is involved in late-onset Alzheimer's. One form of this gene, APOE ε4, increases a person's risk of developing the disease and is also associated with an earlier age of disease onset[20]. Those who carry one copy of the ε4 form have three times higher risk of developing Alzheimer's than those without the ε4 form, while those who inherit two copies of the ε4 form have an 8- to 12-fold higher risk. Researchers estimate that 40 percent to 65 percent of people diagnosed with Alzheimer's have one or two copies of the APOE ε4 gene [6]. However, carrying the APOE ε4 form of the gene does not mean that a person will definitely develop Alzheimer's disease. Some people with an APOE ε4 allele never get the disease, and others who develop Alzheimer's do not have any APOE ε4 alleles. In addition, so far there are more than 20 recently identified genes (GSK3β , DTRK1A, Tau,TOMM40,etc) that also appear to affect the risk of Alzheimer's. However, compared to APP, PS1,PS2 and ApoE, these recently identified genes are believed to have a limited effect on the overall prevalence of Alzheimer's because they are rare or only increase the risk slightly[21] .

1.2.4 Oxidative stress and inflammation hypothesis

Another event that promotes AD pathogenesis is oxidative stress and inflammation. There are multiple free species, atoms or molecules with an unpaired electron in the outer shell present in the body. The most common radicals are derived from the reduction of molecular oxygen to water during oxidative phosphorylation (OXPHOS) and this group of radicals is called reactive oxygen species (ROS). In normally functioning tissues, a balance is maintained between ROS generation and antioxidant protection, mediated through antioxidant enzymes like copper/zinc superoxide dismutase (SOD) and glutathione peroxidase [22] and small antioxidant molecules such as vitamin E, vitamin C and glutathione. When the balance between free radical generation and antioxidant capacities shifts toward free radical generation, oxidative stress occurs and causes oxidative

damage to lipids, proteins, RNA and DNA[23]. Our brain is particularly susceptible to oxidative damage due to its high oxygen consumption rate (1/5th of all consumed oxygen), its high-energy demands, rich abundance of polyunsaturated fatty acids and lipids and the relatively limited antioxidant capacity compared to other organs [24]. In subjects with impaired OXPHOS such as AD, >2% of oxygen consumed by cells during OXPHOS is converted to ROS [25]. The free radical-mediated damage will accumulate in the brain over time and lead to pathological changes, including promotion of Aβ deposition, tau hyperphosphorylation and the subsequent loss of synapses and neurons in the development of AD. Several studies suggest that ROS are involved in Aβ fibrillization and NFT formation in AD and increases with Aβ and NFT pathology in AD [26-28]. Both soluble and fibrillar Aβ may further accelerate oxidative stress, as well as mitochondrial dysfunction [29]. Meanwhile, the peroxidative attack on cell and organelle membrane lipids yields mitochondrial toxins such as hydroxynonenal (HNE) and malondialdehyde [30] [30]. This mechanism could damage the membrane-bound, ion-specific ATPases and stimulate the calcium (Ca2+) entry system which further activates the glutamate (N-methyl-d-aspartate [NMDA]) receptors (NMDAr) and membrane-attack complex (MAC) of complement. Once the NMDAr is under high activity, the accumulation of glutamate at synaptic cleft will induce neurotoxicity and plasticity[31].

Inflammatory processes have also been reported to play an important role in the AD pathology. The two major types of brain cells that participate in the immune/inflammatory response that leads to the death of neurons are astrocytes and microglia. Astrocytes becomes more active in AD,   producing prostaglandin/arachidonic acid which mediates inflammation accompanied by the activated microglial cells, which can produce damaging free radicals [32]. Some hypothesize that the reason for this is Aβ can activate microglia, which leads to an increase

in cell surface expression of major histocompatibility complex II (MHC II) along with increased secretion of the pro-inflammatory cytokines interleukin-1β (IL-1β), interleukin-6 (IL-6), tumor necrosis factor α (TNF α),chemokines- interleukin-8 (IL-8), macrophage inflammatory protein-1 α (MIP-1 α), and monocyte chemo-attractant protein-1[33]. Aβ also induces a phagocytic response in microglia and expression of nitric oxide synthase (NOS), resulting in neuronal damage. Microglia may also play a role in the degradation of Aβ with the release of insulin degrading enzyme (IDE). Astrocytes can cluster at sites of Aβ deposits and secrete interleukins, prostaglandins, leukotrienes, thromboxanes, coagulation factors, and protease inhibitors. Neurons themselves are able to express significantly higher levels of classical pathway complement and pro-inflammatory products that trigger inflammatory processes. Furthermore, the complement system, cytokines, chemokines, and acute phase proteins (especially pentraxins) contribute to the inflammatory response in AD [34, 35]. But the question of whether neuroinflammation is a primary cause or secondary effect in Alzheimerogenesis remains as one of the chicken-and-egg variety [36].

1.2.5 Cholesterol hypothesis

There is a growing body of evidence suggesting that a high level of plasma cholesterol is associated with increased risk of AD. The role of cholesterol in the pathology of AD is also shown by the ability of statins to reduce the prevalence of AD by up to 70%[37]. Several studies have demonstrated that statins reduce the turnover of brain cholesterol at standard therapeutic doses, although the steady-state levels of Aβ in the cerebrospinal fluid (CSF) remain unaltered [38].Similarly, inhibition of cholesterol biosynthesis by statins and another cholesterol synthesis inhibitor was found to reduce amyloid burden in guinea pigs and murine models of AD[39]. In another animal study, it was found that rabbits fed cholesterol had twice the β-amyloid in the

hippocampal cortex compared to the controls[40]. In the AD brain, cholesterol can bind to aggregated amyloid-beta, reducing clearance and contributing to amyloid plaque. Apparently, the subcellular distribution of cholesterol affects amyloid-beta production. Both β-secretase & γ-secretase activity increase with elevated cholesterol, whereas the reverse effect is seen with α-secretase,which is more active with lower cholesterol. Increase in cellular cholesterol also contributes to altered membrane lipid metabolism. Abnormal cholesterol synthesis, efflux, or influx might destablize the membrane structure in which polyunsaturated fatty acids (PUFAs) contents are degraded to start lipid peroxidation and make the neurons more vulnerable to free radical-induced injury[41]. However, it is true that plasma cholesterol levels do not normally regulate production of brain Aβ due to the blood brain barrier (BBB)[42]. One possible reason explaining the risk of an atherosclerosis diet to AD resides is the fact that high non-HDL cholesterol is associated with low HDLand apoA-I levels, a pro-inflammatory systemic status and increased atherogenic/ischemic pathology. Supporting this hypothesis, serum levels of adipocytokines, markers of inflammation, have been associated with cognitive impairment and progression of AD, as well as atherogenic/ischemic disease [43] . Moreover, the metabolic syndromes associated with the atherogenic diseases were also reported to promote the development of dementia by affecting myelin integrity and white-matter connective functions[44].

1.2.6 Other hypothesis

In addition to the hypotheses described above, the cholinergic hypothesis was developed decades year ago, and it identifies basal forebrain cholinergic cell loss as a consistent feature of AD. Most of the brain's supply of acetylcholine is derived from the nucleus basalis of Meynert in the basal forebrain. In AD brains, research has shown that the nucleus basalis seems to be particularly vulnerable to the neurodegeneration. There were decreased numbers of healthy

neurons in this area and decreased cholinergic projections to the hippocampus and entorhinal cortex, suggesting that patients with AD may have decreased acetylcholine. A loss of cholinergic function in the central nervous system can impair the cortical cholinergic neurotransmission, contributing significantly to the cognitive decline associated with advanced age and AD. Therefore, damage or abnormalities in the pathway of the basal forebrain appeared to correlate well with the level of cognitive decline [45, 46]. It was based on this cholinergic hypothesis that the FDA approved drugs were developed. Today, the primary pharmacological approach for AD is to employ cholinesterase inhibitors developed in the 1990s and 2000s, which can block acetylcholinesterase that prevent the breakdown of the neurotransmitter acetylcholine into acetate and choline. As a result, levels of acetylcholine in the synapse are increased and restore signaling to the postsynaptic cell[47].

Above all, the exact aetiopathogenesis of AD is still obscure. Neurobiological mechanisms likely involved in AD include hypotheses explaining the genesis of excitotoxic fibrillar Aβ and defective clearance of toxic amyloid. Agents which interfere with cleavage (BACE 1 Inhibitor), reduce aggregation of Aβ, and accelerate the clearance of neurotoxic amyloid may provide better cognitive advantage in AD. There is also emerging evidence that neuropeptides/modulator systems and estrogen are likely to play a role in memory dysfunction or AD. Additionally, other neurobiological mechanisms including insulin signaling, metallobiology, cell cycle aberrations and more have been put forward to serve as possible therapeutic targets in areas of active research [48-50].

1.3 Symptoms and Diagnosis

AD patients typically suffer from the problems with memory, cognition and behavior. Symptoms usually develop slowly and worsen over time, becoming severe enough to interfere

with daily tasks. When the initial changes occur, the brain compensates for them, enabling individuals to continue to function normally. As neuronal damage increases, the brain can no longer compensate for the changes and individuals show subtle cognitive decline. Later, neuronal damage becomes so significant that individuals show obvious cognitive decline, including symptoms such as memory loss or confusion as to time or place. Later still, basic bodily functions such as swallowing are impaired. The rate of progression varies greatly [51]. The course can take anywhere from two to 20 years, and AD patients live an average of eight years. In early stages, brain regions important in memory,thinking and planning start developing plaques without symptoms; when AD progresses to the moderate stage, more plaques and tangles develop . Thus, individuals develop problems with memory and/or thinking that become serious enough to interfere with work or social life. They may also get confused and have trouble handling money, expressing themselves and organizing their thoughts. In the advanced stage (at which point many patients are first diagnosed), most of the cortex is seriously damaged. The brain shrinks dramatically due to widespread cell death, which causes individuals lose their ability to communicate, to recognize family and to care for themselves[52]. Therefore, it is very important to diagnose AD at its early stage to dramatically enhance its treatment.

AD is usually diagnosed clinically from patient history, collateral history from relatives and clinical observations, based on the presence of characteristic neurological and neuropsychological features and the absence of alternative conditions[53]. Advanced medical imaging including computed tomography (CT), magnetic resonance imaging (MRI), single photon emission computer tomography (SPECT) or positron emission tomography (PET) can be used to help exclude other cerebral pathology or subtypes of dementia[54] .The diagnosis can be confirmed with very high accuracy post-mortem, when brain material is available and can be examined

histologically. Hence, the current diagnostic measures of AD are invasive (cerebrospinal fluid analysis), expensive (neuroimaging) and time-consuming (neuropsychological assessment) and thus have limited accessibility as frontline screening and diagnostic tools for AD. Therefore, there is an increasing need for additional noninvasive and/or cost-effective tools, allowing identification of subjects in the preclinical or early clinical stages of AD who could be suitable for further cognitive evaluation and dementia diagnostics. Molecular imaging technologies are among the most active areas of research aimed at finding new approaches to diagnose Alzheimer's in its earliest stages. In 2012, the U.S. Food and Drug Administration approved the first molecular imaging tracer for use in patients being evaluated for possible Alzheimer's disease or other causes of cognitive decline. This tracer, florbetapir F-18, is a molecule that binds to beta-amyloid in the brain [55]. Because the beta-amyloid is labeled with a radioactive tracer it can be visualized during a positron emission tomography (PET) brain scan, thereby revealing the presence of amyloid plaques in the brains of living patients. In addition, researchers are also investigating whether pre-symptomatic   Alzheimer's disease causes consistent, measurable changes in urine or blood levels of tau, beta-amyloid or other biomarkers. Scientists are also exploring whether early Alzheimer's leads to detectable changes elsewhere in the body, i.e. the lens of the eye [56].

1.4 Treatment the therapeutic strategies

1.4.1 Traditional pharmaceutical treatment

Alzheimer's has no current cure, but treatments for symptoms are available. The available therapeutic agents target only neurotransmitter dysfunction in AD. They can temporarily slow the worsening of dementia symptoms and improve quality of life, though the side effects of these drugs remain a major concern. Cholinesterase inhibitors such as donepezil (Aricept), rivastigmine (Exelon), and galantamine (Razadyne) prevent the breakdown of acetylcholine, a brain chemical

that is important for memory and thinking. By preserving high levels of this chemical messenger, the patient may retain cognitive function longer. About 50 percent of patients on these medications see a modest improvement in cognitive symptoms [55]. Moderate-affinity NMDA-Receptor Antagonist is the first of a new class of Alzheimer's medications in which memantine (Namenda) is approved for the treatment of moderate-to-severe Alzheimer's disease. It works by regulating glutamate, a chemical messenger in the brain that triggers certain receptors to allow calcium into the nerve cells, so the cells can produce the necessary chemical environment to process and store information[57].

1.4.2 New therapeutic strategies and Phytochemicals: OPP and Curcumin

Given the fact that there is still no promising treatment that can slow or stop its progression, scientists have turned to investigating the beneficial effects of food supplements and other natural products for an alternative therapy for AD patients. It has been found that a diet rich in vegetables, especially green leafy vegetables and cruciferous vegetables like broccoli, is associated with a reduced rate of cognitive decline. One epidemiological study reported that people who ate a "Mediterranean diet" had 40 % less risk for development of AD [58]. A Mediterranean diet includes vegetables, legumes, fruits, cereals, fish, olive oil andmild to moderate amounts of alcohol, as well as low amounts of saturated fats, dairy products, meat, and poultry. DHA (docosahexaenoic acid), an omega-3 fatty acid found in salmon and certain other fish, also has been found to reduce beta-amyloid plaques, abnormal protein deposits in the brain that are a signatureof Alzheimer's. Although a clinical trial of DHA showed no impact on people with mild to moderate Alzheimer's disease, it is possible that DHA supplements could be effective if started before cognitive symptoms appear[59].

To date, a growing number of herbal remedies, dietary supplements and "medical foods" are promoted as memory enhancers or treatments to delay or prevent Alzheimer's disease and related dementias such as Coenzyme Q10, ginseng and gingko biloba[60-62]. Of a number of ingredients that have been extracted from plants and fruits as antioxidant agents to treat AD, oil palm (Elaeis guineensis),a high oil-producing tropical plant, appears to have an effective anti-oxidative component to counter the oxidative stress exerted by high temperature and intense sunlight. [63]. Although the fruits of oil palm are mainly used for extraction of edible oils, successful recovery of the aquoeus by-products following palm oil production has identified a water soluble complex rich in phenolics and organic acids collectively referred as Oil Palm Phenolics (OPP). Major components of OPP include three isomers of caffeoylshikimic acid (3-,4- and 5-caffeoylshikimic acids), protocathecuic acid and ρ-hydroxybenzoic acid with the three caffeoylshikimic acid isomers. The chemical structure of the main compounds is shown in Fig. 2. The therapeutic effects of OPP on cardiovascular diseases, diabetes and cancers have been reported by Sambanthamurthi et al[63, 64]. They concluded that OPP could be used as a dietary agent for prevention of many oxidative stress-related chronic diseases, including neurodegenerative ailments [65]. Other polyphenol mixes such as high cocoa flavanol have been reported to enhance the hippocampus dentate gyrus function and improve cognition in older adults, most likely by its high efficiency in removing free radicals [66]. Since AD and the associated amyloid plaque buildup has an underlying component of oxidative stress, we hypothesized that OPP may reduce amyloid beta burden *in vivo*. In a previous pilot study we found OPP can decrease the β amyloid in the cell culture. Because of these results, we have begun further investigation on its effects by using an animal model with AD.
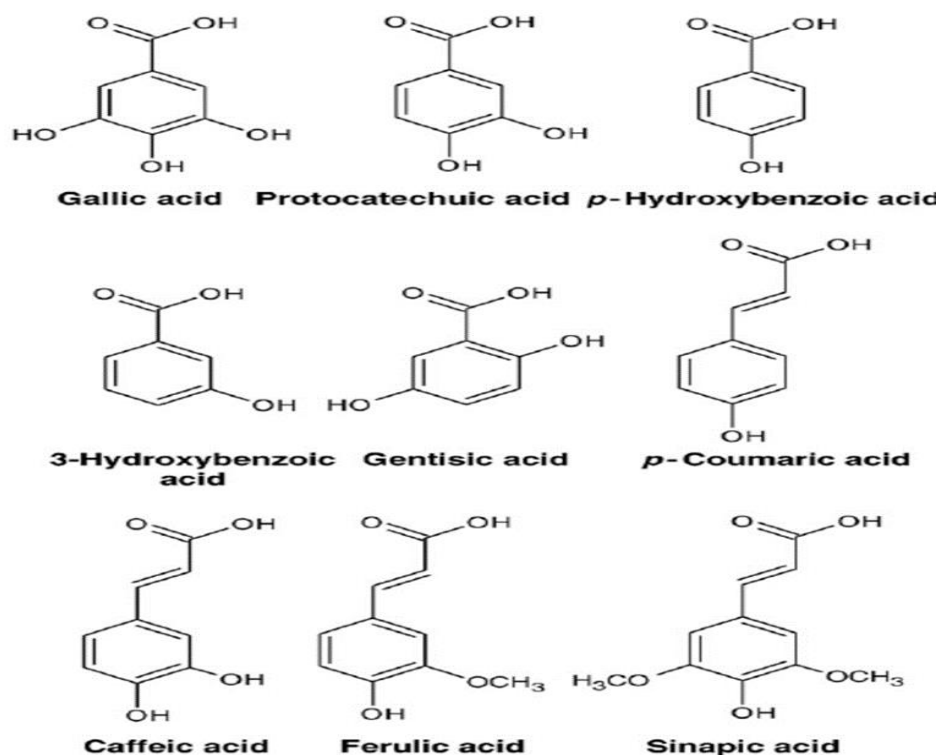
Fig.2 Main compounds in oil palm phenolics (OPP).

Another compound that has been thought to reduce oxidative stress associated with AD is curcumin (Cur), a major component of the yellow curry spice turmeric [67]. Turmeric has been used for thousands of years for medicinal purposes, as a preservative and as a coloring agent in foods. Curcumin was isolated as the major yellow pigment in turmeric, and as is shown by figure 3, it has a polyphenolic molecular structure similar to other plant pigments in green tea (catechins) or in certain fruit juices (blueberries, strawberries, pomegranates etc.)[68]. These polyphenols share antioxidant and anti-inflammatory properties with associated health benefits. Curcumin has been extensively studied for the treatment of various medical conditions, including cancer, atherosclerosis, and dementia. Curcumin also has a potential role in the prevention and treatment of AD. Various studies and research results indicate a lower incidence and prevalence of AD in India. The prevalence of AD among adults aged 70-79 years in India is 4.4 times less than that of adults aged 70-79 years in the United States[69]. The curry consumption and cognitive level in

1010 Asians between 60 and 93 years old was studied and compared as well. The results indicated that those who often (more than once a month) consume curcumin performed better on a standard test (MMSE) of cognitive function than those who ate curry never or rarely [70]. The process through which curcumin can deliver a preventive effect on AD is believed to relate to reducing inflammation and oxidative stress, which are the leading causes of amyloid plaques and metal toxicity (Fig.4). It has been reported that curcumin serves as a free radical scavenger protecting the brain from lipid peroxidation [71]. Oral administration of curcumin has been shown to be centrally neuroprotective by reducing oxidative damage and amyloid pathology in an APPSw mouse model (Tg2576) [72, 73]. Because the lipophilic nature of curcumin, it can cross BBB (blood brain barrier) binds to plaques. Based on the various findings that support the benefits of its oral intake, it is believed that curcumin could lead to a promising treatment for Alzheimer's disease. Therefore, we included curcumin in our experimental high cholesterol diet to serve as a positive control, which enables us to compare it with our testing supplement OPP in their therapeutic effects and potential mechanisms.
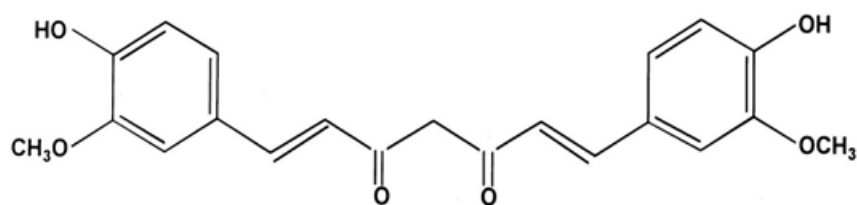
Fig.3. Chemical structure of curcumin[1,7-bis-(4-hydroxy-3-methoxyphenyl)-1,6-heptadiene-3,5-dione]
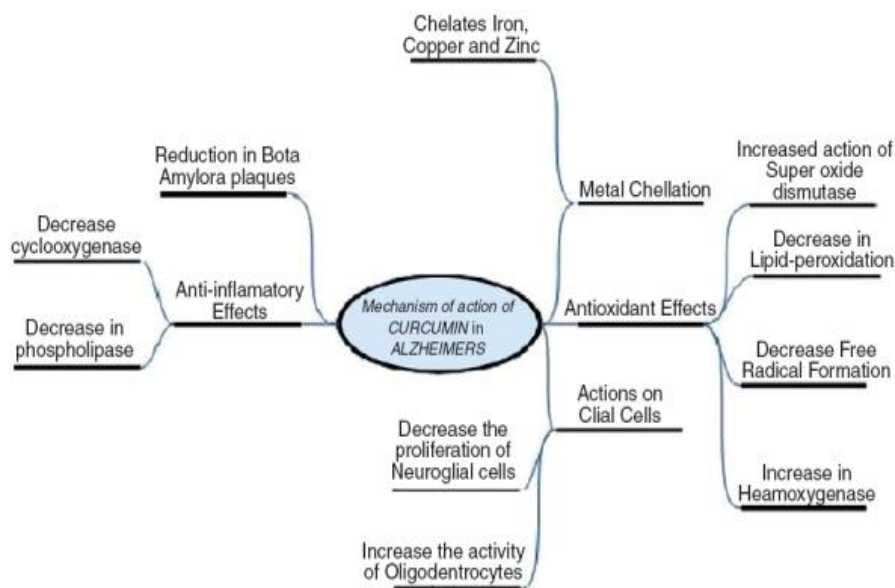
Fig.4. Different mechanisms of action of curcumin in AD [74]

1.5 Hypothesis and Specific Aims

The overall goal of the study is to evaluate the effects of OPP in the treatment of Alzheimer's disease. In order to achieve this goal, we hypothesized that an atherogenic diet (2% cholesterol) will lead to AD-like pathological changes in aging rats. Furthermore, OPP will attenuate the disease progression with their antioxidant & anti-inflammatory effects, which might also be reflected by the changes in the urinary metabolomic profile. Curcumin treatment serves as a positive control group and its effect on AD will also be examined in this study. The following specific aims were proposed to meet our hypothesis:

Specific Aim 1: To evaluate the effect of an OPP supplemented diet on atherogenic diet induced Alzheimer's disease in aged rats;

a, To determine changes in lipid profile and gene expression;

b, To evaluate changes in cognitive behavior;

c, To evaluate amyloid plaque development and neuron loss in hippocampus.

Specific Aim 2 : To examine the possible mechanisms of action of OPP in AD rat model;

a, To investigate effect of OPP on lipid peroxidation (malondialdehyde [MDA] & 3-hydroxybutyrate);

b, To investigate a inflammatory marker (IL-6);

c, To measure effect of OPP on expression of the genes (APP,BACE1, ApoE) in the brain that lead to the plaque formation;

Specific Aim 3, To investigate the urinary metabolomics profile of AD rats for possible non-invasive markers of AD;

a, To observe the difference among groups in metabolomic profiles;

b, To determine the correlations between the urinary metabolomic profiles and cognitive behavioral changes, amyloid burden, oxidative and inflammatory markers;

c, To identify the metabolites responsible for the differences in the metabolomic profile and explore the pathways related to AD pathology.

CHAPTER 2 METHODOLOGY

2.1 Animals

Thirty-two in-bred Brown Norway (BN) rats were obtained from the aged rodent colonies of the National Institute of Aging (Bethesda, MD). Since effects of estrogen on cholesterol metabolism is well known and altered Aβ metabolism by estrogen was reported in several animal species [75], we used male rats exclusively for this study. Pigmented BN strain was chosen for behavioral studies using visual cues.

All animals were housed in individual cage at Wayne State University Division of Laboratory Animal Resources (DLAR) facility under standard conditions as approved by the Wayne State University Animal Investigation Committee (AIC). Each were kept in the same room with alternating 12 hours light and 12 hours darkness under normal humidity and at room temperature. Cage bedding and water was replaced weekly and their health was monitored regularly.

2.2 Experimental conditions and protocols

The study design and experimental conditions are presented in Figure 5. The protocol for this study was approved by Wayne State University IACUC (approval number: A 3310-01). Upon arrival at the facility, all animals were allowed to acclimatize for one week prior to start of the experiment. Following acclimatization period, all rats were assigned in equal number to a control group (n=8), a high cholesterol group (n=8), a high cholesterol + OPP group (n=8) and a high cholesterol + curcumin diet group (n=8) on a pseudo-random basis with the constraint that both diet groups had the same mean body weight. Animals were fed ad libitum supply of diet and had free access to tap water. Cage bedding, diets and water were replaced every week and their health were monitored regularly. Criteria for early euthanasia included 20% weight loss or abdominal distention with respiratory distress.

2.3 Experimental diets

OPP for this study was provided by the Malaysian Palm Oil Board (Kajang, Malaysia) at the stock concentration of 1500 mg/ml gallic acid equivalents (GE). Both the 5% OPP and the standard purified diets were formulated and produced by Dyets Inc. (Bethlehem, PA), and sufficient diet was obtained for the entire duration of the study. The diets were kept at -20°C, and sufficient diet were removed weekly as needed and kept refrigerated at 4°C. Composition of both diets is shown in Table 1.

2.4 Experimental procedures

All rats were provided with their respective diets for 23 weeks. Diet intake was measured weekly and body weight of the animals was measured twice weekly. Weekly urine collections were carried out for a urinary metabolomic study. Upon completion of the experiment at endpoint, each animal was euthanized using carbon dioxide chamber and decapitated followed by exsanguination and tissue collection. Trunk blood was collected into K_2EDTA coated tubes and kept on ice. Plasma was isolated and stored at -80ºC until ready to be used for analysis. Tissues were excised and weight was recorded prior to being flash-frozen in liquid nitrogen. Brain was extracted immediately (generally within 3-5 minutes) and the left hemisphere was flash frozen in liquid nitrogen. Right hemispheres of each animal were immersion-fixed in 10% zinc-formalin (Fisher Scientific International) for histological analysis. Hippocampus and cerebral cortex, cerebellum and the rest of the brain were extracted from the left hemispheres and fixed in RNAlater (Ambion, inc. Austin, TX) for RNA extraction. All procedures and protocols were in accordance with and ratified by the Animal Investigation Committee of Wayne State University.
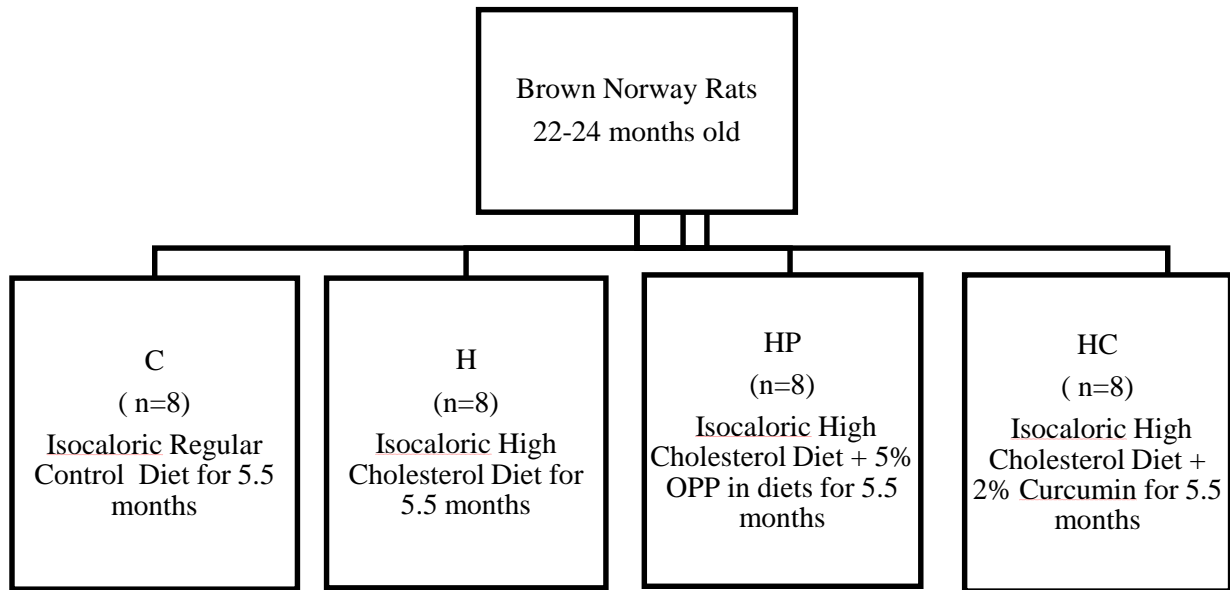
Fig. 5 Study design and experimental conditions

Control groups

C: Rats on standard purified diet.

Experimental groups

H: Rats on standard purified diet + 2% cholesterol;

HP: Rats on standard purified diet + 5% OPP + 2% cholesterol;

HC: Rats on standard purified diet + 2% Curcumin + 2% cholesterol.

Table 1 Composition of purified diets

Ingredient	Isocaloric Control	High Cho (2% Cholesterol)	High Cho +5%OPP	High Cho+2% Curcumin
		g/kg		
Casein	140	140	140	140
L-Cystine	1.8	1.8	1.8	1.8
Sucrose	100	77.5	77.5	77.5
Cornstarch	465.692	465.692	415.692	445.692
Dyetrose	155	155	155	155
Soyabean oil	40	40	40	40
t-butylhydroquinone	0.008	0.008	0.008	0.008
Cellulose	50	50	50	50
Mineral Mix#210050	35	35	35	35
Vitamin Mix#310025	10	10	10	10
Choline Bitartrate	2.5	2.5	2.5	2.5
Cholesterol	_	20	20	20
Cholic Acid	_	2.5	2.5	2.5
OPP	_	_	50	_
Curcumin	_	_	_	20
Total	1000	1000	1000	1000
Calorie	3602	3512	3332	3440

Diets were prepared and pelleted by Dyets Inc. (Bethlehem, PA).

2.5 Total cholesterol measurement

2.5.1 Plasma total cholesterol

Total cholesterol (TC) cholesterol was determined using enzymatic kits (Pointe Scientific Inc. Canton, MI.). Plasma was isolated by centrifugation of blood at 4000 rpm for 20 minutes at 4°C and stored in -80ºC until use. Samples and standards were taken and the test tubes were labeled accordingly. 1ml of reagent was pipetted into each tube and pre-warmed at 37°C for five minutes. 10µL of sample was added into respective tubes, mixed and returned to 37°C for incubation for five minutes. Spectrophotometer was zeroed with blank at 500nm and then the absorbance of all test tubes were recorded. The concentration of unknown samples were calculated by using standard curve.

2.5.2 Liver and brain total cholesterol

The Folch method [76]was used to extract lipids from liver and brain tissues. Briefly, 0.5g of tissue was taken and homogenized in 10mL chloroform-methanol solution 2:1(v/v). The samples were left overnight in a shaking water bath. After water bath, 3mL of 0.5% H_2SO_4 was added for separating the phases. The samples were mixed with vortex and centrifuged at 2000rpm for 20 minutes, the lower phase was taken, and the volume was brought to 10ml by addition of chloroform-methanol mixture. Aliquots of 50µL were made and dried overnight. Before analysis of the total cholesterol, the aliquots were reconstituted with 50µL EtOH. Total cholesterol was determined using an enzymatic kit (Pointe Scientific Inc. Canton, MI.) and same protocol as plasma was followed.

2.6 Plasma HDL level measurement

First, HDL cholesterol was separated by using HDL Cholesterol Precipitating Reagent Set (Pointe Scientific Inc. Canton, MI.). A 0.5 ml (500µL) plasma sample was pipetted into respective

tubes and 0.5ml (500μL) reagent was added to each tube and mixed using vortex. The tubes then were centrifuged at 2000g for 10 minutes. Next, HDL cholesterol was measured by using enzymatic kit (Pointe Scientific Inc. Canton, MI.). A 1ml enzymatic cholesterol reagent, prepared according to package insert instructions, was pipetted into each tube. Then 0.05ml (50μL) standard or clear supernatants from the previous step were pipetted into their respective tubes. All tubes were incubated for 10 minutes at 37°C. The spectrophotometer set zeroed at 500nm with reagent blank and absorbance rate of all test tubes were rerecorded. The concentration of unknown samples then were calculated using standard curve.

2.7 Gene expression analyses

2.7.1 RNA isolation from liver and brain tissue

Total RNA extraction of tissues was performed with a commercial kit (RNeasy Mini Kit, Qiagen Valencia, California, USA) according to the manufacturer's instructions. Tissue samples (30 mg) from liquid nitrogen were taken and were excised, weighed and then placed into 700μL QIAzol Lysis Reagent in a vessel which is suitable for disruption and homogenization using tissue homogenizer. The tube containing the homogenate was then placed at room temperature (15-25˚C) for 5 minutes. Next, 140μL of chloroform was added to the tube, which was capped securely and shaken vigorously for 15 seconds. The tube was kept at room temperature for 3 minutes followed by centrifugation for 15 minutes at 12,000rcf at 4˚C. After centrifugation, the upper aqueous phase was transferred to a new collection tube, and then 525μL of 100% ethanol was added to the tube and mixed thoroughly by pipetting. Next, 700μL of sample, including any precipitate, was pipetted into RNeasy Mini spin column in 2 ml collection tube and centrifuged at 10,000 rpm for 15 seconds. The flow-through was discarded and the previous steps were repeated for the remainder of sample. Buffer RWT (700 μL) was added to RNeasy Mini spin column, then

the sample was centrifuged at 10,000 rpm for 15 seconds and flow-through was discarded. Buffer RPE (500 µL) was then pipetted onto RNeasy Mini spin column and again and centrifuged at 10,000 rpm for 15 seconds. The flow-through was discarded and 500µL of Buffer RPE was added to RNeasy Mini column and then centrifuged at 10,000 rpm for 2 minutes. The RNeasy Mini spin column was then placed into a new 2ml collection tube and centrifuged at full speed for one minute. Afterward, the RNeasy Mini spin column was transferred to a new 1.5ml collection tube after the old collection tube was discarded with the flow through. RNase-free water (40 µL) was then pipetted directly on the RNeasy Mini spin column membrane and centrifuged for one minute at 10,000 rpm to elute the RNA. Then, quantity measurement and the spectrophotometric quality assessment (A260/280 and A260/230 ratios) of RNA were carried out using the Nanodrop spectrophotometer.

2.7.2 Reverse transcription and qRT-PCR

Reverse transcription of the liver RNA was performed using High Capacity RNA to cDNA Master Mix kit (Applied Biosystems, Carlsbad, CA). RT buffer mix (20 µL) including 2µL of RT enzyme mix, 8µL of RNA sample and 10µL of nuclease-free water were taken and mixed into 0.2mL PCR tube and centrifuged for few seconds. The prepared samples were then loaded into an Eppendorf mastercycler realplex 4 (Eppendorf, Hauppauge, NY) for reverse transcription process with the following temperature settings: 25°C for 5 minutes, 42°C for 30 minutes, 85°C for 5 minutes. The samples were then transferred to a -20°C freezer until use for qRT-PCR analysis.

The ApoA1 gene, which encodes apolipoprotein A-I (the major protein component of HDL), was tested in the liver sample. Brain hippocampus expression of the genes (APP, BACE1) that regulate the βAmyloid 42 pathway as well as the whole brain gene expression of the key enzymes (KMO, KYN, HAAO, KAT1,TPH2) that regulate the tryptophan metabolism pathway were

measured. The primer sequence of the genes used in this entire study are listed in Table 2. The final reaction volume of 25 uL was made by using 12.5μL SYBR Green PCR Master Mix (Applied Biosystems, Warrington, UK), 1μL of 20 μM reverse and forward primer mixture, 9.5μL nuclease-free water and 2μL of cDNA. The qRT-PCR was carried out on the Eppendorf mastercycler realplex 4 instrument (Eppendorf, Hauppauge, NY) in Mx3000P 96-Well Plates (Agilent Technologies) using the following settings; initial denaturation: 95˚C for 10 minutes, 45 repetitions of denaturation: 95˚C for 15 seconds and elongation: 60˚C for 1 minute, dissociation curve: 95˚C for 1 minute, 60˚C for 30 seconds followed by gradual temperature increase from 60˚C to 95˚C in 20 minutes and finally at 95˚C for 30 seconds. Each gene was analyzed in triplicate with single non-template control (NTC). GAPDH was used to normalize the expression values (ΔCT). Statistical significance for mRNA expression was obtained by comparing the means of 1/ΔCT values among high cholesterol diet (H), high cholesterol with OPP diet (HP), high cholesterol, curcumin (HC) and the control diet group (C).

Table 2: Primer sequence of the genes in this study

Primers	Forward Sequence	Reverse Sequence
ApoA1	5′- AGGAGCAGACCCAGCAGATA- 3′	5′- AACCCAGAGTGTCCCAGTTG-3′
APP	5'-TGGGTTGACAAACATCAAGACAGAA-3'	5'-GCACCTTTGTTTGAACCCACATC-3'
BACE 1	5′-TGGTGGACACGGGCAGTAGTAA-3′	5′-TCGGAGGTCTCGGTATGTACTGG-3′
ApoE	5'-AGGAGCAGACCCAGCAGATA-3'	5'-GGAGTTGGTAGCCACAGAGG-3'
KMO	5′-TCC ACT TTC ATC CCT CTC TAT-3′	5′- GAG TCC TCT GTT TAT CAC CTTT-3′
Kyn	5′-CAG ACT GCT TAC TGC CAT AC-3′	5′ - CCC AGT GTG TGA GAT TTA CTT-3′
HAAO	5′-TGA TTG AGA GAA GGC GAA TG-3′	5′ - CCT TAC AGT GGA ACC ATT TCT-3′
KAT 1	5'- TGGTCCTCAACACACCCAAC-3'	5'- CCGTCATAGACCAGCCACTG-3'
TPH 2	5'- TAGAGGATGTGCCGTGGTTC - 3'	5'- CTTGAATCCTGGGTGGTCGG -3'

| GAPDH | 5'-ACCCAGAAGACTGTGGATGG-3' | 5'-CAGTGAGCTTCCCGTTCAG-3' |

2.8 Cognitive behavior measurement

A Morris Water Maze test (MWM) was conducted to examine spatial learning and memory. Rats were tested in a circular pool, 60 inches in diameter and 30 inches deep, filled with 10 inches of water made opaque with the addition of a non-toxic dye and maintained at 24-25°C. The swimming pool was placed in a room surrounded by fixed spatial cues such as posters, floor lamp and desk. The rats were trained to locate the hidden escape platform submerged in the water. Latencies for rats to find the platform (seconds) were analyzed as a measure of spatial learning. The rats were given 3 trials/day for 5 consecutive days. They were allowed 90 s to swim around the pool and find the hidden platform. If the animal could not find the platform within this time, it was then gently rescued from the water and placed on the platform. Each trial was separated by 45 min. The platform was always located in the same fixed spot during training and the starting point also remained the same throughout the trials for each rat. All trials were recorded by a video camera as part of the video-tracking system mounted above the pool and the behavioral measures were acquired by a computerized video-tracking system (EthoVision 2.0, Noldus Information Technology, Leesburg, VA).

2.9 Analysis for changes in brain tissue

2.9.1 H&E staining – Histology (1)

All right hemisphere brain tissues were immediately fixed in 10% neutral buffered formalin for 24 hours and then stored in 70% ethanol to prevent excess drying of tissue specimens. Specimens were sent to Histology Lab, Division of Human Pathology, Michigan State University for paraffin section preparation and Hematoxylin and Eosin (H&E) staining and Congo red staining. First, paraffin embedded brain right hemispheres were cut at 6-8 um in the sagittal plane.

Sections then were mounted onto albumin coated slides, deparaffinized, hydrated and nuclei were stained by H&E for visualizing the morphological changes of the neurons. Each prepared H&E slide was later examined under the light microscope (Nikon Eclipse 80i, Melville, NY) for histopathological changes. The outline and the structure of pyramid cells were observed. The healthy neurons were counted in the whole hippocampus which was divided in to CA1, CA3 and DG area defined by the reference[77].

2.9.2 Congo red staining – Histology (2)

Formalin fixed brain tissues of animals were prepared for Congo red staining as described above. Observation under the light microscope (Nikon Eclipse 80i, Melville, NY) was then conducted on the prepared slides to visualize extracellular amyloid deposition. The average number of plaque in the entire hippocampus was calculated among four groups and the size of each plaque as well as the total plaque area were also measured. Amyloid burden in the hippocampus was calculated by comparing the total plaque occupied area to the size of the hippocampus.

2.9.3 Enzyme-linked immunosorbent assay (ELISA) for amyloid β42 concentration

Sample preparation followed as described on the manufacturer's protocol provided with the ß-amyoid 42 Elisa kit (Covance, Princeton NJ). 1g of frozen brain hemisphere was homogenized in TBS with 0.1mM PMSF using a Teflon homogenizer and aliquoted. Formic acid (70%) was added to the homogenate and the mixture was agitated by pipetting up and down. The mixture of each group were spun for 20 minutes at 350,000 g. The supernatant, which represents the whole brain extract, was retrieved for the assay. The supernatant was stored at -80^0C. To begin running the assay, the sample was removed from -80^0C and thawed on ice. Protein content of this formic extraction was determined by the BCA assay. Aβ42 levels were measured using ELISA following

the manufacturer's protocol (Covance, Princeton NJ). Briefly, to start running the assay the sample was removed from -80 ^{0}C and thawed on ice. Wash buffer (300 μL 1X) were added to each well and then dumped out, after which the plate is pat dried on clean paper towel. On day one, 50μL of each standard was added to the plate in triplicate. Each sample (50 μL) as well as 50 μL diluted HRP detection antibody were added to the plate in triplicate. The plate was then covered with a plate sealer. The plate was mixed on a plate shaker for one minute and then incubated overnight at 8^{0}C. On day two, the plate was removed from the refrigerator and the contents were dumped out. The plate was then washed with 300μL of 1X wash buffer per well. The buffer was then dumped and the plate dried pat with clean paper towel. The plate was washed repeatedly with the 1X wash buffer 4 more times for a total of 5 washes. TMB (200μL) substrate was added to each well. The plate was then incubated for 50 minutes at room temperature in the dark. The optical density of each plate was determined using a Bio-tek Elx800 micro-plate reader set at a wavelength of 620nm. The concentration of the unknown (Aβ42) was calculated by using the standard curve.

2.10 Lipid peroxidation

2.10.1 Liver & Brain TBARS (Thiobarbituric Acid Reactive Substances)

2.10.1.1 Tissue homogenization

Tissue (25 mg) was weighed and transferred into a tube. RIPA buffer (250μL) containing protease inhibitor was added to the tube. The tissue was sonicated on ice for 15 seconds and the vial tube was centrifuged at 1600×g for 10 minutes at 4ºC. The supernatant was stored at -80ºC until used for analysis.

2.10.1.2 BCA Protein Quantification

sample using the protein quantification kit (Thermo Fisher Scientific Inc. Grand Island, NY). The standards and working reagents were prepared according to manufacturer's protocol. Each standard or unknown sample replicates were pipetted at 25µL into a microplate well. Working reagent (200 µL) was added to each well and the plate was mixed thoroughly on a plate shaker for 30 seconds. The plate was then covered and incubated at 37°C for 30 minutes. The plate was cooled to room temperature and the absorbance was measured at 562nm on a plate reader.

2.10.1.3 TBARS Assay

A TBARS Assay kit (TCA method) was purchased from Cayman Chemical, Ann Arbor, Michigan. All of the reagents were brought to room temperature before starting the assay. The standards and samples were prepared according to manufacturer's instructions and the vials were labeled accordingly. Sample or standard was taken at 100 µL and added into the vial and 100µL of TCA Assay Reagent was also added to each vial. Then, 800µL of color reagent was added to each vial and vortexed. The vials were capped and placed in foam holder to keep the vials upright during boiling. The vials were then added to vigorously boiling water and left for an hour. Afterward, the vials were taken out and placed in ice bath immediately to stop the reaction and incubated on ice for 10 minutes. The vials were then centrifuged for 10 minutes at 1600×g at 4°C. Solution (200 µL) from each vial was taken and transferred to assigned slots in a plate and absorbance was read at 540nm. The concentration of unknown samples was calculated by using standard curve.

2.10.2 Plasma TBARS The stored plasma from removed from its storage at -80°C and thawed on ice. Plasma TBARS was performed, using the same method as a TBAR assay performed on tissues following the manufacturer's protocol.

2.11 Urine 3-Hydroxybutyrate

2.11.1 Creatinine quantification

The urine creatinine was measured by using a kit purchased from Cayman Chemical, Ann Arbor, Michigan. Stored urine samples from -80°C were taken and thawed on ice. Urine was diluted 1:5 with assay buffer and the standards and reagents were prepared, according to manufacturer instructions. Samples (15 µL) and standards (15 µL) were added to the wells. The reactions were initiated by adding 150µL of alkaline pictrate solution to each well. The plate was covered and incubated at room temperature for ten minutes. The initial absorbance was measured at 500nm after removing the cover. Then 5µL of acid solution was added to each well and the plate was covered, followed by incubation for 20 minutes at room temperature on a shaker. The cover was removed and the final absorbance was read at 500nm. The average final absorbance was subtracted from the average initial absorbance to get the corrected absorbance. The corrected absorbance of standard A was subtracted from itself and all other standards and samples to get adjusted absorbance. This adjusted absorbance of standards was plotted on standard curve to obtain the concentration of creatinine of unknown samples.

2.11.2 Urinary ketone measurement

Urine samples were used for measuring the ketone body 3-hydroxybutyrate by the colorimetric assay kit purchased from Cayman Chemical, Ann Arbor, Michigan. Stored urine samples from -80°C were taken and thawed on ice. Urine was diluted 1:5 with assay buffer and the standards, and reagents were prepared, according to manufacturer instructions. 50µL of standards and samples were added to the wells in triplicates. The reaction was initiated by adding 50µL of developer solution to each well. The plate was incubated in dark at 25°C for 30 minutes. The absorbance was read at 455nm and the values were recorded. The concentration of unknown samples was calculated by using standard curve. The urine samples were normalized using creatinine.

2.12 Inflammatory biomarker

A IL-6 ELISA was measured by immunoassay kit (R&D Systems Inc. Minneapolis, MN). All the reagents, standard dilutions, control, and samples were reconstituted according to manufacturer's protocol. Plasma was taken from -80 ℃ and thawed on ice. Assay Dilent (50 μL) was added into each well and then 50μL of standards or samples were also added into their respective wells. The samples were mixed by gently tapping the plate frame for one minute. The plates was covered with the adhesive strip provided and incubated for two hours at room temperature. Each well was aspirated and washed, repeating the process four times for a total of five washes. The wells were washed by filling each well with Wash Buffer (400 μL) using a squirt bottle. The plate was inverted and blotted against clean paper towels. After this, 100 μL of Rat IL-6 Conjugate was added to each well and covered with a new adhesive strip. The wells were incubated for two hours at room temperature and the aspiration/wash was repeated as explained above. Then 100 μL of Substrate Solution was added to each well and incubated for 30 minutes at room temperature, taking care to protect it from light. After 30 minutes 100 μL of Stop Solution was added to each well and gently tapped the plate to ensure thorough mixing. The optical density of each well was determined within 30 minutes, using a microplate reader set to 450 nm. The concentration of unknown samples was calculated by using standard curve.

2.13 Urine metabolomics analysis

2.13.1 Sample preparation and ^{1}H NMR spectroscopic acquisition

Urine samples were collected from the animal subjects once per month using the metabolic cage. Following collection, samples was centrifuged at 350 x g for 15 min at 4°C to remove any debris, aliquoted and frozen at -80°C till analysis. Stored urine sample was mixed with 60ul of 1:9 D2O diluted reference buffer solution containing 5mM DSS (disodium-2, 2-dimethyl 2-

silapentane-5-sulphonate) and 10mM imidazole (Sigma-Aldrich, Mississauga, Ontario, Canada) to make the final volume of 600ul. Samples were mixed by vortexing and then transferred into 5mm NMR tubes immediately before NMR acquisition. ^{1}H NMR spectra of the prepared samples were acquired on a Varian 500 MHz spectrophotometer fitted with a cryoprobe maintained at 25 K. Single pulse spectra using a solvent pre-saturation pulse sequence to suppress residual water sequences were acquired. The standard spectral acquisition conditions used includes collection of 32 free induction decays (FIDs) into data points in 2 s; spectral width ~ 12000 Hz; temperature = 25°C.

2.13.2 NMR spectra pre-processing and multivariate data analysis

All ^{1}H NMR spectra were batch processed in the form of free induction decay [78] files by using ACD NMR processing software (Advanced Chemistry Development Inc., Toronto, ON, Canada). Peak areas were used to quantify 1H spectra and resonance assignments were made by comparison with nuclear overhauser spectroscopy (NOESY) NMR spectra and by adding reference compounds whenever needed. FID files were Fourier transformed to convert the spectra from the time domain to the frequency domain. The converted spectra were baseline corrected, autophased and binned into 1000 bins. The table of integrals from spectra pre-processing was then imported into Excel and used for multivariate data analysis using SIMCA-P+ software (Version 13, Umetrics, Sweden). For further analysis, the regions δ 4.5 to 6.0, which include the water resonances and cross–relaxation alterations with the urea peaks through exchanging of protons with the solvent, were excluded. Data were also Pareto-scaled prior to the subsequent model generations. Using SIMCA-P+ software, both multivariate pattern recognition techniques, unsupervised (principal component analysis, PCA) and supervised (partial least-squares discriminant analysis, PLS-DA) were employed to the data in order to discriminate sample spectra

of different experimental groups. PCA is an unsupervised multivariate projection method designed

to extract and display the systemic variation in the data matrix X as a score plot. The corresponding

loading plot provides information about the part of the spectrum that is responsible for the

similarities and/or

dissimilarities in the data set as observed in the score plot. Moreover, regression analysis using

orthogonal projections to latent structures (OPLS) was conducted on several investigated variables

(escape latency, βAmyloid 42, MDA and IL-6 concertration). Regression analysis enables the

evaluation of the relationship between urinary metabolite profiles with the variables investigated

independently of the metabolomic profiles. In PLS-DA, the data set was distributed into classes

and its objective was to find a model that separated the classes of observation on the basis of their

X-variables, while using a hypothetical Y-variable. Both OPLS and PLS-DA methods of analysis

were supervised, meaning that some information about the data set was provided to the software

prior to analysis.

2.13.3 Metabolite identification and pathway interpretation

Changes in specific metabolite concentrations that contribute to the difference in metabolomic

profile were quantified by Chenomx-NMR Suite (CHENOMX INC, Edmonton, Alberta). The fid

files from the 1D ^{1}H –NMR spectra were imported to the CHENOMX software. This software has

its own processing interface where spectra were Fourier transformed and base line was corrected.

Phasing was done using DSS reference peak at 0.0 ppm and water peak was deleted. The processed

spectra were further analyzed in the profiler module of the software. The 500 MHz library with

corresponding pH was selected. Identification and concentrations of different metabolites were

calculated by fitting the set of peaks for those compounds in the sample spectrum. If the area was

crowded with many peaks then multiple metabolites were fitted at one time to match the reference

spectrum closest to the sample spectrum. The identified and quantified compounds then were exported in to the Excel sheet and ANOVA was done to calculate the statistical significance of the differences in spectra. Based on results from CHENOMX, MetaboAnalyst3.0 software was used to explore the potential pathway. MetaboAnalyst software utilizes pathway enrichment analysis and pathway topology analysis to translate metabolic trends into defined pathways relevant to the study.

2.13.4 Pathway validation

Whole brain expression of the key enzymes (KMO, KYN, HAAO, KAT1, TPH2) that regulate the tryptophan metabolic pathway were measured by rt-PCR for further validation of the metabolomics data. The sequence of the primers are listed in Table 2 and same method was performed as described above in "2.7 Gene expression analyses."

2.14 Statistical analysis

All statistical analyses were performed by using IBM SPSS 23.0 (SPSS Inc. Chicago, IL). Data was analyzed using ANOVA followed by LSD or Tukey post-hoc tests. Comparisons between two groups was analyzed by using student t-test. Results are presented as the means + SEM with statistical significance level of 0.05 ($p<0.05$).

CHAPTER 3 RESULTS

3.1 Survival of the aging rats

A total of 32 aging BN rats were used for this study. Animals were randomly assigned to four groups for a 23 week dietary intervention to investigate the *in-vivo* effect of OPP on AD induced by an atherosclerosic diet. At endpoint (week 23), each group had lost three animals before the termination of the study due to death or conditions approved by a veteran researcher that demanded an early euthanization (Table. 3).

3.2 Body weight and diet intake

No significant differences were observed among groups at baseline (week 1) and endpoint (week 23) with respect to mean body weight (Fig. 6). For diet intake, average diet intake (g) per week (the total diet intake during the whole experiment period/23 weeks) was calculated and compared among four groups. Differences in weekly diet intake were not found to be significant among the four groups (Fig. 7).

Table 3. The number of animals that survived at each month

	Wk0	M1	M2	M3	M4	M5	Endpoint
C	8	7	7	7	6	5	5
H	8	8	8	8	7	6	5
HP	8	8	8	8	7	5	5
HC	8	8	7	7	6	5	5
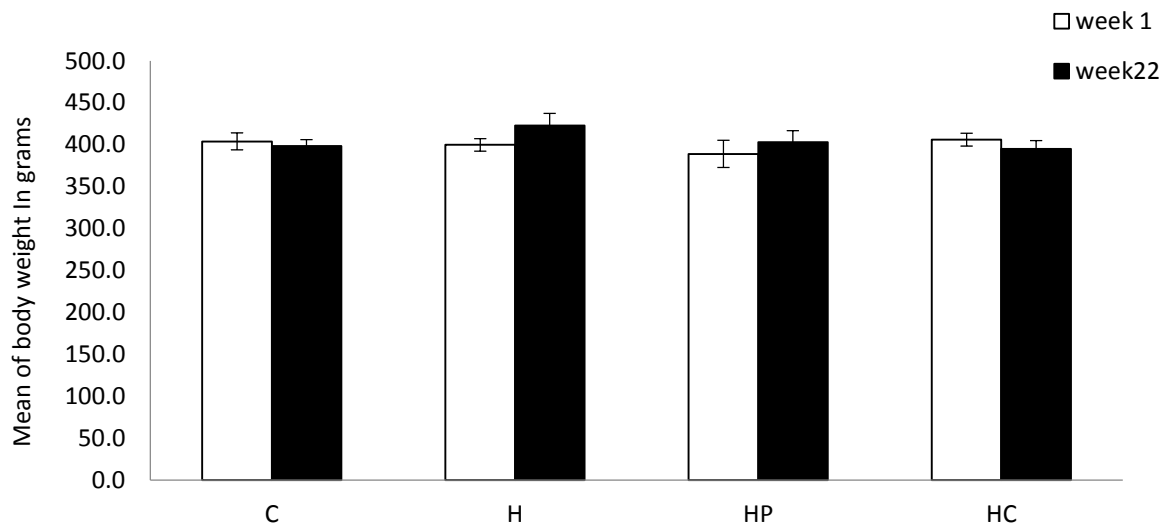
Fig. 6 Mean body weight. Comparison of mean body weight in Control (C), High cholesterol (H), High cholesterol + 5% OPP (HP) and High cholesterol + 2% curcumin (HC) at baseline (week 1) and endpoint (week 23). Data are expressed as mean±SE. No significant differences between groups observed (p>0.05).
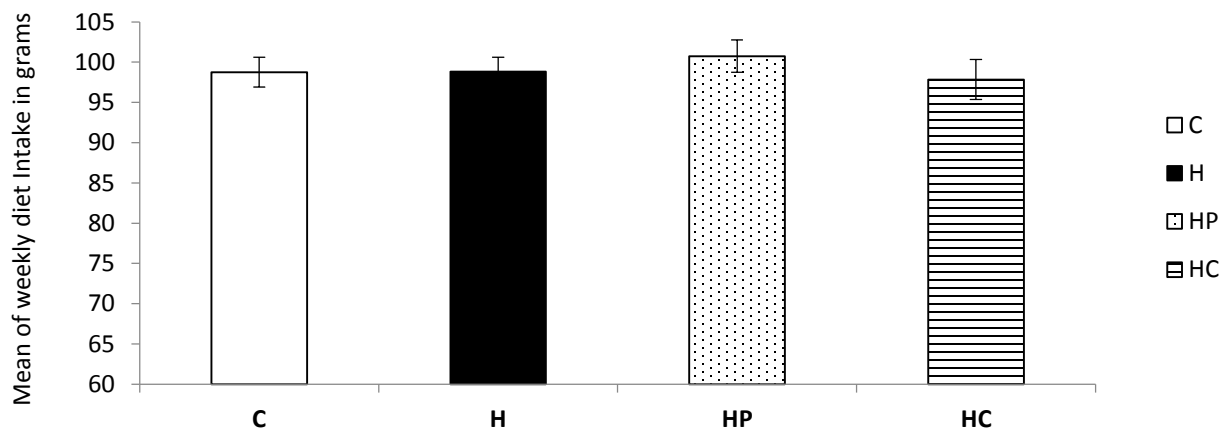
Fig. 7 Mean weekly diet intake. Comparison of mean weekly diet intake in Control (C), High cholesterol (H), High cholesterol + 5% OPP (HP) and High cholesterol + 2% curcumin (HC) over the whole feeding period. Data are expressed as mean±SE. No significant differences between groups observed (p>0.05).

Specific Aim 1: <u>To evaluate the effect of OPP on atherogenic diet induced AD in aged rats with</u> <u>the hypothesis that the high cholesterol diet and hypercholesterolemia will induce the AD</u> <u>pathological changes including Aß deposition, neuron death and cognitive decline, while OPP can</u> <u>improve their progression.</u>

3.3 Effect of diet on lipid profile

In this study, we created a diet-induced hypercholesterolemic rat model without the use of gene transfection or pharmacological supplementation. To confirm the effects of the atherosclerotic diet on creating peripheral hypercholesterolemic conditions, plasma and liver lipid profiles were examined for all rats.

3.3.1 Plasma lipid profile

The mean plasma total cholesterol (TC) (Fig. 8) was significantly increased with the high cholesterol diet (ANOVA,$p<0.05$) as compared to the control diet group. There was no difference in plasma TC among any of the high cholesterol fed animals; The concentration of HDL-C was significantly higher in the control group ($p < 0.05$) as compared to the high cholesterol and high cholesterol+OPP group ($p < 0.05$); There was no significant difference between the control and the high cholesterol + curcumin group (Fig 9). We then calculated the non-HDL cholesterol level using total cholesterol level to subtract the HDL-cholesterol (HDL-C). The result indicated the same changes observed in total cholesterol level (Fig 10). The TC/HDL-C ratio was also significantly lower in control group when compared with the other high cholesterol diet groups ($p<0.05$) as shown in Fig 11. Taken together, the results show that feeding rats with a two percent high cholesterol diet for 23 consecutive weeks resulted in marked hypercholesterolemia. Interestingly, it seems that curcumin may have the ability to maintain the HDL level by alleviating the hypercholesterolemia effects from the diet, as there is no significant difference in HDL when

compared to the control diet group. The curcumin diet group also had a significant lower Non–HDL cholesterol level and TC/HDL ratio when compared to the other two high cholesterol diet group (H & HP). The possible hypolipidemic effects of curcumin demonstrate its potential therapeutic effect in atherosclerotic diseases.

3.3.2 Lipid profile changes in tissues

Since liver is the key organ regulating cholesterol metabolism, we also measured the total cholesterol level in liver tissue due to the diet. The liver/body weight (BWT) ratio of the rats were also examined. The results show liver/BWT ratio was significantly increased in the high-cholesterol fed animals (p<0.05) (Fig.12). The mean liver cholesterol was also significantly increased with the high cholesterol diet (Fig.13, p<0.05) compared to the control group, reflecting the same trend found in the weight of the liver tissue/BWT. This demonstrates that a hypercholesterolemic diet increased the plasma cholesterol as well as hepatic content of total cholesterol. In order to investigate how a high cholesterol diet can impact the brain, total cholesterol concentration in the brain was also measured. There was no significant difference among four groups, indicating the intake of dietary-sourced cholesterol is not associated with brain cholesterol level (Fig.14).

3.3.3 Gene expression of the HDL related gene

In order to explore the mechanism of how curcumin affects plasma HDL level, we next examined the expression of the gene that regulates HDL production. Apolipoprotein A-1 (ApoA-1) is a major component of the high-density lipoprotein (HDL) particle, which is necessary for the efficient transport and clearance of cholesterol from peripheral tissues to the liver through a process called reverse cholesterol transport. The results showed the expression of liver gene ApoA-1 that encodes the apolioprotein A-1 was significantly upregulated by curcumin in the HC group

compared to the high cholesterol (H) group(p<0.05) (Fig.15). There is no significant difference

between control (C) and high choleserol + curcumin (HC) diet group, demonstrating that curcumin

can maintain the HDL level by upregulating the Apo A-1 gene expresion in liver.
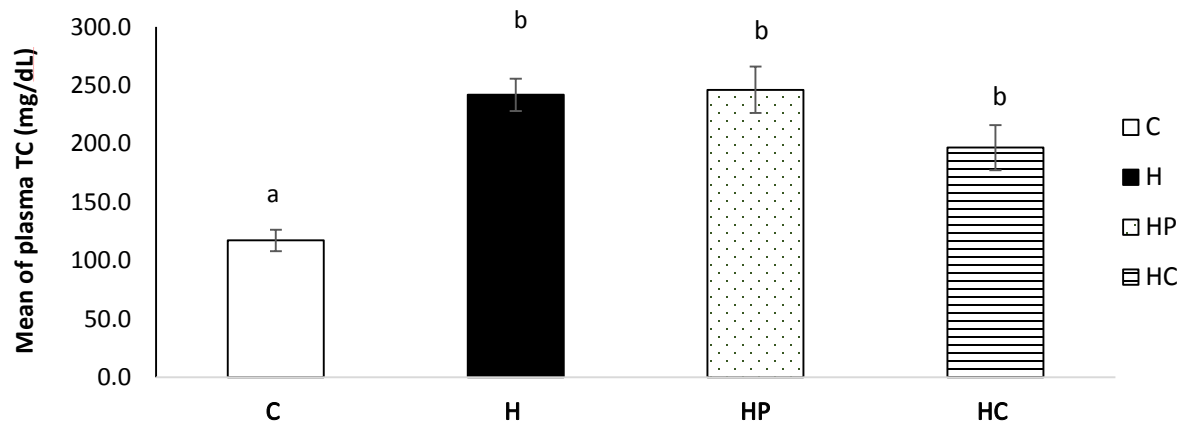
Fig.8 Effect of atherosclerotic diet on plasma total cholesterol level. Comparison of mean
plasma total cholesterol in Control (C), High cholesterol (H), High cholesterol + 5% OPP (HP)
and High cholesterol + 2% curcumin (HC) over the whole feeding period. a,b: C is significantly
different from H, HP and HC (p<0.05). Data are expressed as mean±SE.
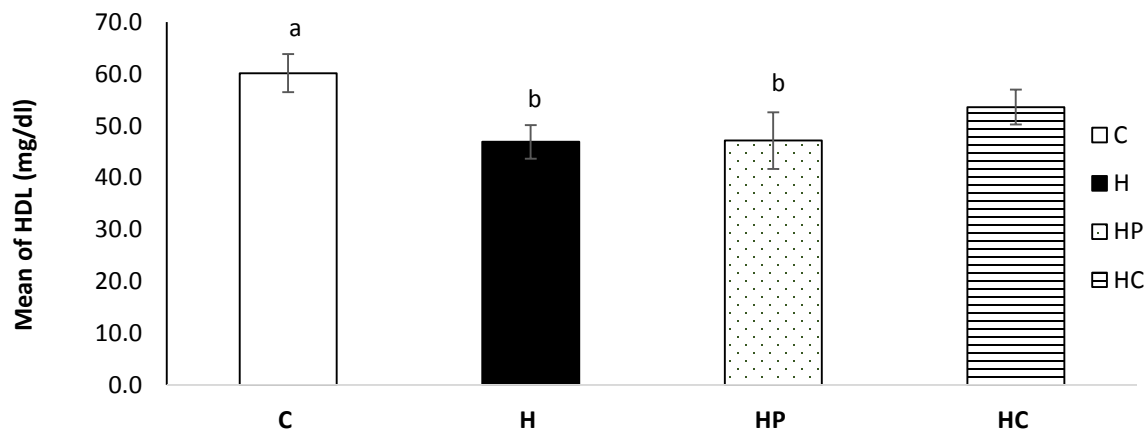
Fig.9 Effect of atherosclerotic diet on plasma HDL-cholesterol level. Comparison of mean
plasma HDL-cholesterol level in Control (C), High cholesterol (H), High cholesterol + 5% OPP

(HP) and High cholesterol + 2% curcumin (HC) over the whole feeding period. a,b : C is significantly different from H, HP (p<0.05). No significant difference between HC and other groups. Data are expressed as mean±SE.
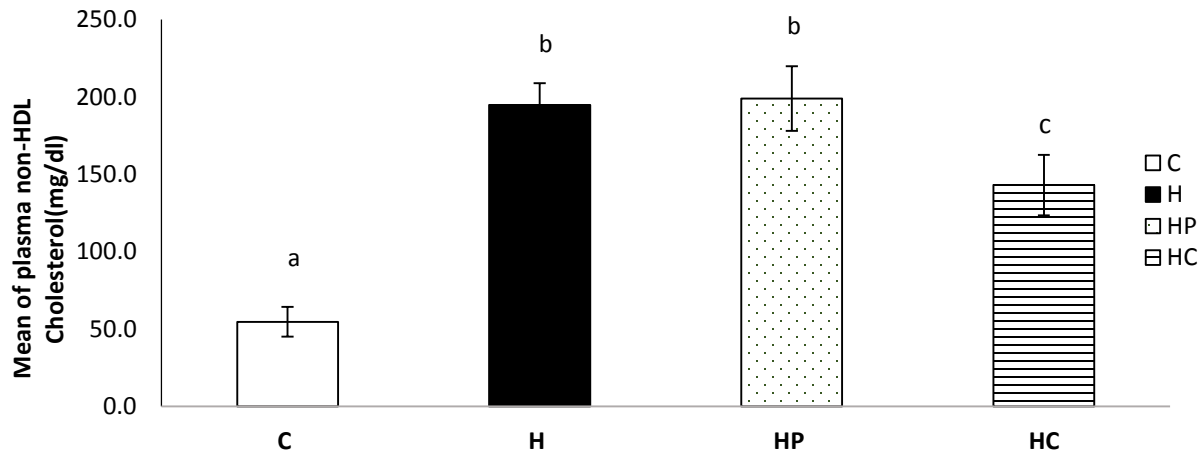
Fig.10 Effect of atherosclerotic diet on plasma non HDL-cholesterol level. Comparison of mean plasma non HDL-cholesterol level in Control (C), High cholesterol (H), High cholesterol + 5% OPP (HP) and High cholesterol + 2% curcumin (HC) over the whole feeding period. a,b: C is significantly different from H, HP and HC (p<0.05). c: HC is significant different from H and HP (p<0.05). Data are expressed as mean ± SE.
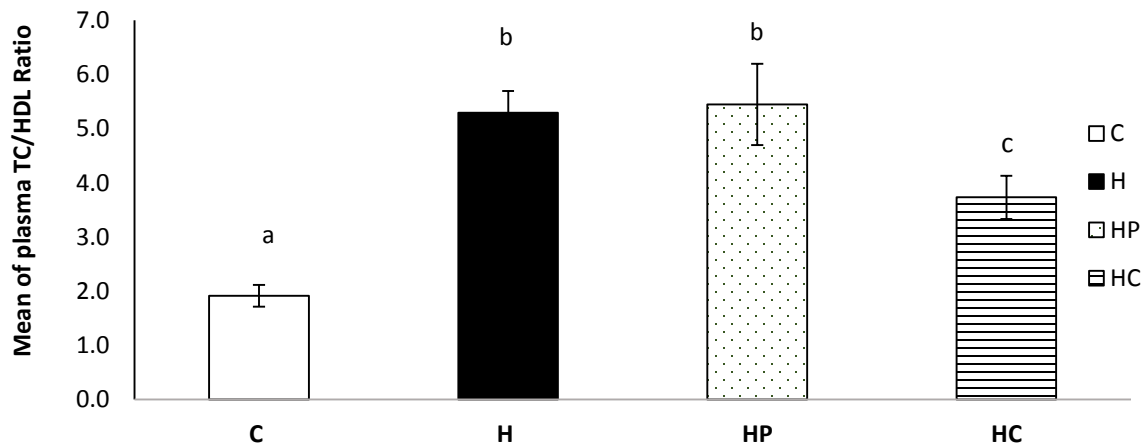
Fig.11 Effect of atherosclerotic diet on plasma Total cholesterol (TC)/HDL ratio. Comparison of mean plasma TC/HDL ratio in Control (C), High cholesterol (H), High cholesterol + 5% OPP (HP) and High cholesterol + 2% curcumin (HC) over the whole feeding period. a,b: C is significantly different from H, HP and HC (p<0.05). c: HC is significant different from H and HP (p<0.05). Data are expressed as mean±SE.
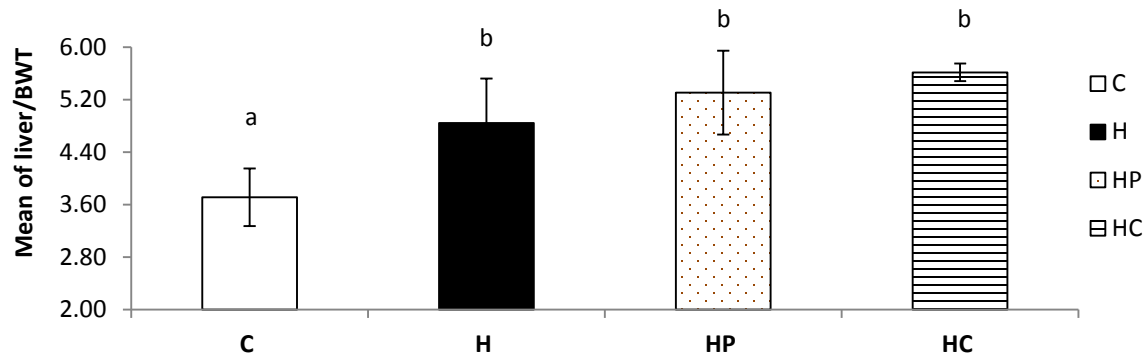
Fig.12 Effect of atherosclerotic diet on liver/body weight (BWT) ratio. Comparison of mean liver/body weight (BWT) ratio in Control (C), High cholesterol (H), High cholesterol + 5% OPP (HP) and High cholesterol + 2% curcumin (HC) over the whole feeding period. a,b: C is significantly different from H, HP and HC ($p<0.05$). Data are expressed as mean ± SE.
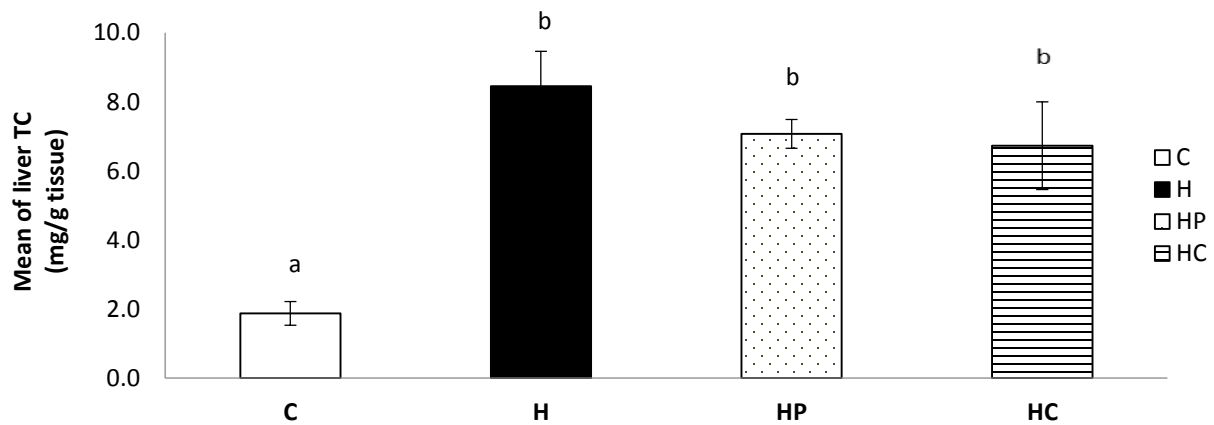
Fig.13 Effect of atherosclerotic diet on liver cholesterol level. Comparison of mean liver cholesterol level in Control (C), High cholesterol (H), High cholesterol + 5% OPP (HP) and High cholesterol + 2% curcumin (HC) over the whole feeding period. a,b: C is significantly different from H, HP and HC ($p<0.05$). Data are expressed as mean ± SE.
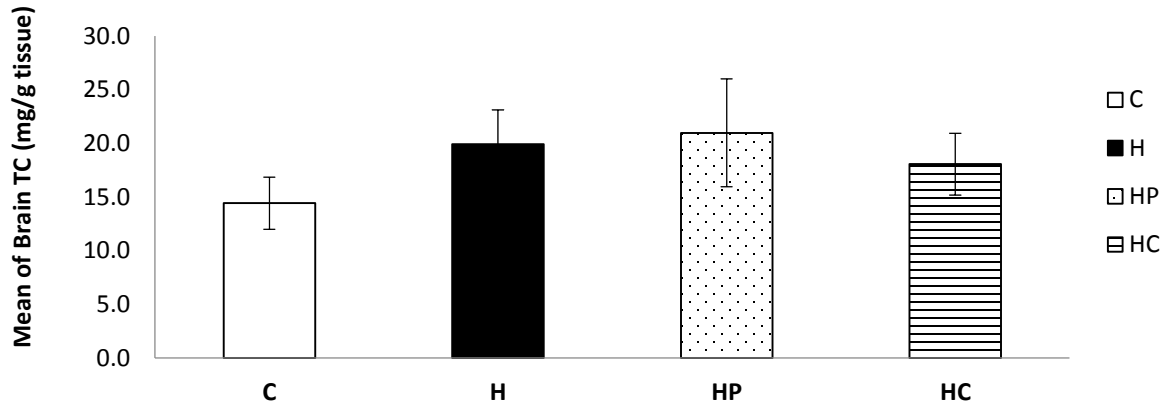
Fig.14 Effect of atherosclerotic diet on brain cholesterol level. Comparison of mean brain cholesterol level in Control (C), High cholesterol (H), High cholesterol + 5% OPP (HP) and High cholesterol + 2% curcumin (HC) at baseline (week 1) and endpoint (week 23). Data are expressed as mean±SE. No significant differences between groups observed (p>0.05).
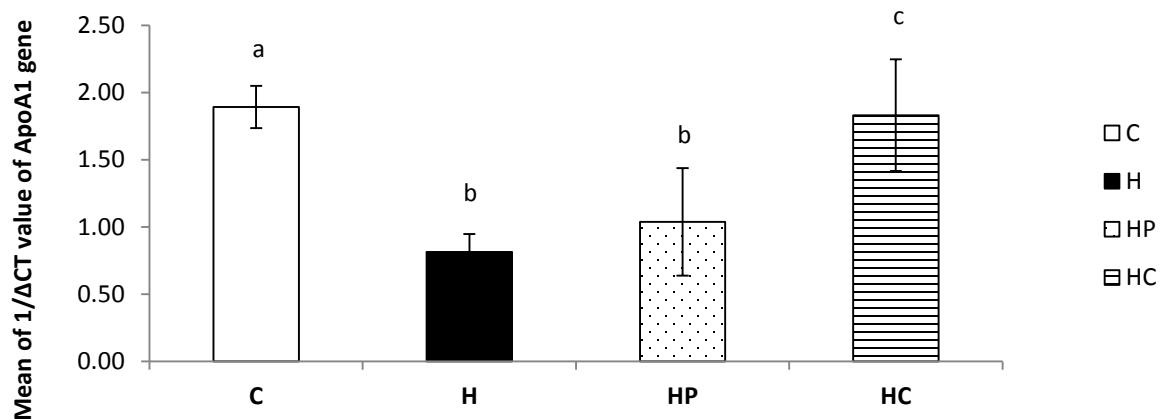
Fig.15 Effect of atherosclerotic diet on liver gene expression of Apo A-1. a,b : High cholesterol diet significantly down regulates Apo A-1 expression in high cholesterol (H) and high cholesterol + OPP (HP) group as compared to control (C) group (p<0.05); c: High cholesterol + curcumin diet group(HC) has a significant higher expression as compared to high cholesterol diet (H) group and OPP supplement group (p<0.05). Data are expressed as 1/ ΔCT values which was normalized against GAPDH (mean±SE).

3.4 Effect of diet on spatial learning ability

Escape latency (EL) using a Morris water maze was measured to determine the rat's spatial learning. Because the aging rats were fatigued on day five, which may interfere with their performance, we compared the means of EL on day three for each group. First, we compared the means of escape latency (EL) among the four groups at each time point from baseline to month five (Fig.16). In month two, the high cholesterol + curcumin (HC) group used the shortest time(s) on average to locate the platform compared to the other three groups ($p<0.05$). In month three, the control group as well as both treatment groups showed significant time differences from the high cholesterol diet group ($p<0.05$). In month four, the average time that HC group animals used was once again significantly less compared to the other three groups($p<0.05$), meaning both OPP and curcumin appear to preserve memory in targeting the underwater platform. However, OPP only shows the significant difference at month three. Reasons for this could include loss of the aging animals during the long term of the study (5.5 month). Therefore, months three and four are more likely to reflect the spatial learning ability of the animals. At month five, the study's endpoint, average time the animals spent in water was longer than month four, which could be a result of aging.

Next, we compared the means of escape latency (EL) over four months for each group (Fig 17). For control group, there was no significant difference across the entire study period; the same trend was observed on the high cholesterol group (H). For the OPP supplement group (HP), significant differences began in month three and continued to month four ($p<0.05$); For the curcumin supplement group, a significant difference started in month two and lasted through month four. ($p<0.05$).

Finally, the improvement in the animals' spatial learning ability during the feeding period was investigated. The improvement was calculated by using the escape latency (EL) at month four subtracted from month one. The means of the difference were compared. It was found that only OPP group had a significant improvement in EL (p<0.05, Fig. 18).
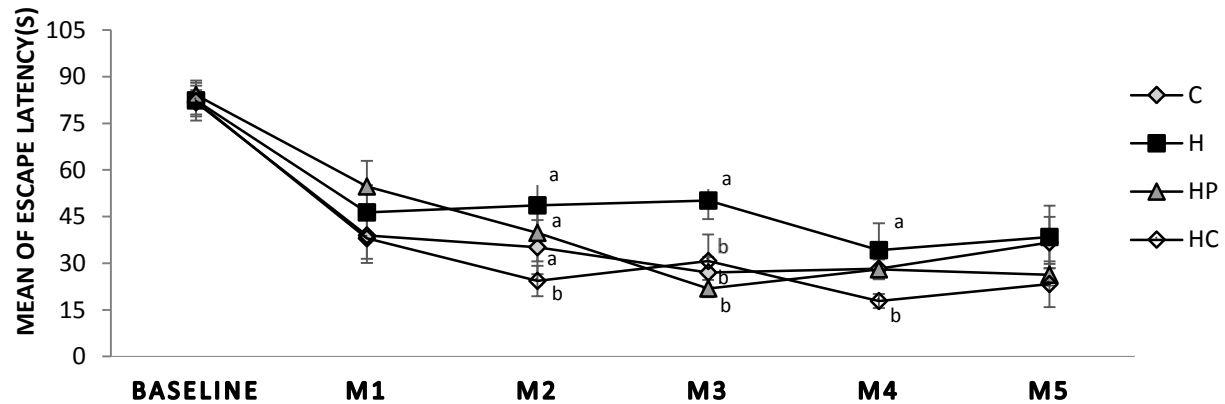
Fig.16 Linear graph of the spatial learning ability throughout whole study. Comparison of the means of escape latency (EL) at day 3 among 4 groups at each time point from baseline to month 5. In month two, high cholesterol + 2% curcumin (HC) group used the shortest time(s) on average to locate the platform as compared to the other three groups. a,b: HC is significantly different from C,H and HP(p<0.05); In month three, control group as well as the other two treatment groups were significantly different from the high cholesterol diet group; a,b: H is significantly different from C, HP and HC groups (p<0.05); In month four, the average time that HC group animals used was once again significantly less compared than in the other three groups. a,b: HC is significantly different from C,H and HP (p<0.05); Data are expressed as mean ± SE.
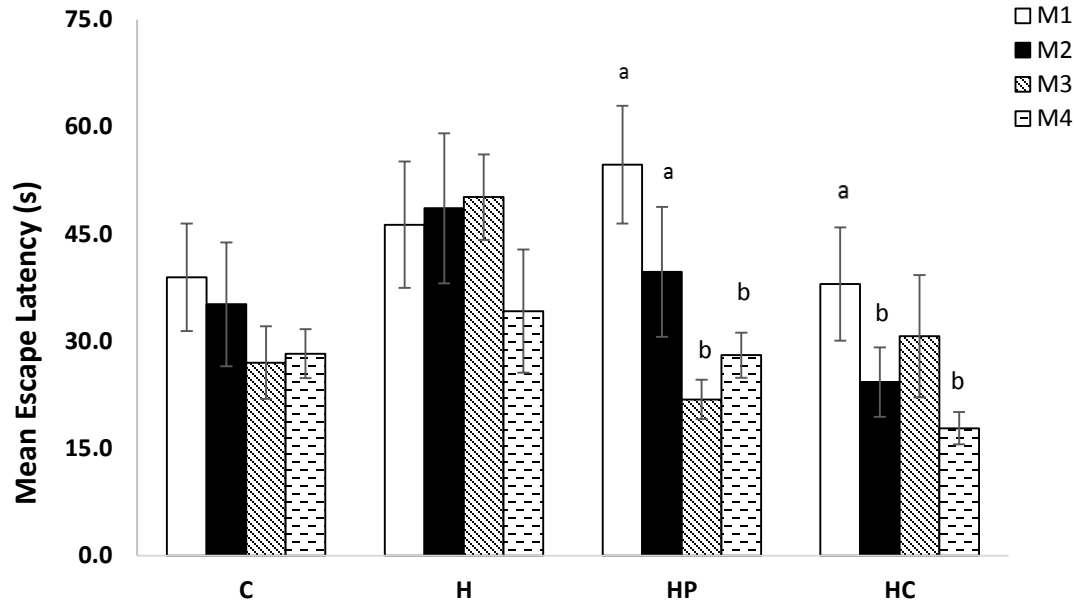
Fig.17 Bar graph of the time course change of spatial learning ability in each group.
Comparison of the means of escape latency (EL) over four months for each group. In the
control group, there is no significant difference over the study period; the same trend was
observed on the high cholesterol group (H). In OPP supplement group (HP), a significant
difference began in month three and continued through month four. a,b: months three and four
are significantly different from months one and two. ($p<0.05$). In curcumin supplement group,
significant differences began inmonth two and lasted through month four. In month three,
animals on average took a longer time to find the platform as compared to month two, but the
difference is not significant. a,b: months two and four are significantly different from month
one ($p<0.05$). Data are expressed as mean ± SE.
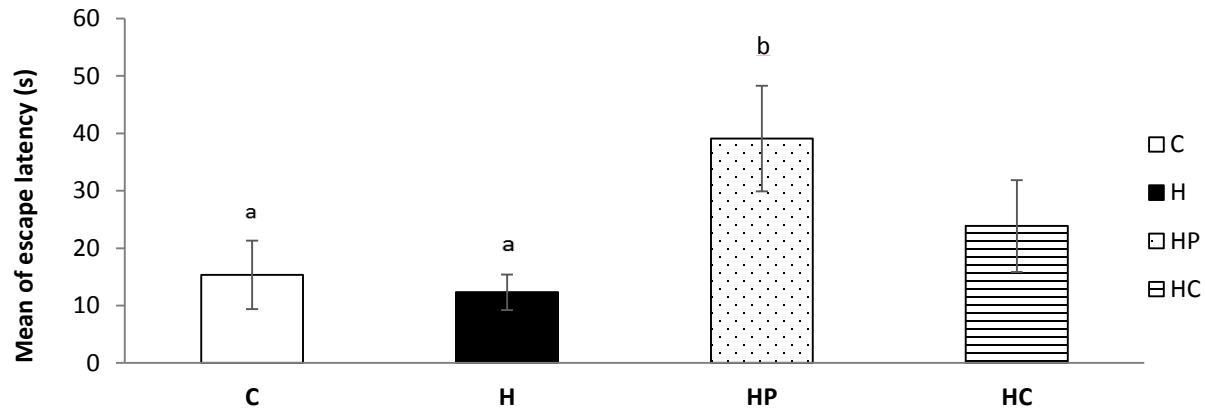
Fig.18 Improvement in spatial memory learning ability in each group. Comparison of the means of the difference by using the escape latency (EL) at month 4 to be subtracted by month 1; a,b: High cholesterol + 5% OPP (HP) has the most improvement in the spatial learning ability compared to the control (C) and high cholesterol (H) diet group ($p<0.05$); No significant difference was observed between high cholesterol + 2% curcumin (HC) group and other groups. Data are expressed as mean ± SE.

3.5 Effect of diet on AD-like histological changes on the rat brain

3.5.1 Morphological changes of neurons in hippocampus

One of the prominent pathological features of Alzheimer's disease is neuronal death and loss, which will ultimately result in brain atrophy. It has been reported that the hippocampus, the brain region responsible for memory and spatial learning ability, is one of the areas that is particularly vulnerable to the degenerative processes by exhibiting neuronal dysfunction in the earliest stage of the disease [79, 80]. Hence, some of the earliest damage can be found in the hippocampus. In this study, rat brain right hemispheres slides were prepared by the histology lab at Michigan State University. The slides were examined under the microscope (Nikon Eclipse 80i, Melville, NY). Sections containing the hippocampus area were first subjected to H&E staining to observe the morphology of the neurons lined up in a pyramidal layer in the hippocampus. The hippocampus was examined by sub-region: CA1 (cornu ammonis region 1), CA3 (cornu ammonis region 3) and DG (dentate gyrus) region based on the "Rat Brain Atlas"[77]. The pyramid cells were

visualized and a healthy neuron was defined by the following characteristics: ①big size and intact oval shape with abundant cytoplasm and ②lined up regularly with full nucleus, sparse nuclear chromatins and clear nucleoli cell shape [81]. The results showed necrotic cells were identified with a shrunken nucleus or nucleus clumping into large round speckles as well as a hyperchromatism (chromatin condensation) in all animals. The high cholesterol group showed more neuron death (shown with an arrow) compared to control, high cholesterol +OPP and high cholesterol+ curcumin groups in CA1, CA3 and DG area (Fig.19). In order to quantify the number of the healthy neurons, we also counted their numbers in the hippocampus area. As shown by Fig. 20, there was a significant decrease in healthy neurons in both control and high cholesterol group compared to the other two treatment groups (HP, HC) ($p<0.05$). A decrease in the number of healthy neurons in control groups might be a result of aging and the dietary supplement (OPP& curcumin) helping to preserve more healthy neurons in those groups.
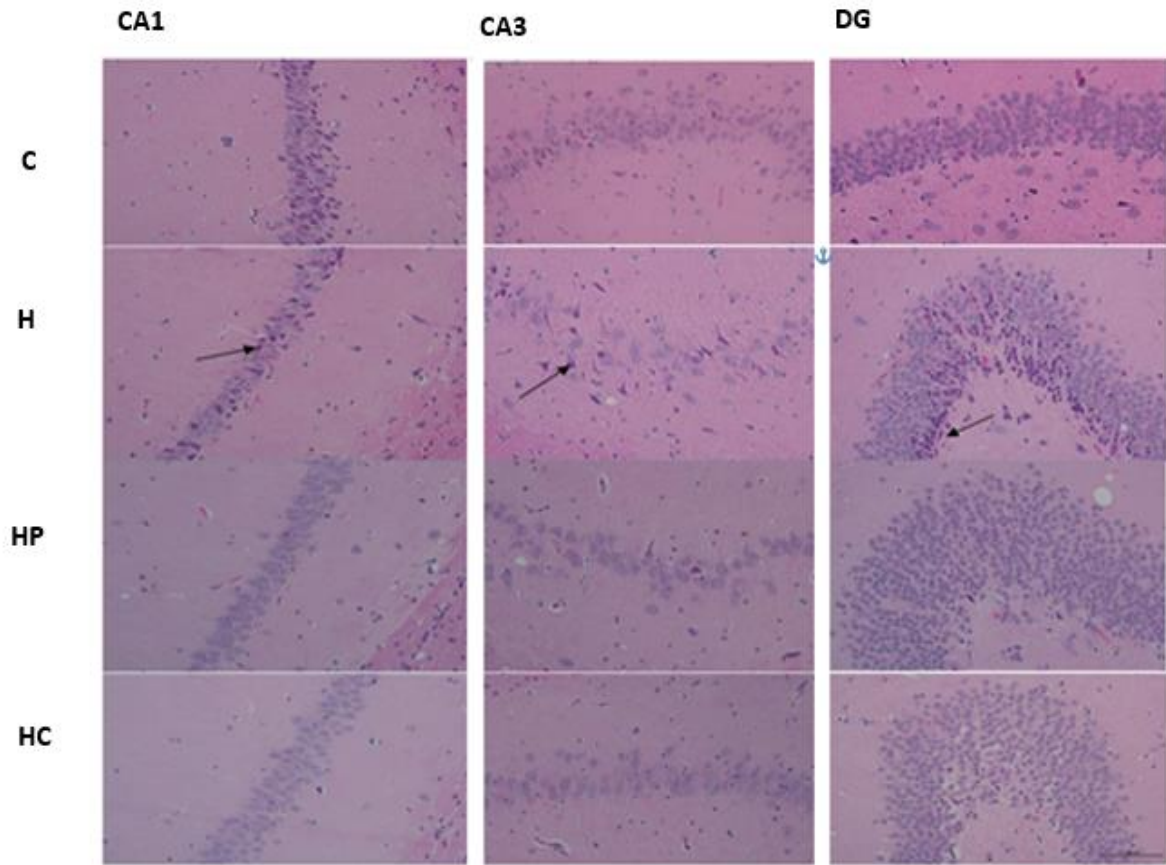
Fig.19 Effects of atherosclerotic diet and OPP treatment on histopathological changes in the hippocampus revealed by hematoxylin and eosin (HE) staining (20 x). Left column: Comparison of the histopathological changes in the hippocampal CA1 region among 4 groups (Control (C), High cholesterol (H), High cholesterol + 5% OPP (HP) and High cholesterol + 2% curcumin (HC)). Middle column: Comparison of the histopathological changes in the hippocampal CA3 region among four groups. Right column: Comparison of the histopathological changes in the hippocampal DG region. Necrotic neurons (nucleus shrinkage, condensed chromatin and loss of cytoplasm structure) were easily observed, as the arrow indicates. In the H group, there is a loose and disordered arrangement of cells and more neuron shrinking deformations as compared to other groups. CA1, cornu ammonis region 1; CA3, cornu ammonis region 3; DG, dentate gyrus.
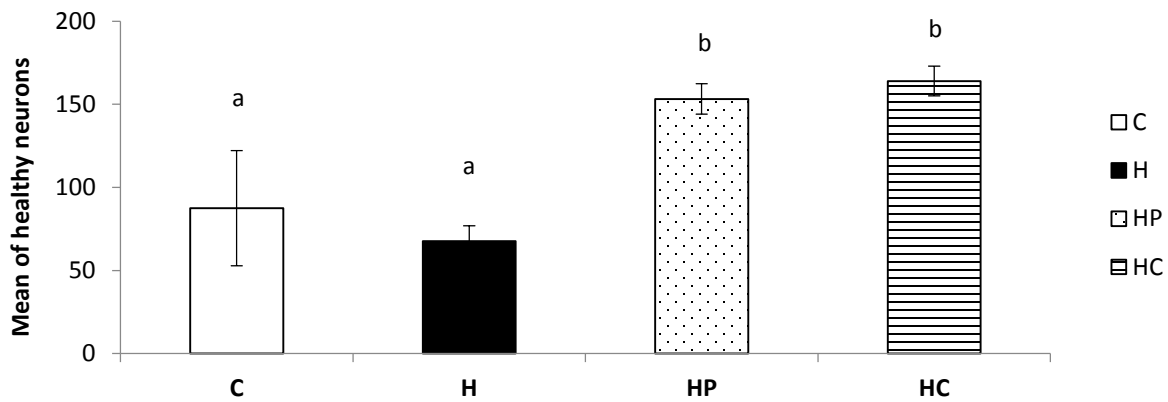
Fig.20 Quantification of the healthy neurons in the hippocampus. Comparison of the means of the number of health neurons among 4 groups (Control (C), High cholesterol (H), High cholesterol + 5% OPP (HP) and High cholesterol + 2% curcumin (HC)); a,b: the OPP fed group (HP) and the curcumin (HC) fed group had higher number of healthy neurons as compared to the control as well as high cholesterol diet group (p<0.05, n=4); Data are expressed as mean±SE.

3.5.2 Extracellular amyloid plaque deposition

Another important pathological feature of Alzheimer's disease is the formation and deposition of the amyloid plaque, which can lead to the neuron death and loss. Congo red staining was used to detect the amyloid plaques deposited in the hippocampus area. As is shown by Fig.21&22, high cholesterol diet-induced plaque formation was seen in the CA1 area as well as the DG area in all four groups, while only a few plaques were observed in the control group. A higher density of plaque deposition in the CA1 and DG areas was observed in animals from the H group as compared to those of other two treatment groups (i.e. HP and HC). In addition, amyloid load was calculated by comparing the total area occupied by the amyloid plaque to the total area of hippocampus. The high cholesterol group had the highest average plaque load (total plaque area/total hippocampus area %) compared to other two treatment group (p<0.05) (Fig. 23).
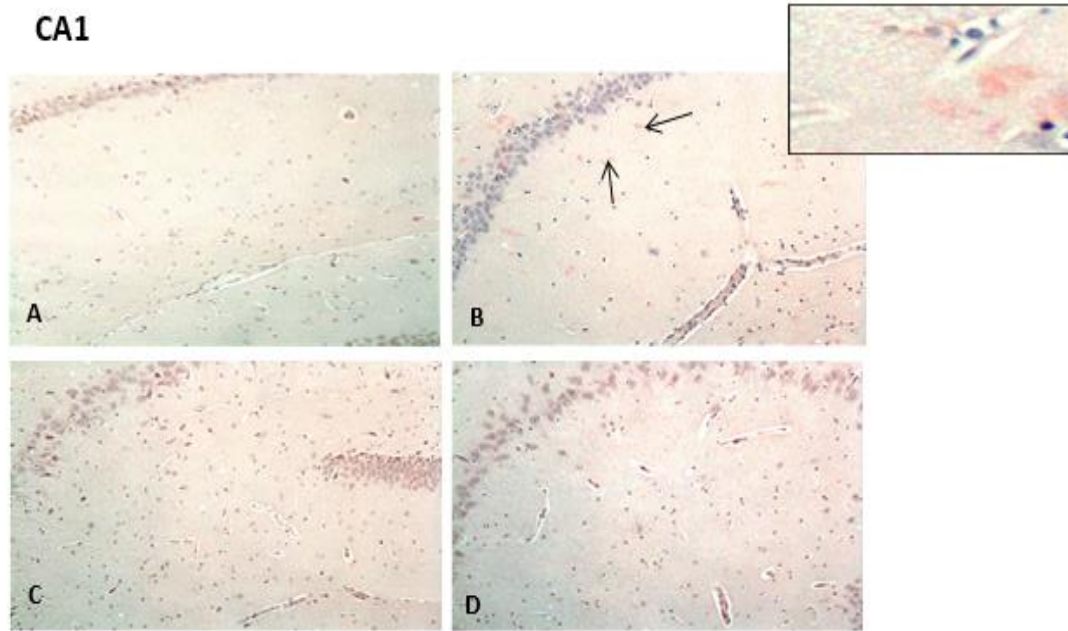
Fig.21 Effects of atherosclerotic diet and OPP treatment on histopathological changes in the hippocampus CA 1 area revealed by Congo red staining (10 x). A: The CA1 area was clean in control group (C), no plaque was detected; B: many plaques spread throughout the CA 1 area which were observed as the arrow pointed in high cholesterol group (H); C: the CA 1 was clean in high cholesterol + OPP group (HP); D: sporadic small plaques were observed in high cholesterol + curcumin group (HC).
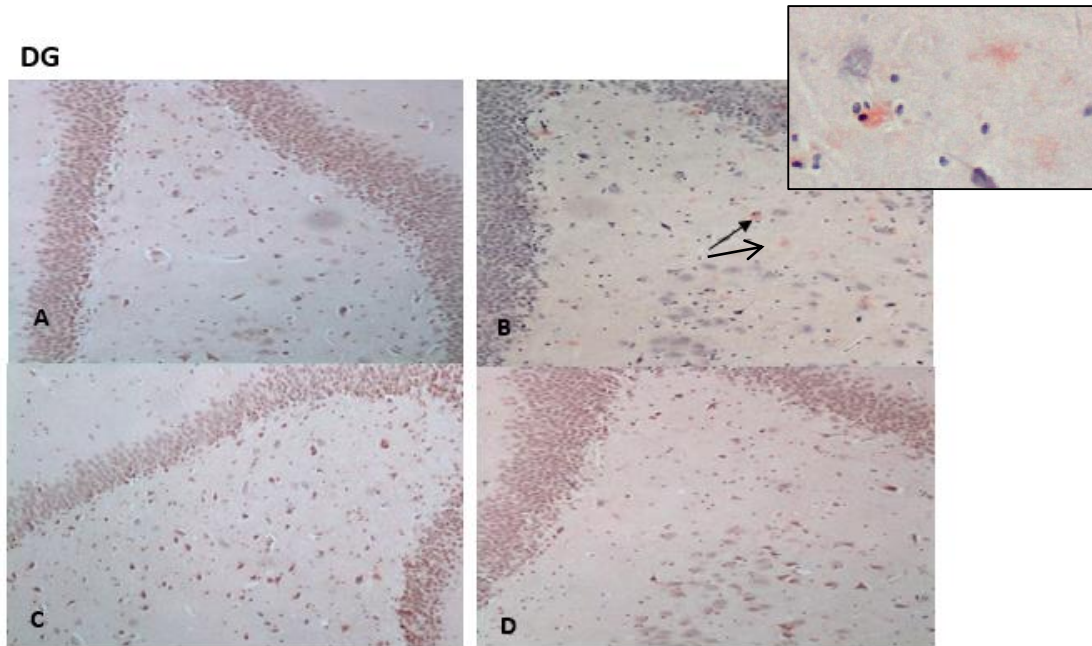
Fig.22 Effects of atherosclerotic diet and OPP treatment on histopathological changes in the hippocampus DG area revealed by Congo red staining (10 x). A: The DG area was clean in control group (C), no plaque was detected; B: many plaques were spotted throughout the DG area which were observed as the arrow pointed in high cholesterol group (H); C: the DG was clean in high cholesterol + OPP group (HP); D: sporadic small plaques were observed in high cholesterol + curcumin group (HC).
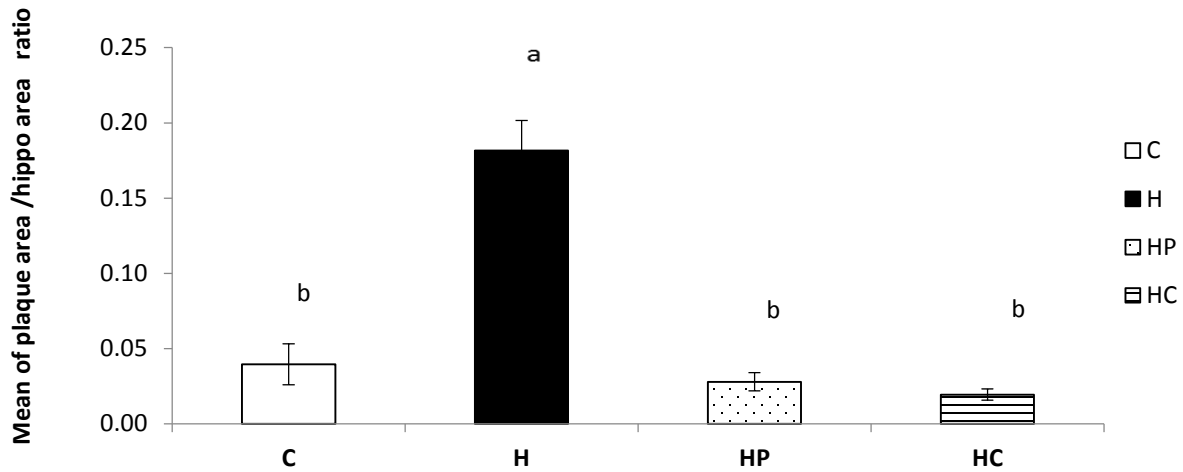
Fig.23 Amyloid plaque load in the hippocampus. Comparison of the means of the ratio between total area occupied by amyloid plaques and total hippocampus area among 4 groups; a,b: the high cholesterol diet group had highest amyloid burden and the difference is significant after comparing the H group to C, HP and HC ($p < 0.05$, n=4); Data are expressed as mean $\pm$ SE.

3.5.3 Hippocampal total β-amyloid 42 level

β-amyloid 42 is the main component of the senile amyloid plaque [82]. Therefore, we also measured β-amyloid 42 concentration in the hippocampus of rats' brain by using enzyme-linked immunosorbent assay (ELISA). The results showed the same trend as the histological changes (Fig.24); the high cholesterol group had a higher concentration as compared to other two treatment group (HP & HC) ($p < 0.05$), which explains the amyloid evidence that was observed in the histology. However, a higher level of β-amyloid 42 was also found in the control group, where no plaque deposition was seen in histology. The reason could be that more soluble amyloid peptide was produced and it was not visible under the microscope.
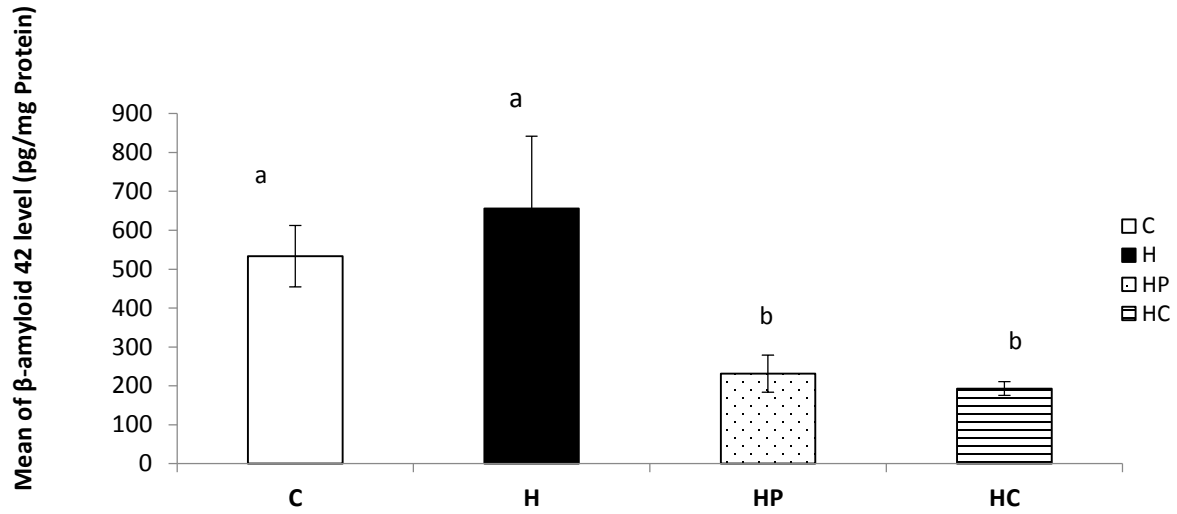
Fig.24 Total β-amyloid 42 level of hippocampus. Comparison of the means of the total β-amyloid 42 level among 4 groups (Control (C), High cholesterol (H), High cholesterol + 5% OPP (HP) and High cholesterol + 2% curcumin (HC)); both control and high cholesterol diet group had a significant higher amyloid concentration compared to the other two treatment groups; a,b: comparison of the C, H group with HP and HC ($p < 0.05$, n=4); Data are expressed as mean ± SE.

Specific Aim 2: To examine the possible mechanism of actions of OPP in AD rat model by investigating its effects on improving the lipid peroxidation, inflammation and oxidative stress induced gene expression in brain that lead to the plaque formation

3.6 Lipid Oxidation

3.6.1 MDA measurement on plasma, liver and brain tissues

It has been proposed that oxidative stress is associated with amyloid plaque, neuron loss and other AD pathological features. The phospholipid composition of neuronal membranes, such as the ratio of membrane -3 to -6 long-chain PUFAs, can be attacked by free radicals from the periphery and the CNS. The lipid peroxyl radical generated will then take a hydrogen atom from a nearby PUFA and form lipid hydroperoxide. These lipid hydroperoxides then decompose into aldehydes, ketones, and hydroxynonenal (HNE) with the help of transition metal ions [83]. As a main product of the lipid oxidation and a biomarker of the oxidative stress, we first looked at the MDA level to examine the antioxidative effect of OPP and curcumin [30]. Because the toxic aldehydes resulting from lipid peroxidation in the brain in AD can diffuse from the primary site and into the blood stream, we measured the MDA level in plasma as well as liver and brain tissue by using TBAR method. The result showed that the MDA level in plasma was increased in the animals from high cholesterol diet group. We found a significant difference between H group and C, HP and HC groups ($p<0.05$) (Fig.25). The same effect was found in the liver tissue (Fig.26), which indicates that the liver is a primary organ in the generation of oxidized lipids, which are further released into the blood circulation. Both OPP and curcumin can reduce the lipid peroxidation in the liver tissues and also lower the toxic aldehyde level in blood. However, in the brain MDA level, only the HP group is significantly lower than the H group (Fig 27). HC seems to lower the MDA, for the p value is close to 0.05 ($p=0.07$). The results indicate that both OPP and curcumin can bring down the whole brain oxidative level. However, it remains in question whether

OPP and curcumin reduce active aldehydes in blood, indirectly improving levels of brain stress or

if they directly impact the CNS.
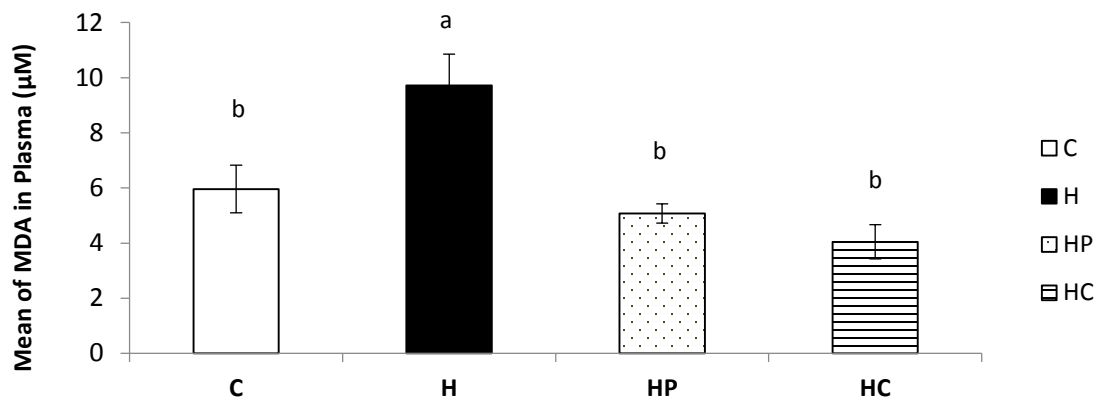
Fig. 25 Effect of atherosclerotic diet and OPP treatment on the lipid peroxidation in plasma. Comparison of the means of the MDA level (uM) among 4 groups (Control (C), High cholesterol (H), High cholesterol + 5% OPP (HP) and High cholesterol + 2% curcumin (HC)); a, b: H is significantly different from C, HP and HC ($p<0.05$). Results represent mean + SE.
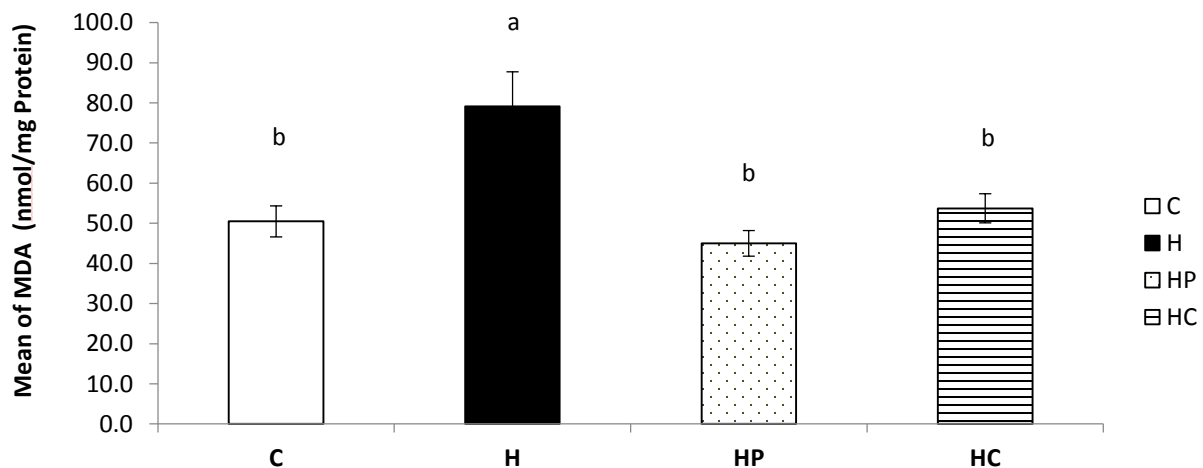
Fig.26 Effect of atherosclerotic diet and OPP treatment on the lipid peroxidation in liver tissue. Comparison of the means of the MDA level (nmol/mg tissue) among 4 groups (Control (C), High cholesterol (H), High cholesterol + 5% OPP (HP) and High cholesterol + 2% curcumin (HC)); a, b: H is significantly different from, HP and HC ($p<0.05$). Results represent mean + SE.
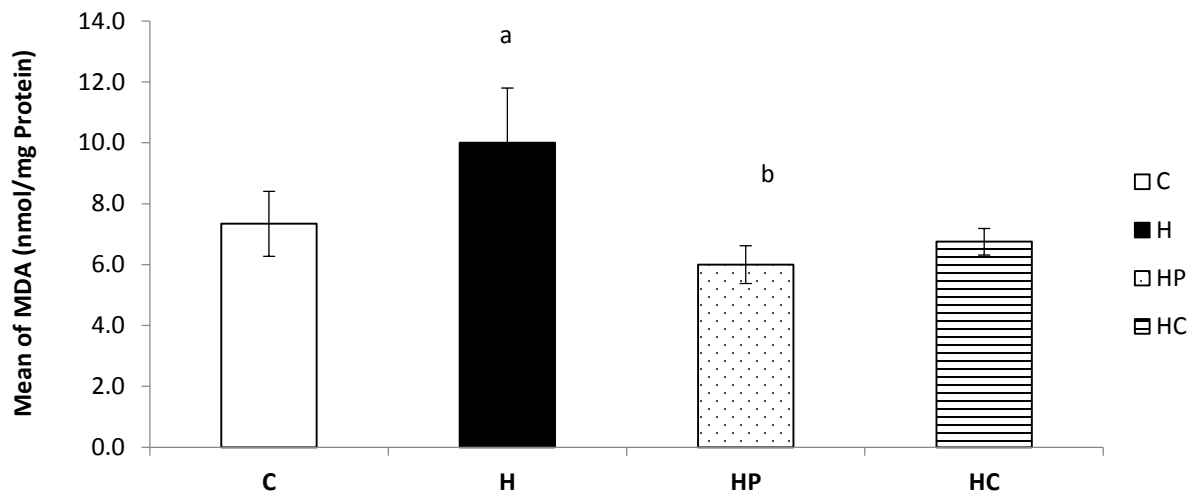
Fig.27 Effect of atherosclerotic diet and OPP treatment on the lipid peroxidation in brain tissue. Comparison of the means of the MDA level (nmol/mg tissue) among 4 groups (Control (C), High cholesterol (H), High cholesterol + 5% OPP (HP) and High cholesterol + 2% curcumin (HC)); a, b: H is significantly different from HP ($p<0.05$); no significant difference was found when compared H to C and HC group while HC show a trend that close to the significance ($p=0.07$). Results represent mean + SE.

3.6.2 Urinary ketone measurement

Ketone formation has been observed in radical termination reactions in the oxidation of fatty acids [84]. We measured the ketone concentration in rat urine samples and all results were normalized by the creatinine concentration. The results show that urinary 3-hydroxibutyrate (3HOB) was increased in the animals from high cholesterol diet group. There is a significant difference between H group and the C, HP and HC groups ($p<0.05$) (Fig.28). This further confirms the high oxidative levels in the body of the animal fed with high cholesterol diet and the antioxidant effect of OPP and curcumin at the whole body level.
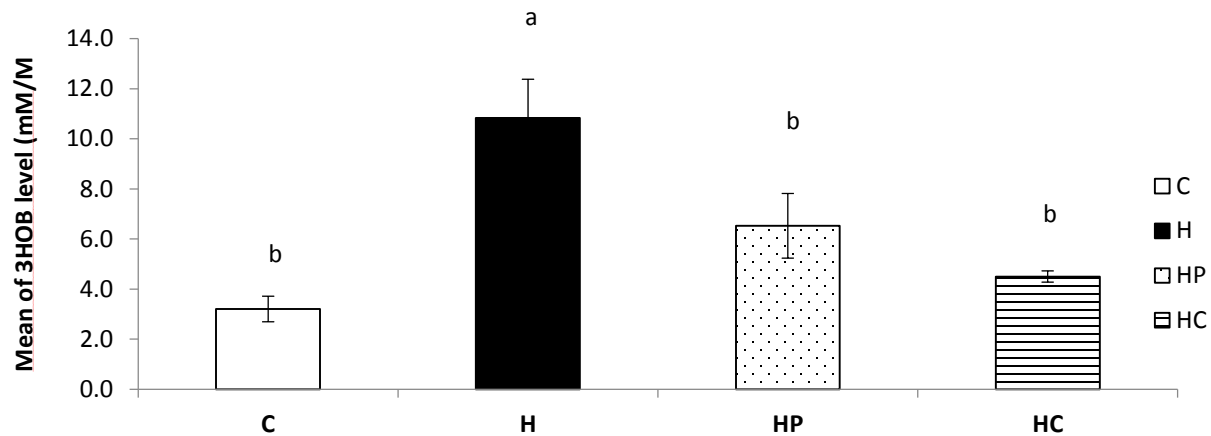
Fig. 28 Effect of atherosclerotic diet and OPP treatment on ketone formation in urine samples. Comparison of mean 3-hydroxybutyrate level (mMol/M creatinine) among 4 groups (Control (C), High cholesterol (H), High cholesterol + 5% OPP (HP) and High cholesterol + 2% curcumin (HC)); a, b: H is significantly different from C, HP and HC ($p < 0.05$); Results represent mean + SE.

3.7 Inflammation biomarker

Inflammation is another important contributor to AD pathology, as cytokines amplify the local inflammatory response and promote the progression of plaque formation. Detectable levels of circulating cytokines might be used for monitoring the progression of brain inflammation associated with AD. Interleukin-6 (IL-6), a circulating cytokine, has been identified as a marker of inflammation in chronic diseases including AD [85]. As is shown by Fig.29, the plasma IL-6 level was significantly increased in the animals on the high cholesterol diet when compared to the curcumin diet group ($p < 0.05$). Therefore, curcumin shows some impact in repression of whole body inflammation, which might also affect the CNS, as the BBB is permeable to inflammatory factors when it is damaged and has lost its integrity.
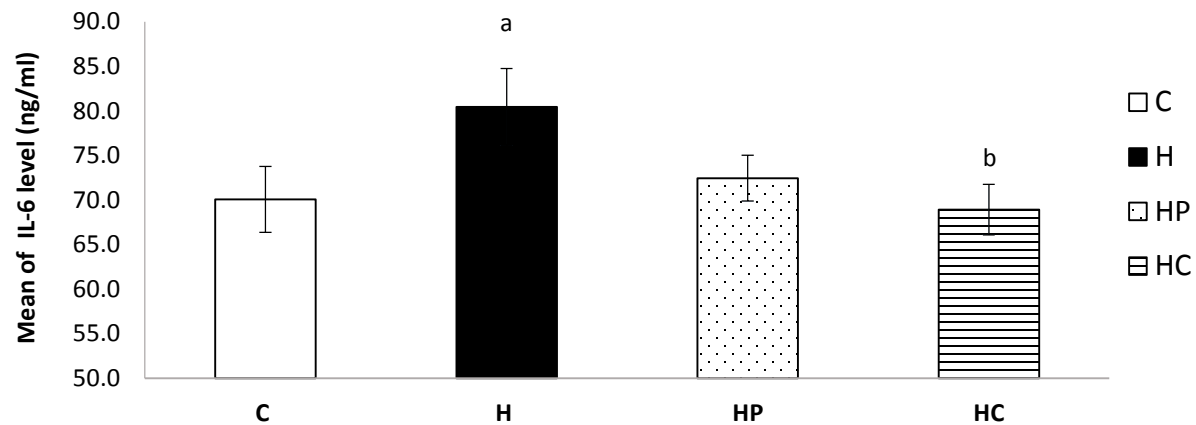
Fig.29 Effect of atherosclerotic diet and OPP treatment on plasma cytokine level.
Comparison of mean IL-6 (ng/ml) among 4 groups (Control (C), High cholesterol (H), High cholesterol + 5% OPP (HP) and High cholesterol + 2% curcumin (HC)); a, b: H is significantly different from HC ($p<0.05$); Results represent mean + SE.

3.8 Expression of the genes in brain that lead to the plaque formation

As the critical enzymes of the amyloid cascade pathway, over-expression of the APP and BACE1 genes will trigger the overproduction of the β-amyloid 42 peptides, the primary component of amyloid plaque deposition found in brain. The Apo E gene is another important gene encoding the ApoE lipoprotein. ApoE lipoprotein is the major transport protein for extracellular cholesterol and it mediates cholesterol exchange between neuronal and non-neuronal cells. Defects of homeostasis of cholesterol in brain are linked to extracellular deposition of the β amyloid 42 peptide. It has also been reported that there is a close relationship between abnormal expression of these genes, and oxidative stress, and inflammation in amyloid pathology. To test this, we measured the APP, BACE and Apo E genes expression from the hippocampus. The results showed that expression of APP gene is significantly higher in high cholesterol-fed group and the control diet group when compared to the OPP and curcumin supplement groups ($p<0.05$) (Fig 30); the same effect was observed on the expression of the BACE 1 gene (Fig 31). Therefore, OPP and curcumin can help down-regulate these two enzymes and prevent the amyloid pathway shunt

toward the plaque formation direction. The control group also had a higher gene expression, implying that aging also contributes to the plaque formation pathway. These gene expression results reflect the same trend as observed in the β-amyloid 42 level by ELISA. For ApoE, high cholesterol diet-fed animals had a significantly higher gene expression when compared to the other three groups (p<0.05) (Fig 32). This demonstrates that dietary high cholesterol can affect the normal transportation and distribution of the cholesterol in brain.
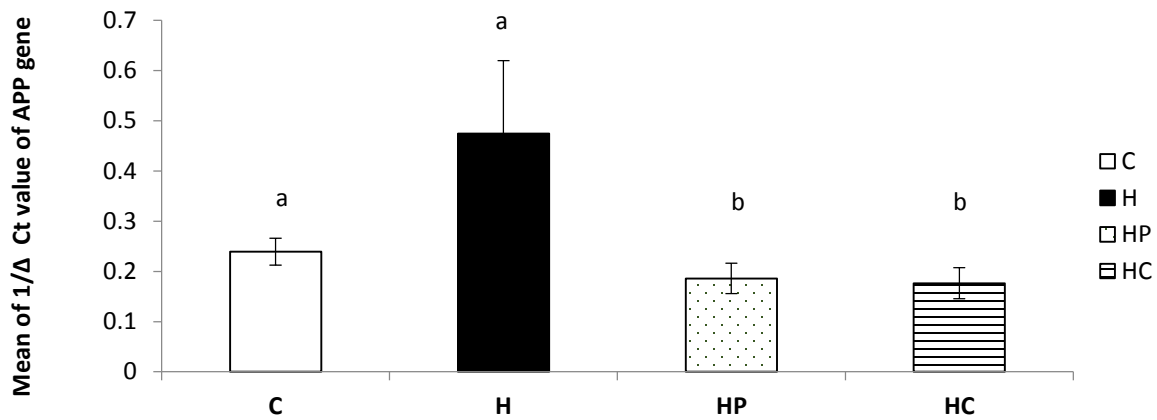
Fig.30 Hippocampus gene expression of APP gene. a,b: a significantly higher expression of APP gene in high cholesterol (H) and control (C) groups was found as compared to the high cholesterol + OPP (HP) group as well as high cholesterol + curcumin (HC) group (p<0.05);). Data are expressed as 1/ ΔCT values which was normalized against GAPDH (mean±SE).
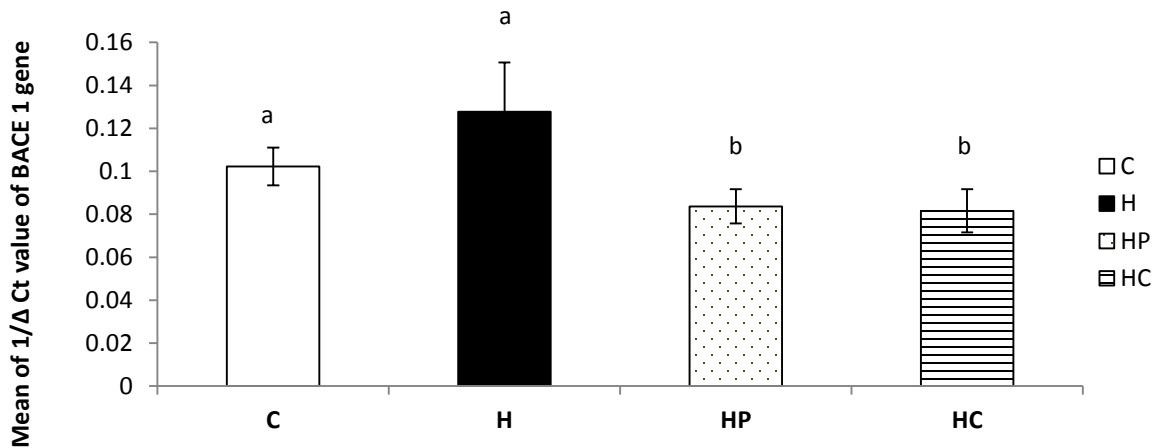
Fig.31 Hippocampus gene expression of BACE 1. a,b: a significantly higher expression of BACE 1 gene in high cholesterol (H) and control (C) groups was found as compared to the high cholesterol + OPP (HP) group as well as high cholesterol + curcumin (HC) group ($p<0.05$); Data are expressed as 1/ ΔCT values which was normalized against GAPDH (mean±SE).
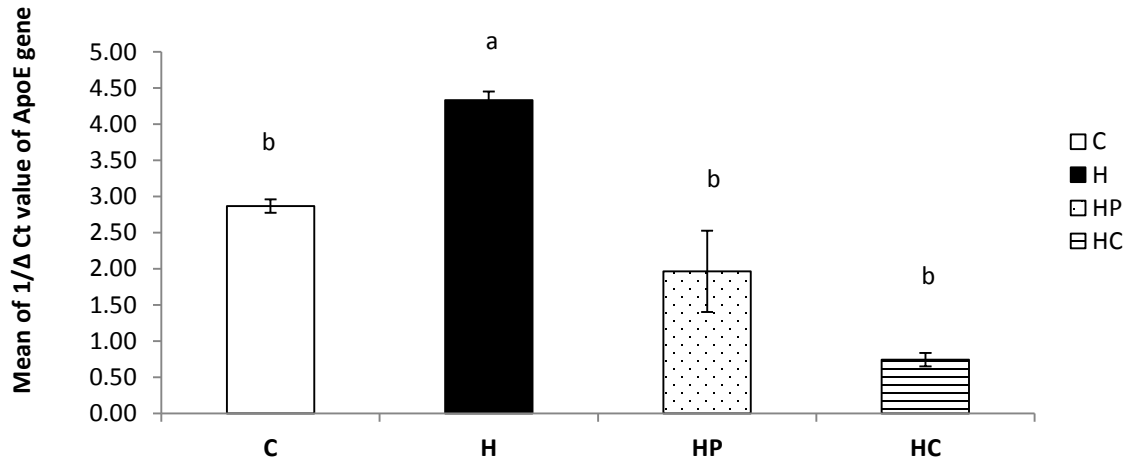
Fig.32 Hippocampus gene expression of ApoE. a,b: a significantly higher expression of ApoE gene in high cholesterol (H) was found as compared to the control (C) group, high cholesterol + OPP (HP) group as well as high cholesterol + curcumin (HC) group ($p<0.05$); Data are expressed as 1/ ΔCT values which was normalized against GAPDH (mean±SE).

Specific Aim 3: To identify changes in urinary metabolomics profile and the metabolites altered in AD for pathway exploration

3.9 Exploration of the time-course changes in the urinary ¹H NMR metabolomic profiles of four groups

Differences in the metabolomic profiles of these aging rats subjected to different diets (standard control diet, 2% high cholesterol diet, 2% high cholesterol diet+5% OPP diet, 2% high cholesterol diet+2% curcumin diet) in this study were evaluated using proton nuclear magnetic resonance spectroscopy, ¹H NMR. Spectra separation or discrimination analysis was carried out using SIMCA-P+ software, utilizing both unsupervised (PCA) and supervised techniques (PLS-DA). We aimed to find possible distinctions in urinary metabolomic profiles by comparing four groups at three different timepoints. We began our analysis with an unsupervised principal component analysis (PCA) which provided a basic overview of the similarities and differences in the metabolomics profiles of groups of animals on different diets. The PCA score plot in Fig. 33 A shows there is no clear separation among four groups at the baseline (week 0), indicating all animals arrived at the same level of health. Next, using the supervised technique, a PLS-DA score plot confirmed what was observed on the PCA plot: no separation among the four groups (Fig. 33 B). At the intermediate timepoint (week 12), the PCA score plot showed a separation of the urinary NMR spectra of control diet animals from the other three high cholesterol diet groups (Fig 34 A). The curcumin supplement group was also well separated from the other groups and OPP began to separate from the high cholesterol diet group. The clear separation was also obvious in the supervised PLSDA score plot as shown in Fig.34 B. As depicted by the diagram, the four groups are clearly separated along the principal component 1 (t1). The principal component 1 (t1) accounts for the most variation in the data and the subsequent component (t2) accounts for the second most

variation in the data. The control group was well separated from the other three high cholesterol diet groups, reflecting the effects of the hypercholesterolemia; the curcumin group has already become well separated from high cholesterol group at week 12, showing an influence the curcumin supplement on the higher cholesterol diet. Animals from the OPP group are clustered between the high cholesterol and curcumin groups on the diagram. This may indicate the start of a trend, where the OPP group separated from the high cholesterol diet group at that time point.

The corresponding loading plot in Fig. 34 C illustrates the regions in the spectra comprising metabolites that are influential in the separation of the four groups. The regions of variables that are responsible for the separation of control group are seen at ppm 3.02-3.42, 2.5-2.6; the regions of the variable that separated the curcumin group are 7.2-7.4. At the endpoint (week 20), the high cholesterol diet group was clearly separated from the other three groups, as is shown by the PCA score plot in Fig.35 A. The OPP group and curcumin group are clustered together while also being pulled closer toward the control diet group as the feeding trial proceeded. Using the supervised technique, PLS-DA score plot showed a more pronounced separation between the high cholesterol diet group and other three groups (Fig. 35 B). Class discrimination of the supervised method improved the transparency and interpretability of the model. Therefore, OPP were more influential when the study was approaching its end. The PCA loading plot reveals the regions in the spectra that separated out the high cholesterol-diet group, including 3.5-3.9, 3.04-3.06, 4.33-4.35,4.03-4.05; the regions of spectra responsible for separation of OPP and curcumin are 2.65-2.67, 7.2-7.3 (Fig. 35 C).
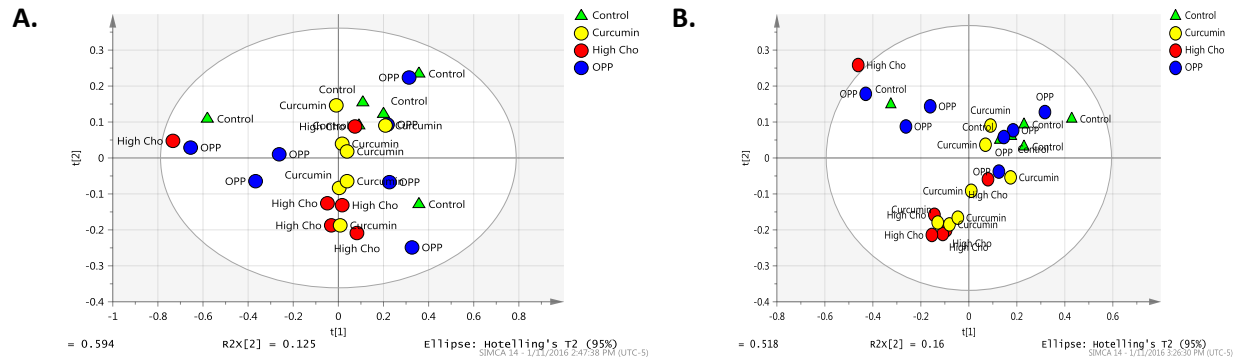
Fig.33 Multivariate analysis of all four groups at baseline (Week0). (**A**) The unsupervised method, PCA score plot based on urinary ^{1}H NMR spectra of rats of four groups with control (Control), high cholesterol (High Cho), high cholesterol + OPP(OPP), high cholesterol +curcumin (Curcumin) at study baseline. (**B**) The supervised method, PLSDA score plot based on urinary ^{1}H NMR spectra of rats of four groups at study baseline. There is no significant difference in the urinary metabolomics profile of rats from either of the four groups at baseline.
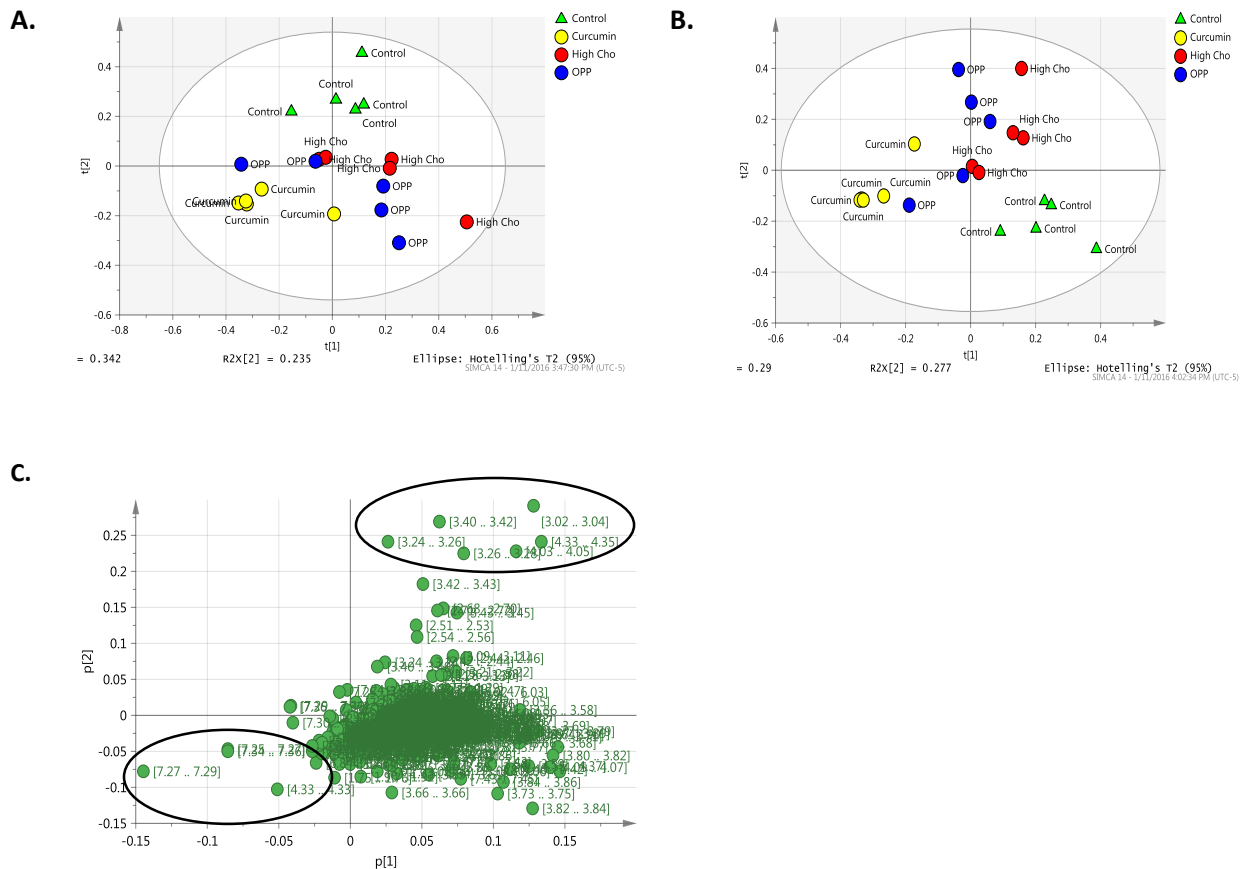
Fig.34 Multivariate analysis of four groups at intermediate time point (Week12). (**A**) The unsupervised PCA score plot based on urinary ^{1}H NMR spectra of rats of four groups with control(Control), high cholesterol (High Cho), high cholesterol + OPP(OPP), high cholesterol + curcumin (Curcumin) at intermediate timepoint. **(B)** The supervised method, PLSDA score plot based on urinary ^{1}H NMR spectra of rats of four groups at intermediate time point. **(C)** Corresponding loading plot manifesting the regions in the spectra comprising metabolites that are influential in the separation of the four groups. Control and curcumin groups were well separated from high cholesterol and high cholesterol + OPP groups in the urinary metabolomics profile of rats at week 12.

Fig.35 Multivariate analysis of four groups at endpoint (Week20). (**A**) The unsupervised PCA score plot based on urinary ^{1}H NMR spectra of rats of four groups with control (Control), high cholesterol (High Cho), high cholesterol + OPP(OPP), high cholesterol + curcumin (Curcumin) at intermediate timepoint. (**B**) The supervised method, PLSDA score plot base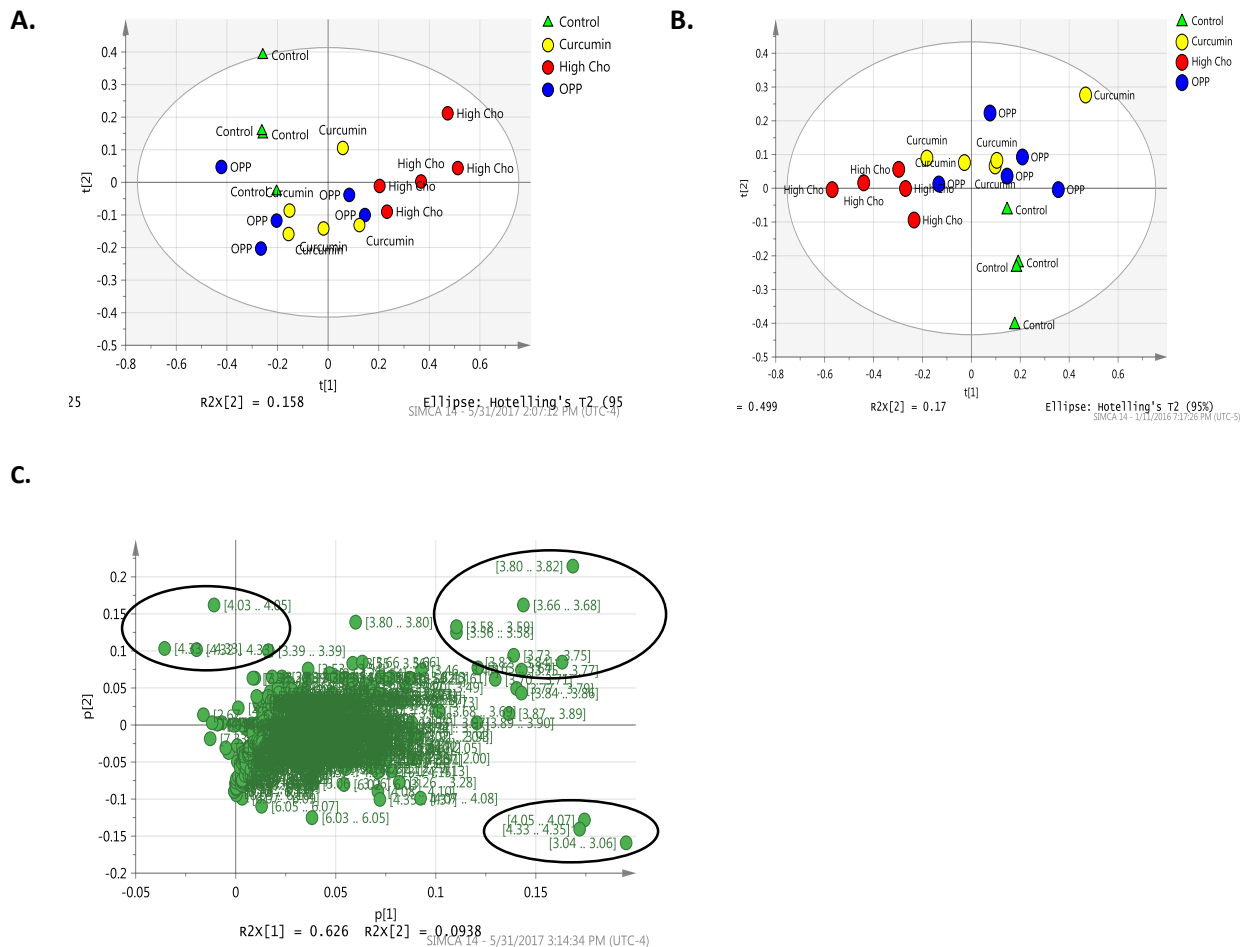d on urinary ^{1}H NMR spectra of rats of four groups at endpoint. (**C**) Corresponding loading plot manifesting the regions in the spectra comprising metabolites that are influential in the separation of the four groups. Control and high cholesterol groups were well separated from other two treatment groups in the urinary metabolomics profile of rats at week 20.

3.10 Regression analysis

The relationship between urinary metabolite profiles and variables related to AD progression including spatial learning ability (Escape Latency), hippocampal βamyloid 42 concentration, brain oxidative stress, and peripheral inflammation (IL-6) was measured by regression analysis. As seen from Fig.36 A, an OPLS regression plot shows a weak correlation (R^2=0.2384) between escape latency (EL) with urinary 1H NMR profiles of the four groups at baseline (week 0) and a high correlation (R^2=0.7956) at endpoint (week 20)(Fig.36 B). Fig.36 C shows the S-plot obtained from OPLS model at endpoint, which indicates the regions of the metabolites that are respectively positively and negatively correlated with EL. Regions of the spectra on the upper right side including 4.05,4.07,4.35,4.37,7.4,7.5,3.04,3.06 are metabolites positively correlated with the EL and those on the lower left side including 7.34,7.36,7.13,7.14 are metabolites negatively correlated with EL. Similar regression analysis on the hippocampus βAmyloid 42 concentration also revealed a strong correlation with urinary NMR profiles (R^2=0.7406) at endpoint (week 20) and a weak correlation at baseline (R^2=0.3076) (Fig.37 A&B). An S-plot of the OPLS score plot at the endpoint shows the regions (upper right and left lower side) of the metabolites which could be potential biomarkers of βAmyloid 42 accumulation. The metabolites that are positively correlated with amyloid level are located at 2.56, 2.71, 2.72, 3.24, 3.25, 4.03, 4.05 and those negatively correlated with amyloid levels are found at 7.4, 7.3 and 2.84 (Fig.37 C). As to the correlation of urinary NMR profile with peripheral and CNS oxidative stress, both correlations show a moderate-to-high R^2 value: 0.6008 for IL-6 (Fig.39 B) and 0.6665 for MDA level (Fig. 38 B) at the endpoint as compared to the weak correlation at baseline: R^2=0.3526 for IL-6 (Fig. 39 A) and R^2=0.2925 for MDA (Fig. 38 A). The regions circled in the S-plots also show the location of metabolites that are involved in inflammation (Fig.39 C) and lipid oxidation (Fig.38 C). Having observed that

urinary metabolomic profiles of the animals with high cholesterol diet-induced AD correlated well with escape latency and β amyloid concentration, we then used the Chenomx software to identify and quantify the metabolites that are indicated by the S-plot, which will be discussed in next section. These could potentially be evaluated as noninvasive biomarkers of AD progression.

A.
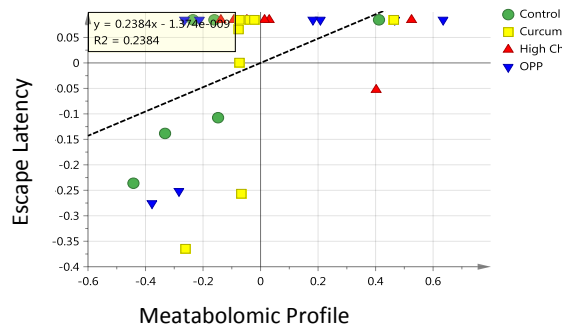
B.
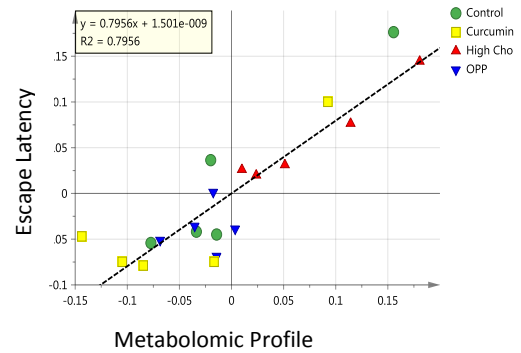
C.
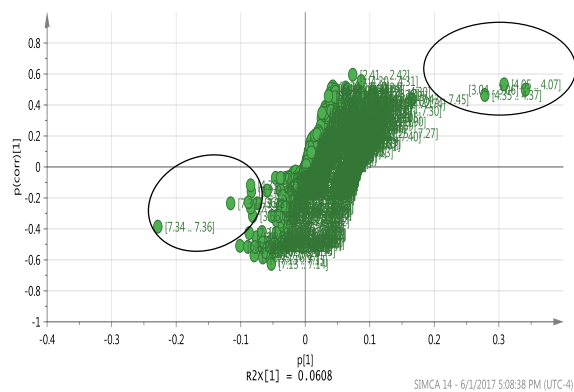
Fig.36 OPLS regression of escape latency (EL) with urinary ^{1}H NMR profiles of the four groups at two time point. (**A**) OPLS score shows a weak correlation (R^2=0.2384) at baseline (week 0). (**B**) OPLS score plot shows a high correlation (R2=0.7956) at endpoint (week 20). (**C**) S-plot obtained from OPLS model at week 20. The circle on the upper right side includes the regions of metabolites in the spectra that is correlated with higher EL; Regions containing regions of the metabolites are circled at lower left side are correlate with shorter EL.
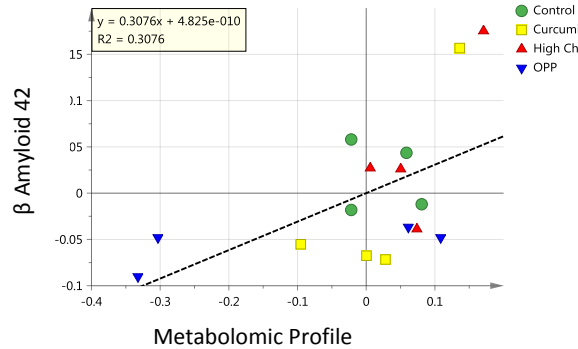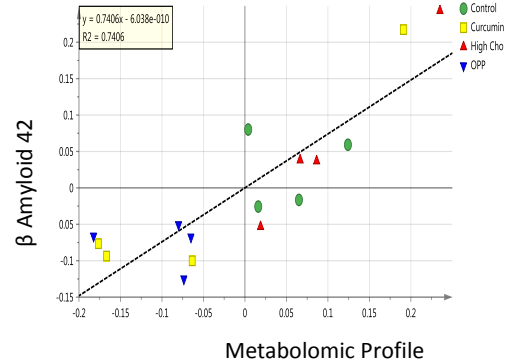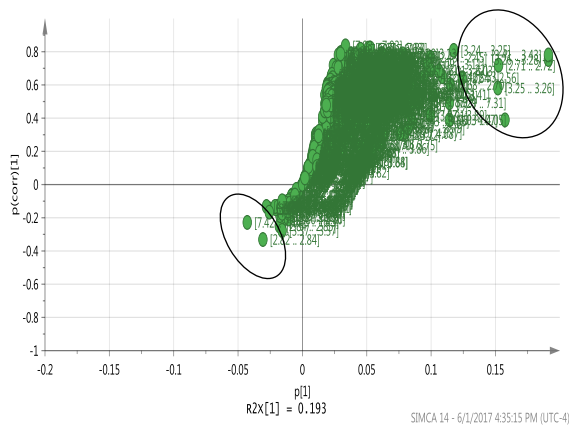
Fig.37 OPLS regression of hippocampus βAmyloid 42 concentration with urinary ^{1}H NMR profiles of the four groups at two time point. (**A**) OPLS score shows a weak correlation (R^2=0.3076) at baseline (week 0). (**B**) OPLS score plot shows a high correlation (R^2=0.7406) at endpoint (week 20). (**C**) S-plot obtained from OPLS model at week20. The circle on the upper right side includes the regions of metabolites in the spectra that is correlated with higher βAmyloid 42 concentration; Regions containing regions of the metabolites are circled at lower left side are correlated with lower βAmyloid 42 concentration.

A.
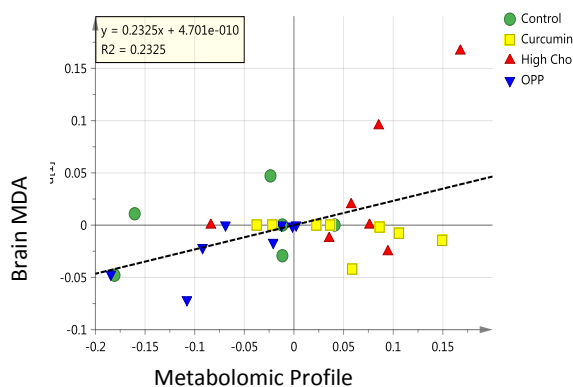
B.
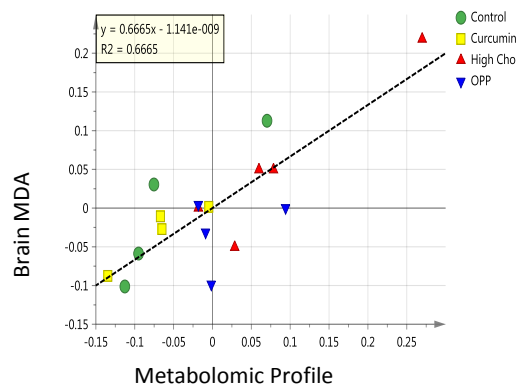
C.
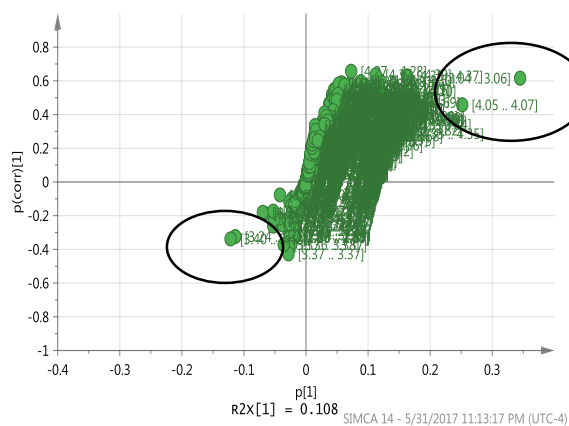
Fig.38 OPLS regression of brain oxidative stress level (MDA) with urinary ^{1}H NMR profiles of the four groups at two time point. (**A**) OPLS score shows a weak correlation (R^2=02925) at baseline (week 0). (**B**) OPLS score plot shows a moderate-high correlation (R^2=0.6665) at endpoint (week 20). (**C**) S-plot obtained from OPLS model at week 20. The circle on the upper right side includes the regions of metabolites in the spectra that is correlated with higher MDA level; Regions containing regions of the metabolites are circled at lower left side are correlated with lower MDA level.

A.
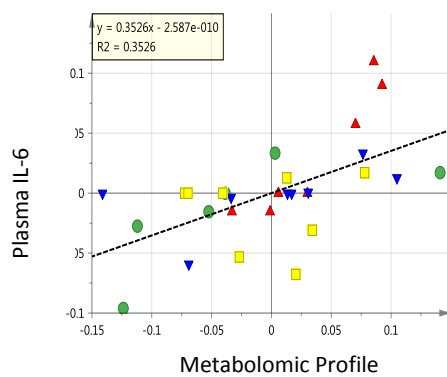
B
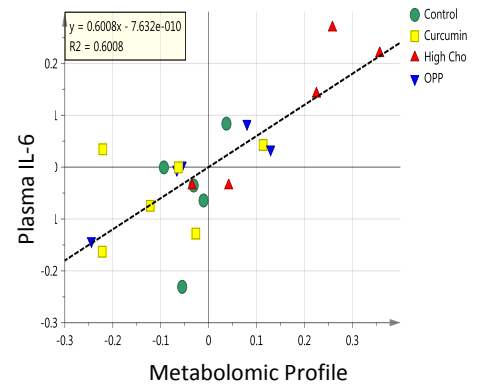
C.
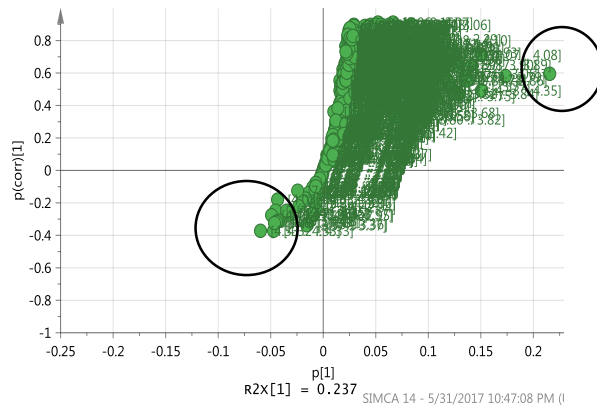
Fig.39 OPLS regression of plasma inflammation level (IL-6) with urinary ^{1}H NMR profiles of the four groups at two time point. (**A**) OPLS score shows a weak correlation (R^2=0.3526) at baseline (week 0). (**B**) OPLS score plot shows a moderate-high correlation (R^2=0.6008) at endpoint (week 20). (**C**) S-plot obtained from OPLS model at week 20. The circle on the upper right side includes the regions of metabolites in the spectra that is correlated with higher IL-6 level; Regions containing regions of the metabolites are circled at lower left side are correlated with lower IL-6 level.

3.11 Identification and quantification of metabolite as a potential biomarker and pathway exploration

The Chenomx NMR Suite software (Chenomx Inc., Edmonton, Canada) was used to identify and quantify the metabolites responsible for separation observed in the PCA, PLS-DA and OPLS score plots. Metabolites were identified and measured for their concentrations by fitting the spectral peaks found for each compound in the compound library. Then, the concentrations of metabolites were subjected to an ANOVA test (SPSS Inc. Chicago, IL) for comparison of the concentration changes among the four groups. A post-hoc test was also run to observe the differences within the groups. Details about the metabolites with significant differences in concentration are shown in Table 4. To further confirm the changes in concentration, we subjected our data to MetaboAnalysis 3.0, an online data analysis software. All metabolites represented above the 0.05 threshold line in that software are considered to be significantly different (Fig.40). The results from MetaboAnalysis corroborated results from the Chenomx software, so metabolites found significantly different were subject to pathway analysis. Impacted pathways and networks analysis and their statistics are shown in Figure 41 and Table 5. The key aberrant pathways identified through this process include Tryptophan metabolism, Tyrosine metabolism, Ketone bodies synthesis and degradation, Butanoate metabolism, Taurine and hypotaurine metabolism, Methane metabolism, Glutathione metabolism, and Citrate cycle. The metabolites associated with individual pathways and their concentrations are shown in the figures below (Fig.42-44). Significant decreases ($p<0.05$) in concentration of tryptophan, 3-hydroxykynurenine, quinolinic acid were found in HP and HC groups when compared to the high cholesterol group (Fig 42 A-D). In addition, the concentration of serotonin, 5-hydroxytryptophan and melatonin was significantly higher in HC

when compared to the other three groups (p<0.05, Fig 42 F-H). Meanwhile, as shown in Fig.43 (A, B, C), it was observed that when subjects were given a high cholesterol diet, ketone bodies and ketone metabolite (2-oxoglutarate) were higher than the control group. These effects were brought down to a similar level as control group with intervention of OPP as well as curcumin supplements, which implies an antioxidant effect on lipids in the rats on a high cholesterol diet.

Urinary concentration of serine was also found to be significantly higher in the high cholesterol diet group as compared to the control group (Fig.43 D). The HC groups were found to be significantly higher in tyrosine concentration, while a lower level of homogentisate was found in both HP and HC groups (p<0.05. Fig 44 A&B).   Taurine concentration was significantly higher in the control group as compared to the other three groups (p<0.05, Fig 44 C). A higher citrate level was found in control group after being compared to the HP and HC groups (p<0.05, Fig.44 D). The HP and HC groups had lower levels of trimethylamine and allantoin than high cholesterol group (p<0.05, Fig 44 E&G) and the group subjected to intervention with curcumin (HC) was found have lower level of homocysteine (p<0.05, Fig 44 F). As these results indicate, some metabolites from tryptophan metabolism were significantly higher in the cholesterol fed animals as compared to the control. Because this pathway has been shown to be involved in neurodegenerative diseases [86], we investigated it in further detail. The effects of treatment with OPP or curcumin on the concentration of these metabolites are shown in Figure 45.

Table 4. Concentration of metabolites with significant change in the metabolomic profile measured by Chenomx and compared by using ANOVA and post hoc test

Compounds	NMR Chemical shift (ppm)	P value	Fisher's LSD post-hoc
Kynurenate	7.0 7.3 7.6 7.8 8.2	<0.01	HC - C; HC - H; HC - OPP
2-Oxoglutarate	4.0 2.3 2.2 2.0 1.8	<0.01	C- HC; C - HP; H - HC; H - HP
3-Hydroxykynurenine	7.5 7.0 6.7 4.1 3.7	<0.01	H - C; H - HC; HC-HP
Melatonin		<0.01	HC - C; HC - H; HC - HP
5-Hydroxytryptophan	10, 7.4,7.3,7.1,6.9 4.0,3.4 3.2	0.01	HC- C; HC - H; HC – HP
Urea	5.8	<0.01	C - HC; C - H; C - HP
Quinolinate	7.5 8.0	<0.01	H - C; H - HC; H - HP
4-Hydroxyphenylacetate	7.2 6.9 3.4	<0.01	HC - C; HC - H; HC - HP
Catechol	6.9 7.0	<0.01	HC - C; HC - H; HC - HP
dTTP	1.9 2.4 4.2 4.6 6.3 7.7	<0.01	HC - C; HP - C; HC - H
Phenol	7.0 7.3 6.9	<0.01	HC - C; HC - H; HC - HP
Acetoacetate	2.3 3.4	0.02	H - C; H - HC; H - HP
Riboflavin	2.5 2.6 3.7 3.9 4.0 4.4 5.0 8.0	0.02	C - H; C - HP
Taurine	3.2 3.4	0.02	C - HC; C - H; C - HP
Allantoin	8.0 7.3 6.0 5.4	0.02	H - C; H - HC; H - HP
Citrate	2.7 2.5	0.03	C - HC; C - HP
Tryptophan	3.3 3.5 4.1 7.2 7.3 7.5 7.7	0.03	C - H; HC - H; HP - H
Serotonin	3.1 3.3 6.9 7.1 7.3 7.4 10	0.03	HC - C; HC - H
Homoserine	2.0 2.2 3.8 3.9	0.03	HC - C; HC - H; HC - HP
Phthalate	7.5	0.03	HC - C; HC - HP

Theophylline	8.0 3.6 3.4	0.03	HC - C; HC - H; HC - HP
Tyrosine	7.2 6.9 3.9 3.2 3	0.03	HC - C; HC - H
Ethanolamine	3.1 3.8	0.03	C - HC; H - HC; H - HP
N-Phenylacetylglycine	3.7 7.3 7.4 7.9	0.04	HC - C; HC - H; HC - HP
Homocysteine	2.2 2.3 2.8 2.9 3.9	0.04	H - C; H - HC
3-hydroxybutyrate	1.2 2.3 2.4 4.1	0.04	H - C; H - HC; H - HP
Trimethylamine	2.9	0.04	H - HC; H - HP
Gentisate	6.8 7.0 7.3	0.04	H - C; H - HC; H - HP
Serine	4.0 3.9 3.8	0.04	H - C
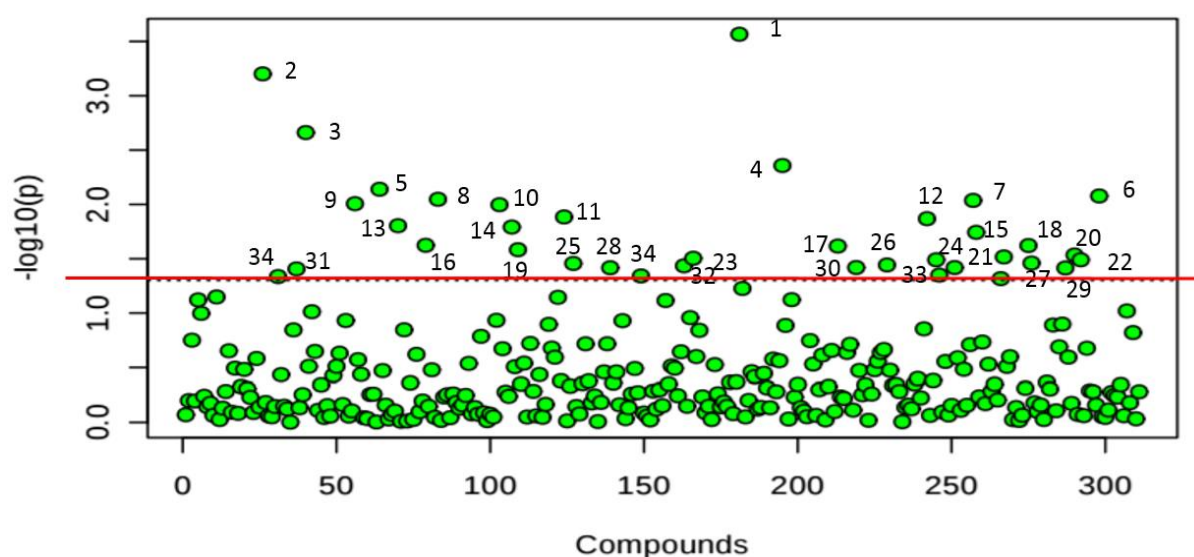
Fig .40 Manhattan Plot (A) based on Chenomx measured with MetaboAnalyst 3.0 software. The concentrations of all the metabolites measured by Chenomx was subjected to MetaboAnalyst 3.0 software. The red line represents 0.05 threshold. Metabolites with significant difference were labeled in number above the threshold. The p values are transformed by -log10 so that the more significant features (with smaller p values) is plotted higher on the graph. 1 – Kynurenate; 2 - 2-Oxoglutarate; 3 -3-Hydroxykynurenine; 4-Melatonin; 5- 5-Hydroxytryptophan; 6 - Urea; 7 -Quinolinate; 8 - 4-Hydroxyphenylacetate; 9 - Catechol; 10 - Anthranilate; 11 - dTTP; 12- Phenol; 13 – Acetoacetate; 14- Riboflavin; 15 - Taurine; 16 - Allantoin; 17 - Citrate; 18 - Tryptophan; 19-Serotonin; 20 - Homoserine; 21 – Phthalate; 22 - Theophylline; 23 - Tyrosine; 24 - Ethanolamine; 25 - N-Phenylacetylglycine; 26 -

Homocysteine; 27 - 3-hydroxybutyrate; 28 - Trimethylamine; 29 - Gentisate ; 30 - Serine; 31- ;31 - N Acetylserotonine; 32 - Glutathione ; 33 - Gentisate ; 34 - Tartrate ;
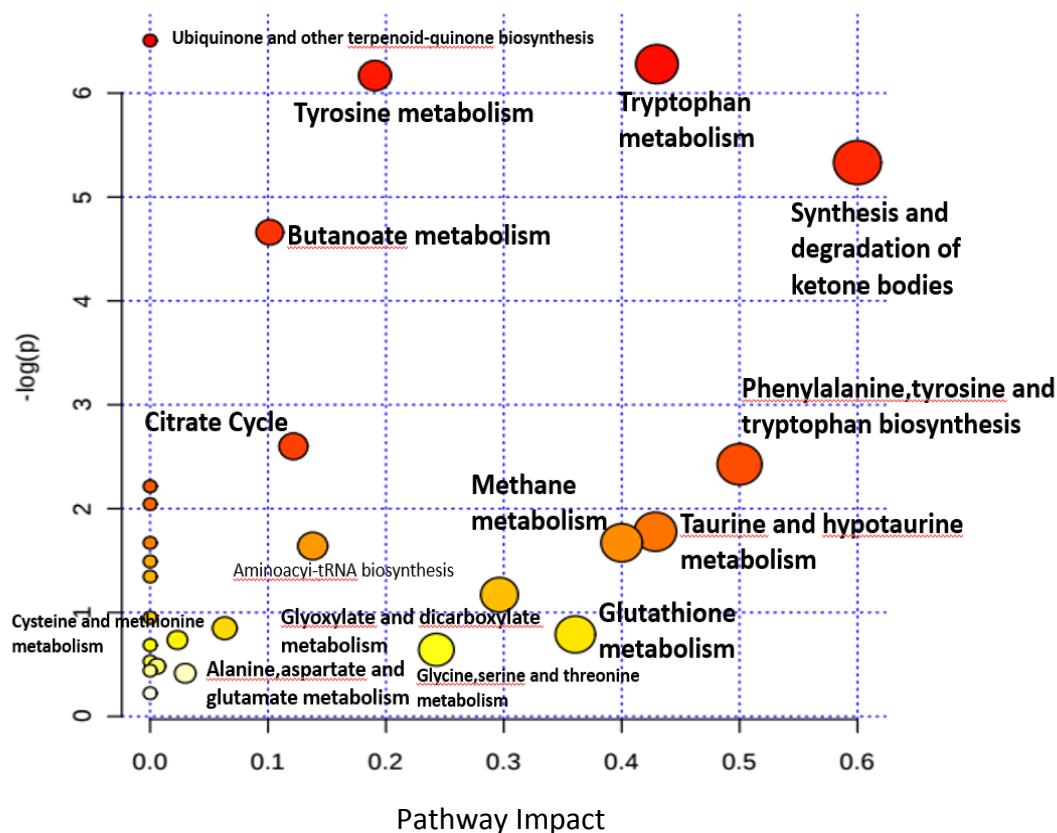
Fig 41. Pathway analysis by MetaboAnalyst 3.0 software. MetaboAnalyst 3.0 output illustrating the most predominant metabolic pathways that correspond to the significant metabolites changed in the urinary metabolomic profiles. The larger a circle and higher on the y axis, the higher impact of pathway.

Table 5. Pathways with the highest impact analyzed by MetaboAnalyst 3.0.

Pathway name	Hits	p-value	–log(p)	Impact
Tryptophan metabolism	5	0.001874	6.2794	0.42989
Tyrosine metabolism	5	0.0020934	6.169	0.19071
Synthesis and degradation of ketone bodies	2	0.0048373	5.3314	0.6
Butanoate metabolism	3	0.0094628	4.6604	0.10145

Metabolites with the most significant difference in the urinary metabolomic profile were subjected to MetaboAnalyst 3.0 for pathway analysis. MetaboAnalyst 3.0 identified highly significant pathways these metabolites involved ($p<0.01$); log-transformed values of p-value reflects the same trend with the significance of the pathway. The pathway with the highest impact has the highest -log (p) value.
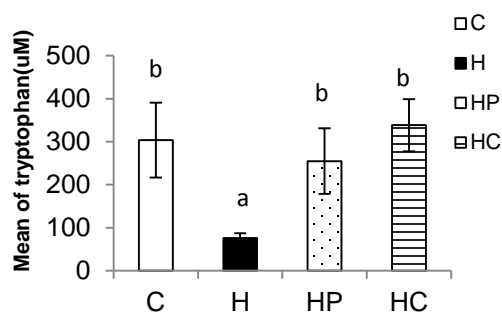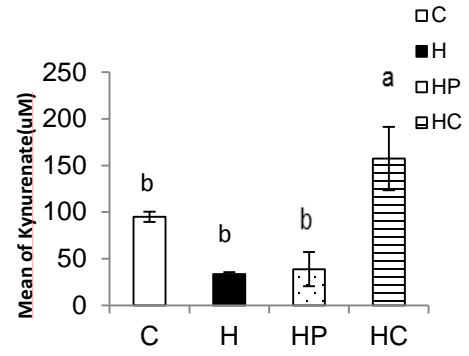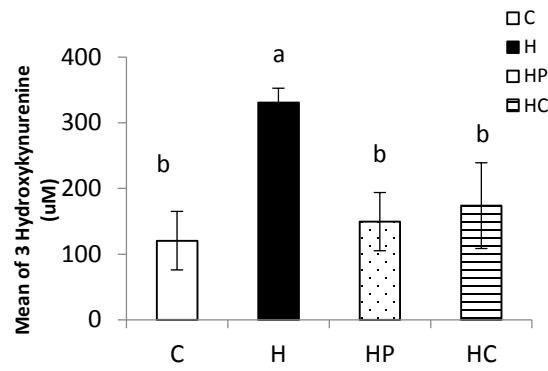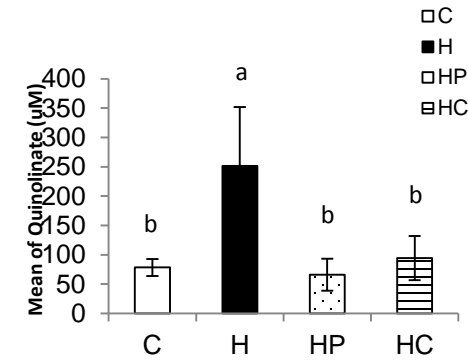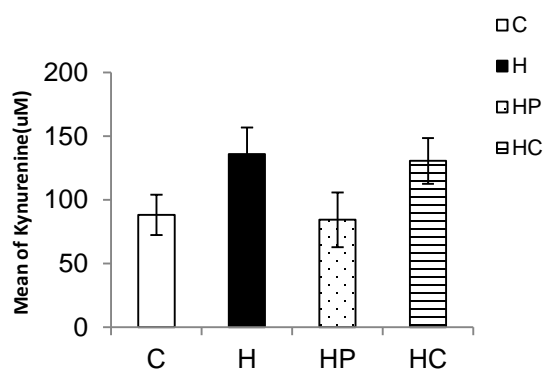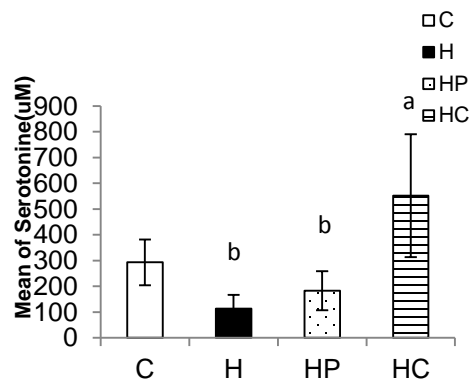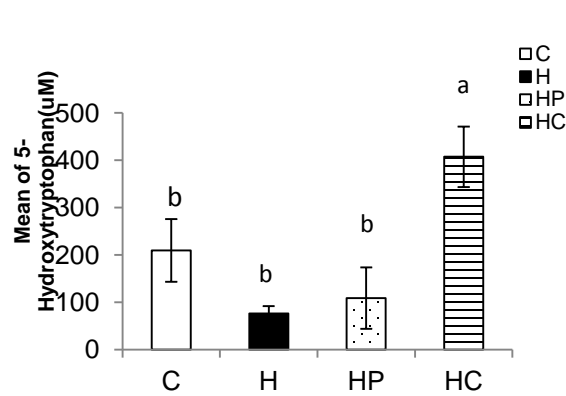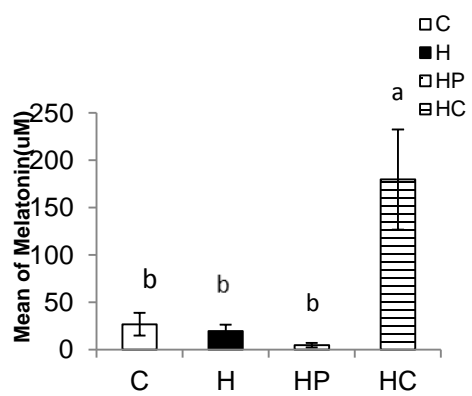
Fig.42 Selected urinary metabolites associated with the diet effect found in Tryptophan metabolism by the pathway analysis . Urinary metabolites identified to be significantly lowered at $p<0.05$ (detail see Table 4) when comparing the four groups.
 (A) Tryptophan; (B)Kynurenate; (C) 3 Hydroxykynurenine (D) Quinolinate
(E) Kynurenine (F) Serotonin (G) 5-Hydroxytryptophan (H) Melatonin. Data are expressed as mean±SE.
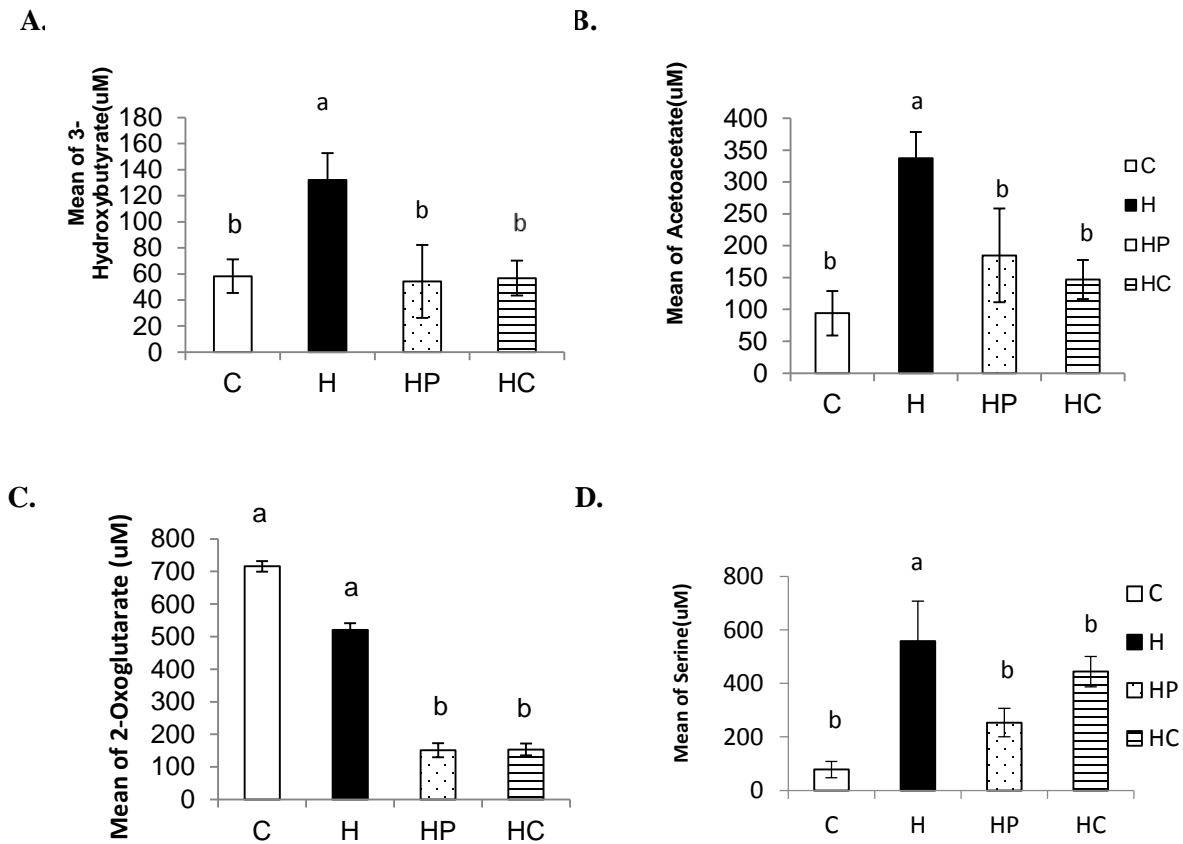
Fig.43 Selected urinary metabolites associated with diet effect found in ketone pathway, butanoate pathway and methane pathway by the pathway analysis. Urinary metabolites identified to be significantly lowered at $p<0.05$ (detail see Table 4) when comparing the four groups. (A) 3 hydroxybutyrate; (B) Acetoacetate; (C) 2 oxoglutarate (D) Serine. Data are expressed as mean±SE. (A), (B) were found in ketone pathway and butanoate pathway; (C) was found in butanoate pathway; (D) was found in methane pathway.
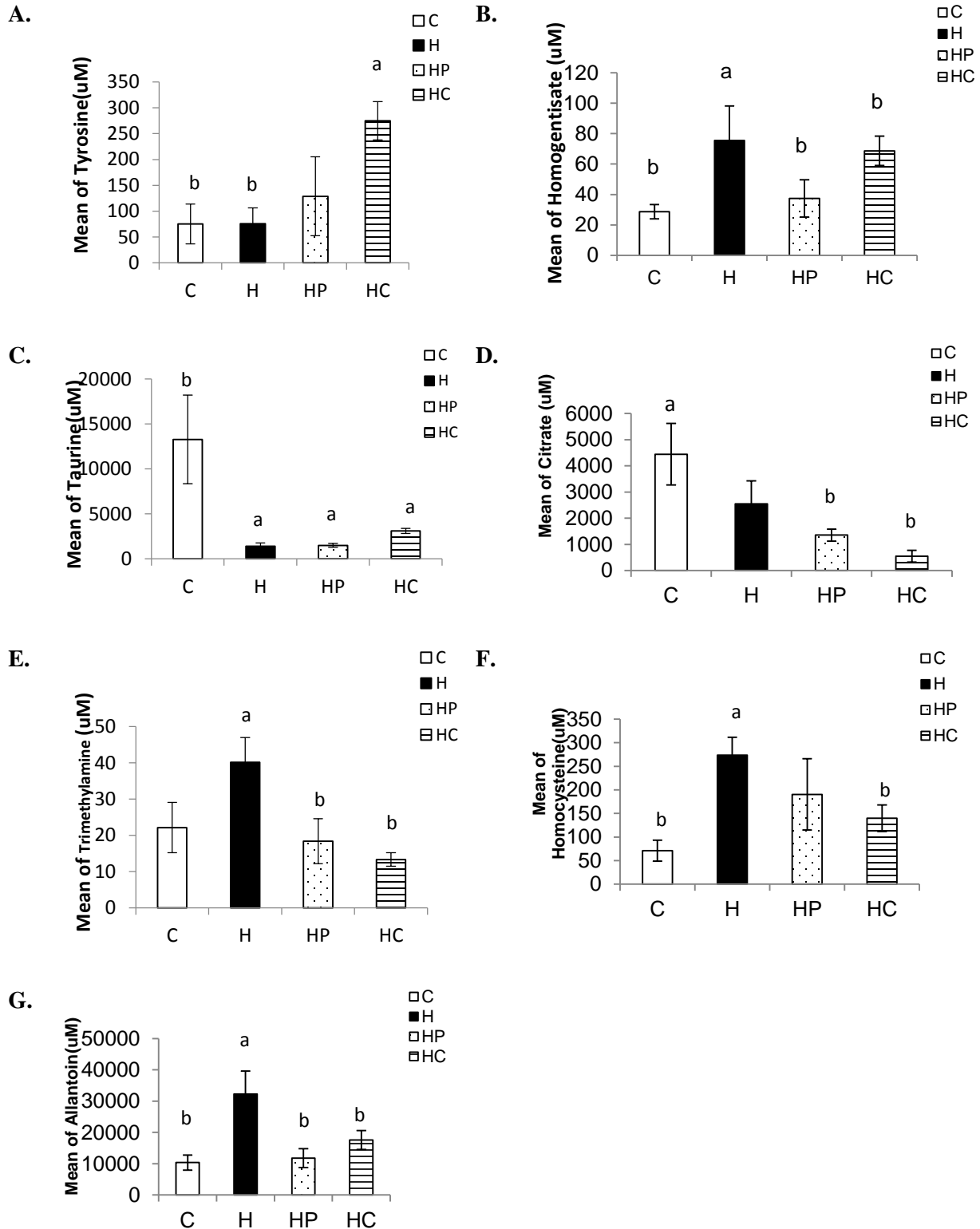
Fig.44 Selected urinary metabolites associated with diet effect found in tyrosine pathway, taurine pathway and citrate pathway by the pathway analysis. Urinary metabolites identified to be significantly lowered at p<0.05

(detail see Table 4) when comparing the four groups. (A) Tyrosine; (B) Homogentisate; (C) Taurine (D) Citrate (E) Trimethylamine (F) Homocysteine (G) Allantoin. Data are expressed as mean±SE. (A), (B) were found in tyrosine pathway; (C) was found in taurine pathway; (D) was found in citrate pathway; (F) was found in cysteine and methionine pathway;(G) was found in uric acid pathway.
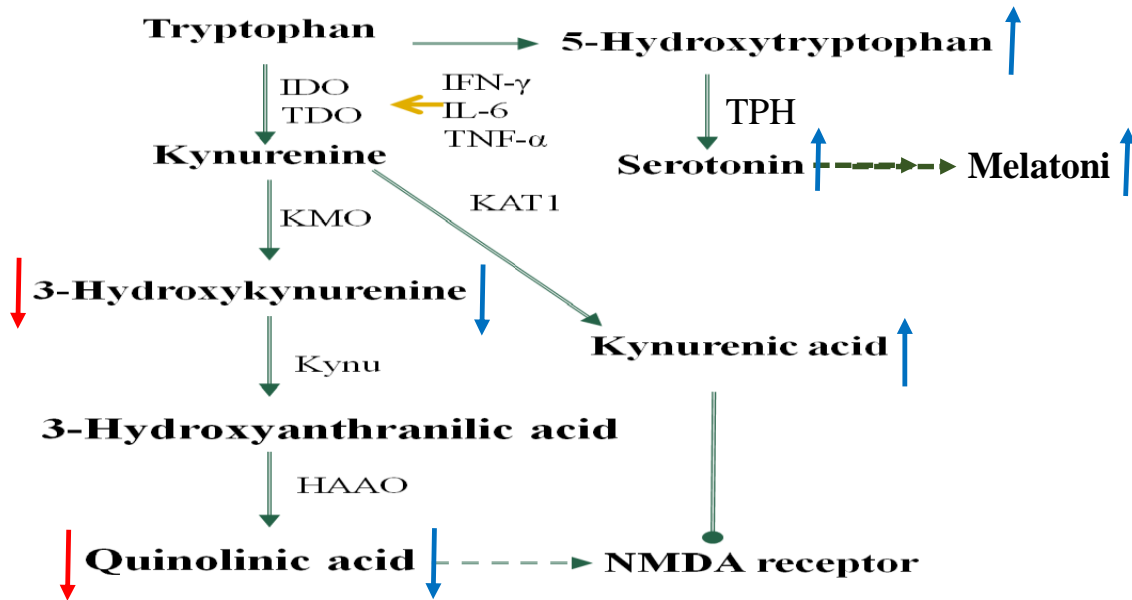
Fig 45. Effect of OPP and curcumin on the alteration of the urinary metabolites from pathway of tryptophan metabolism. Schematic diagram outlining the changes of the metabolites in tryptophan pathway due to the effect OPP and curcumin diet. Red arrows (left side) are associated with OPP diet; blue arrows (right side) are associated curcumin diet. The down-pointed arrows means down regulated; up-pointed arrows mean up regulated. Serotonin pathway: TPH=tryptophan hydroxylase; kynurenine pathway: KAT1 =kynurenine aminotransferase 1 ; KMO=kynurenine 3-monooxygenase; Kyn= kynureninase; HAAO = 3-hydroxyanthranilic acid oxygenase

3.12 Investigating the gene expression for pathway regulation

To correlate and further explore the mechanism behind the urinary metabolomics profile described above, we performed the rtPCR to analyze the gene expression of genes that regulate the tryptophan metabolism. In the tryptophan metabolic process, 95% of tryptophan is metabolized along the kynurenine pathway, which includes two steps: the formation of kynurenine from tryptophan, regulated by the enzymes IDO and TDO and further metabolization of kynurenine along the two distinct routes competing for KYN as a substrate, the KYN–kynurenic acid (KYNA) pathway and the quinolinate (quinolinic acid) pathway. The KYN –KYNA pathway is regulated by KYN aminotransferases (KAT 1), the major biosynthetic enzyme of KYNA formation in the brain. In the KYN–Quinolinate pathway, kynurenine produces 3-hydroxykynurenine regulated by kynurenine 3-monooxygenase(KMO), and KMO is then converted to 3-hydroxyanthranilic acid regulated by kynureninase (Kyn) and further converted with 3-hydroxyanthranilic acid oxygenase (HAAO). 3-hydroxyanthranilic acid becomes quinolinic acid, which serves as an NMDA agonist. At the same time, five percent of TRY is metabolized along the pathway for neurotransmitter serotonin (5-HT) biosynthesis. The rate-limiting step in this pathway is the hydroxylation of TRY catalyzed by TRY-hydroxylase (TPH). The formation of 5-hydroxytryptophan(5-HT) from this step then serves as a substrate for melatonin synthesis.

In this study we performed the rtPCR on the investigation of the gene expression of KMO, Kyn, HAAO, KAT 1, and TPH 2 (Fig 46). For the KMO, a significant difference was found between the control group and OPP groups ($p<0.05$) (Fig 46 A); The effect of OPP was also observed in the expression of the Kyn gene when compared to the control and high cholesterol diet groups ($p<0.05$, Fig 48 B). Significant difference were seen between the curcumin and

control groups as well the high cholesterol diet group in HAAO gene ($p<0.05$, Fig 46 C). Although no significant differences were found in KAT 1 gene expression when comparing the four groups (Fig 48 D1), a separate student T-test was run between the high cholesterol diet group and the curcumin group. This test found a higher gene expression in the curcumin group than in the high cholesterol diet group ($p<0.05$ Fig 46 D2). The same trend was found in the TPH gene; no significant difference was found when comparing the four groups (Fig 46 E1), but after running the student T-test, a significantly higher expression of TPH2 gene was found in the H group when compared to the HP group and HC group separately ($p<0.05$ Fig.46 E2 & E3). Therefore, OPP helped down-regulate KMO and Kyn and also upregulate TPH 2 genes, and the curcumin supplement intervention helped downregulate the HAAO gene and while also upregulating the KAT 1 and TPH 2 genes. These gene expression results reflect the same trend as observed in the urinary metabolomic profile. Some metabolites like 3-hydroxykynurenine and quinolinic acid can cross the BBB, and therefore the peripheral levels might reflect their changes in CNS. A summary of the effects of OPP and curcumin on brain gene regulation of the enzymes in tryptophan metabolism are shown in Fig.47.

E2

E3
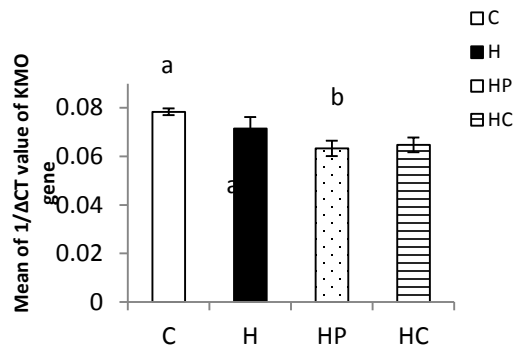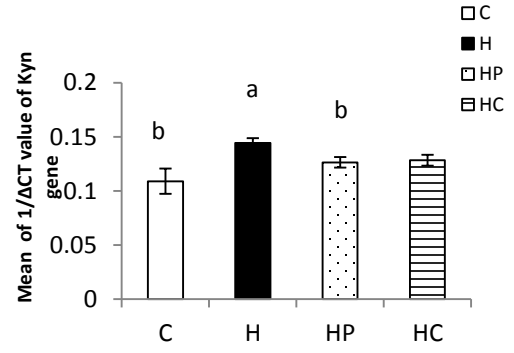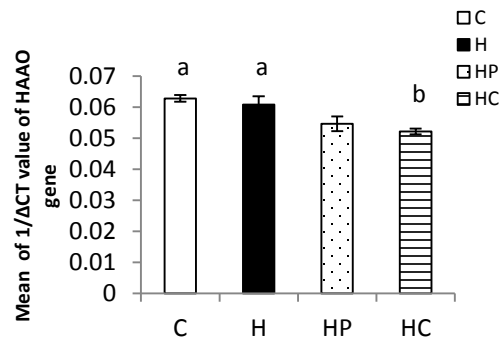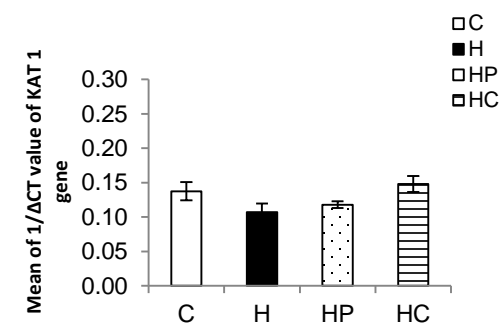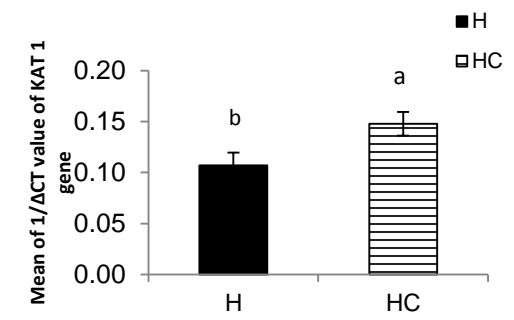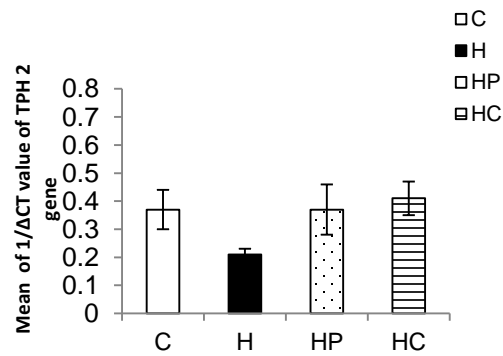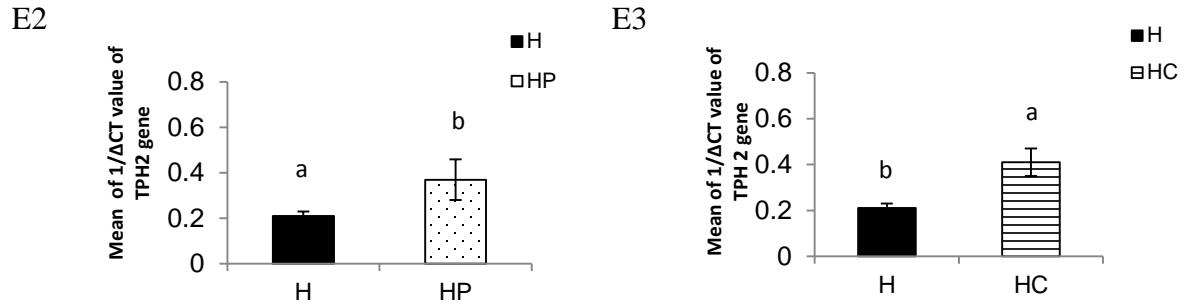
Fig.46 Brain gene expression of genes regulating the tryptophan-serotonin pathway.
A. Gene expression of KMO gene. a,b : significantly higher expression of KMO gene in control (C) groups as compared to the high cholesterol + OPP (HP) group (p<0.05). B. Gene expression of the Kyn gene. a,b: significantly higher expression of Kyn gene in C groups and H as compared to the high cholesterol + OPP (HP) group (p<0.05). C. gene expression of the HAAO gene. a,b: significantly higher expression of HAAO gene in C and H groups as compared to the HP group (p<0.05). D1. Gene expression of the KAT1 gene; no significant differences were found after comparing the four groups. D2. Gene expression of the KAT 1 gene between two groups. a,b : significantly higher expression of KAT1 gene in HC group as compared to the H group (p<0.05). E1. Gene expression of the TPH2 gene; no significant difference was found after comparing the four groups. E2. Gene expression of the TPH gene between two groups (H &HP). a,b: significantly higher expression of TPH2 gene in HP group as compared to the H group (p<0.05). E3. Gene expression of the TPH gene between two groups (H &HC). a,b : significantly higher expression of TPH2 gene in HC group as compared to the H group (p<0.05); Data are expressed as 1/ ΔCT values which was normalized against GAPDH (mean±SE).
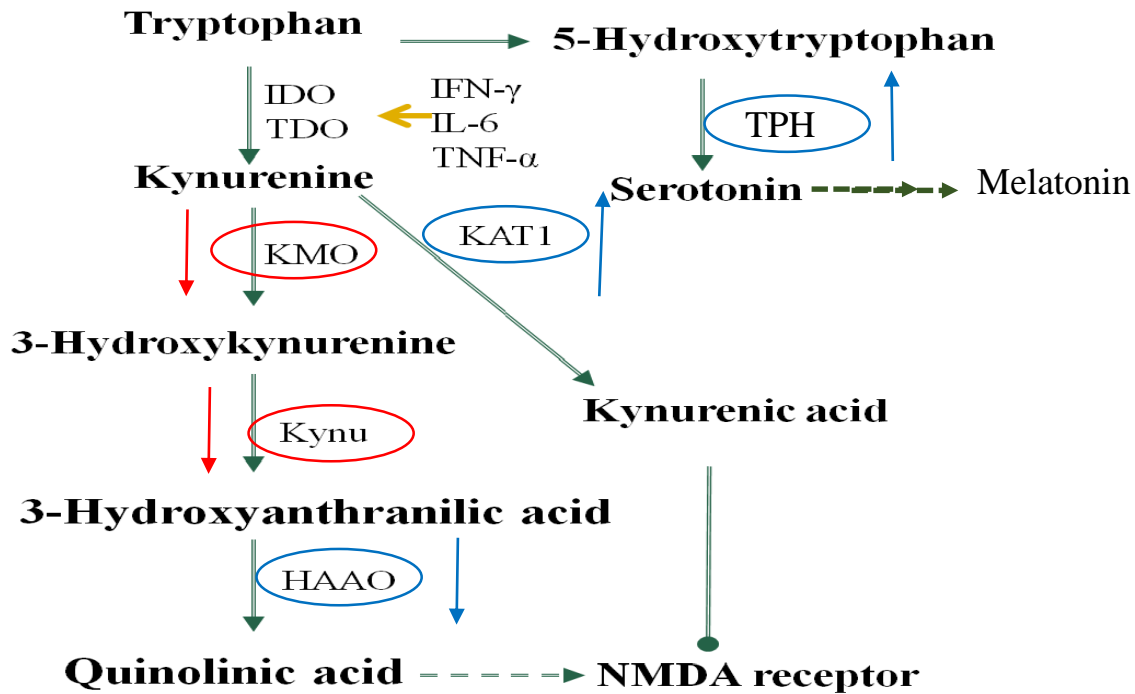
Fig. 47 Effect of OPP and curcumin on gene expression in the pathway of tryptophan metabolism. Schematic diagram outlining the changes of the metabolites in tryptophan pathway due to the effect OPP and curcumin diet. Red circle and arrows (left side) are the genes that are associated with an OPP diet; Blue circles and arrows (right side) are the genes that are associated with a curcumin diet. The down-pointed arrows indicate down-regulation; up-pointed arrows indicateup-regulation. Serotonin pathway: TPH=tryptophan hydroxylase; kynurenine pathway: KAT1 =kynurenine aminotransferase 1; KMO=kynurenine 3-monooxygenase; Kyn= kynureninase; HAAO = 3-hydroxyanthranilic acid oxygenase.

CHAPTER 4 DISCUSSION

The vast majority of AD cases are sporadic, occurring more often in the population with an age above 65. Although some comprehensive evaluations including mental status assessments, analysis of blood and urine, and imaging exams such as CT or MRI can assist its diagnosis, absolute confirmation requires examination of brain tissue at autopsy. In addition, some pathological features have already occurred in the brain before the symptoms show up, which cause the patient to lose the best chance for early diagnosis and treatment of AD. Therefore, animal models have been developed and applied to elucidate the AD pathological progression and mechanisms. However, these animal models have relied on the utilization of genetic mutations associated with familial AD (FAD). Although genetic models have been invaluable in determining the molecular mechanisms of disease progression and for testing potential therapeutics, there are some translational concerns that transgenic models cannot replicate, including complex disease components such as age, diet and other risk factors. There is an increasing awareness that lifestyle, especially a high fat/cholesterol diet, plays a detrimental role in cognitive function. Granholm et al. fed 16-months old rats a high cholesterol diet (2% cholesterol) and saturated fat diet (10% saturated fat) for eight weeks. The lipid profiles of these rats revealed elevated plasma triglycerides, total cholesterol, and LDL for the high fat/cholesterol group as compared to those on an iso-caloric control diet. Additionally, high fat/cholesterol treated rats had more working memory errors in the water radial arm maze and more dendrite loss as well as microglial activation in the hippocampus, which indicated a profound impaired memory and hippocampal morphology when subjects had a high cholesterol and fat diet [87] . In another study, rabbits were fed a 2% cholesterol diet for four, six, and eight weeks. They found that β amyloid immunoreactive features were observed in the hippocampus and adjacent cortex starting from week four. There was an increasing accumulation

of immunolabeled β-amyloid in hippocampus starting from week six. Neurons in the pyramidal cell layer were mostly affected. The β-amyloid deposition increased in severity with time on the hypercholestorol diet when comparing animals at weeks four, six,and eight[88] . Another study reported the application of statin drugs can strongly reduce levels of AD β-amyloid peptides as well as tangle formation both in vitro and *in vivo* by maintaining the plasma's total cholesterol and LDL level [89-91]. Therefore, in our study, we used aging rats which arrived 22-24 months, approximately 60-70 years old in human age, and fed them with humanized hypercholesterolemia to create an AD model. With a dietary supplementation of two percent cholesterol plus cholic acid, we observed a significantly elevated plasma total cholesterol, non-HDL cholesterol level and a higher total cholesterol/HDL ratio in the animals on this experimental diet (Figure 8, 10, 11). Meanwhile, except for the curcumin supplement group, the other two high cholesterol diet groups failed to maintain their HDL level compared to the animals from the control group (Fig.9). The liver cholesterol deposition as well as the liver/body weight ratio were also significantly higher in the high cholesterol diet fed animals (Fig 12-13), while no significant difference was obtained from the brain tissue total cholesterol among four groups (Fig.14). Interestingly, when we compared the lipid profile of the four groups of animals, we found that rats fed a high cholesterol diet supplemented with curcumin for 23 weeks had an improved plasma HDL cholesterol level compared with the groups fed a high cholesterol diet only and a high cholesterol + OPP diet (Fig.9). Gene expression of ApolipoproteinAI (apoAI), a major component of the high- HDL particle, also showed the same trend (Fig.15). Because plasma HDL cholesterol is an independent negative risk predictor of cardiovascular disease (CVD), curcumin has been reported by the other studies to counteract the progression of atherosclerosis by increasing the HDL level and improving HDL

funtionality [92, 93]. Thus, our result also implies a protective role of curcumin on chronic heart disease.

Through this process, we have created an animal model demonstrating all high cholesterol diet group animals developed hypercholesterolemia via a high cholesterol diet but did not create a change in brain cholesterol content. Using this model, we further tested the AD-like pathological changes, including behavior changes and amyloid evidence in the brain induced by an elevated peripheral cholesterol, and also examined the therapeutic effects of the dietary supplement OPP curcumin.

Spatial learning tasks, such as the Morris Water Maze (MWM), have been commonly used to screen aged rats and mice for cognitive status. This task was developed for use in rats, which are good swimmers compared to the mice whose performance are highly affected by other physiological or behavioral traits such as impaired thermogenesis or high anxiety. Because there are no local cues that mark the position of the platform, the rat's ability to locate it efficiently depends on the rat's use of a configuration of cues surrounding the pool. Normally, after a few training trials from a start location at the perimeter of the pool, rats can learn to swim directly to the escape platform. A good learning ability is reflected in shorter latencies to escape by reaching the platform. MWM was prevalently used in neurocognitive disorder studies. Anderson et al. used the Morris Water Maze to measure the spatial working memory changes in rats with transient neurodegeneration induced by NMDA receptor antagonist phencyclidine (PCP) prenatally. When they compared the escape latency over the four daily trials, they found that the placebo group reduced their latency to locate the platform as training progressed, but the PCP-treated rats did not show an equivalent overall improvement. In their second experiment, D-serine was also applied with PCP in these animals and their spatial learning performance in the MWM was measured and

compared with the PCP-only group. The result indicated a significant disruptive effect of PCP treatment on the latency of rats to locate the platform, and the co-administration of D-serine led to a significant improvement. In our study, by comparing the EL among four groups at each time point (baseline, month 1, month 2, month 3, month 4 and month 5), it was found that all of the groups started learning to locate the platform by cues at month 1 (Fig.16). The curcumin supplement group showed a significantly shorter EL time, beginning at month two, when compared to the high cholesterol group. Control and OPP supplement groups animals performed better than the high cholesterol diet group, although the difference is not significant (Fig.17). At month three, the average time that control as well as the other two treatment groups spent in water to locate the platform was significantly less than the high cholesterol group, which means the animals fed a high cholesterol diet had the most impaired memory among the four groups. In month four, although high cholesterol diet group showed some improvement, a significant longer EL could still be observed when compared to the curcumin supplement group. In month five, all four groups showed some deficit in memory function as their EL were higher than the previous month, which is potentially the result of losing animals and aging.

When comparing the time-course performance within individual groups as indicated by figure 18 and 19, we found that no significant difference in EL for the control group from month one through month four, meaning this group of animals maintained their memory and learning ability in four month study period. For the high cholesterol diet group, despire showing a trend in learning and memorizing the location of target at month four, there is still no significant difference in EL among the four time points; A significant improvement of EL was observed in OPP group at month three and month four when compared with month two and month one, which means the OPP supplement showed an effect in memory maintenance after three months of the dietary trial. As

curcumin served as a positive control group, this group kept the shortest time in platform searching as compared to the other groups. This result demonstrated that curcumin has a strong effect on the preservation of the memory and spatial learning ability.

Finally, we looked at the difference of EL between month one and month four and then compared the average differences among the four groups. The result showed that the OPP group had the biggest improvement in their performance in the MWM,implyings that OPP might have a function beyond memory improvement; it may also have an anti-aging effect as the improvement gained by this group is significantly higher than in the group with the high cholesterol diet as well as the control diet group (Fig.18). Therefore, our MWM results indicated the detrimental effect of high cholesterol diet on cognitive function. Similarly to our results, plasma cholesterol levels and its association with MWM performance has also been found in several studies using animal models of AD [1, 8]. Both OPP and curcumin show some ability to alleviate dementia. As curcumin serves the positive control in our study, it is not surprising that curcumin created its effect earlier (month two) and lasted longer (until month four) compared to the OPP treatment group.

Next, we have also investigated the effect of OPP on AD brain hallmarks in this study. Amyloid plaque formation and associated neuron loss in the hippocampus were examined via histology. Neuronal loss is a common pathway for a large number of degenerative processes in AD. The hippocampus, the brain structure in charge of spatial and episodic memory, is particularly vulnerable to the degenerative processes and may exhibit neuronal dysfunction in the earliest stage of the disease. To visualize the cell morphological alteration in the hippocampus area, Hematoxylin and Eosin (H&E) staining was used in this study. From the H&E staining (Fig.19), we found more necrotic neurons and pyramidal neuron loss in the hippocampus of animals fed a high cholesterol diet. As a comparison, neurons in this region of the OPP and curcumin group rats

were more neatly arranged and in an intact shape. After quantification of the healthy cells, healthy

neurons were significantly higher in number in the hippocampus area from OPP and curcumin

supplemented groups (Fig.20). Because the pyramidal cells depend on the synaptic inputs they

receive to integrate information, the loss of these neurons is associated with synaptic dysfunctions.

As the memory deficits observed in aged rodents are the consequence of hippocampal synaptic

plasticity[94], our histological results agree with what we found when studying behavior changes:

the high cholesterol diet group showed more memory impairment. More healthy neurons were

preserved in the OPP as well as the curcumin groups, which explained the better learning ability

of the rats from these two groups. Hence, the loss of synapses and the neurotic alterations are

correlated with cognitive decline from our result, and the cognitive deficit was successfully

reversed by chronic treatment with OPP as well as curcumin by rescuing more dead neurons.

Additionally, amyloid plaque formation was observed using Congo red staining, which is a specific

staining for the β-pleated sheet conformation. Soluble β amyloid (Aβ) is normally secreted by

neurons and then cleared from the brain [18]. However, in abnormal conditions, protein mis-folds

and aberrantly aggregates as oligomers and amyloid fibrils. The accumulation of these insoluble

fibrous proteinns exhibits an affinity for Congo red dye with concomitant apple-green

birefringence under plane polarized light, which is considered a gold standard in diagnosis of

amyloid disorders [20]. Our Congo red results showed a higher density of plaque deposition and

significantly larger amyloid burden in the animals' hippocampus region for those in the high

cholesterol diet group compared to the other three groups (Fig 21-23). This result was confirmed

by a higher concentration of amyloid ß42 in the high cholesterol diet group by enzyme

immunoassay (Fig 24). As numerous studies have observed, the key event leading to AD appears

to be the cluster of peptides and fibrils into amyloid plaques (senile plaques), and we have observed

pathological changes occurring in the rats' brains as response to their diet. Many other studies also found that Aβ 42 significantly increased in AD [95]. Compared to another major product, Aβ40, in amyloid pathway, Aβ 42 peptide is the most neurotoxic form. It has two extra hydrophobic amino acids that promote greater fibrillar formation and been found predominant in neurotic plaques of AD patients [96]. Both cell culture and mouse models have shown that familial AD mutations result in an increase in Aβ42: Aβ40 ratio, suggesting that elevated levels of Ab42 are critical for AD pathogenesis [97, 98]. In addition, Aβ42 has higher *in vitro* propensity of aggregation to form oligomers [99]. Some studies have reported that Aβ42 oligomers are highly toxic to mouse cortical culture as well as more destructive to memory when injected into the brains of young rats [95, 100]. These observations led to the hypothesis that the deposition of amyloid, comprised principally of Aβ42, was the central event in the initial pathogenesis of AD.

Above all, our high cholesterol diet model clearly exhibited AD pathologies, both in abnormal brain Aβ metabolism (overproduction of Aβ 42 and higher amyloid plaque deposition) and learning deficit (longer escape latency). However, whether hypercholesterolemia can interpret the brain cholesterol metabolism is still contested in the field, as plasma lipoprotein cholesterol does not cross the BBB. Since peripherally circulating cholesterol cannot cross the BBB, there may be body-brain communication signals which mediate AD-like pathology in the brain under the condition of hypercholesterolemia such as oxidative stress, inflammation factors and abnormal gene expressions. Compared to the detrimental effect of hypercholesterolemia, a diet supplemented with OPP has shown some neuroprotective effects which are similar to the positive control curcumin group. Leow et al. also nvestigated OPP's neuroprotective effects. They fed BALB/c mice OPP for six weeks and animals were tested in a water maze for cognitive and motor function. They found that mice given OPP showed a downward trend in latency to the platform

and OPP-fed rats had improved balance and motor coordination. Microarray gene expression analysis showed OPP compounds could up-regulate genes involved in brain function, such as Arc, Cast or D14Er*td171e* and Gria3 which were under the regulation of Bdnf (brain-derived neurotropic factor). Genes involved in inflammation were also down-regulated by OPP such as Spp1 (secreted phosphoprotein1 or osteopontin), Saa3 (serum amyloid A3), and Apod (apolipoprotein D)[65]. Additionally, the AD-improving effects of OPP in the brain were aligned with the findings made by Hamaguchi et al., who investigated the effects of phenolic compounds (myricetin, nordihydroguaiaretic acid (NDGA) and rosmarinic acid (RA) on AD model transgenic mice. Mice were fed with these phenolic compounds for ten months from the age of five months. They found Aβ deposition was significantly decreased in the in both the NDGA- and RA-treated groups' brains. The RA-treated group also showed increased (TBS)-soluble Aβ monomers. They concluded that oral administration of phenolic compounds prevented the development of AD pathology by affecting different Aβ aggregation pathways *in vivo*[101].

So this raises the question: what is the mechanism of OPP resulting in its therapeutic effects in AD-like pathology? Because oxidative stress and inflammation have been recognized contributing to the brain amyloidogenesis, we further measured the antioxidant and anti-inflammatory abilities carried by this agent. We began with the knowledge that atherosclerosis and cardiovascular disease are now linked to an increased risk of AD [102]. The lipid peroxidation products generated from the atherogenic diet are possible markers of Alzheimer´s disease in blood. In the Aβ-induced oxidative stress hypothesis, an overproduction of Aβ1–42 inserts as oligomers into the bilayer and serves as a source of ROS to initiate lipid peroxidation [83]. The lipid peroxidation process eventually generates an unsaturated reactive aldehyde [e.g., 4-hydroxy-nonenal (HNE), malondialdehyde (MDA), and acrolein][26]. In one study, Keller et al. assessed

the amount of protein carbonyls and MDA [30] in the postmortem brain of normal subjects and those with MCI and early AD. They found 25% elevated levels of protein carbonyls, and approximately 60% of MDA were observed in the individuals with MCI and early AD compared to normal subjects. The elevation in TBARS was associated with the numbers of neurotoxic plaques and decreased verbal memory performance was observed in these patients[103]. In another study, increased protein-bound free HNE, TBARS, and MDA were found in AD subjects, as well as a higher isoprostane (F2isoP) level in plasma, urine, and CSF, as compared with healthy controls [103, 104]. In our study, we found that the level of both peripheral and CNS MDA increased significantly in high cholesterol diet group while the OPP and curcumin groups' MDA levels were similar to the control group (Fig.25-27). The increase in MDA level and the presence of amyloid plaque following a high cholesterol diet are consistent with findings reported by the studies mentioned above. A lower level of MDA level observed in the OPP group suggested that bioactive aldehyde toxicity may be mediated by the effect of OPP, which serves as a strong antioxidant during the development of peripheral atherosclerosis and plaque deposition in brain. OPP also reduced the urinary ketones as compared to those rats consuming high cholesterol diet only (Fig.28). 3-hydroxybutyrate, which is most abundant in serum and urine, was elevated as a result of excessive oxidation of fatty acid. Ketone bodies have been shown to be also elevated in mice consuming high-fat diets [105]. These results indicated the antioxidant activity delivered by the dietary intake of phenolic compounds.

However, it is still not clear whether the origin of these lipid prooxidants is peripheral circulation/tissues or brains. When the brain is under a oxidative stress conditions, the inhibition of mitochondrial energy metabolism can alter the metabolism of APP from the non-amyloidogenic to the amyloidogenic pathway with an upregulated APP and β-secretases(BACE) gene

expression[106]. The overproduction in APP appears to increase APP cleavage toward a higher generation of total Aβ or more of the amyloidogenic Aβ42 species alone. Meanwhile, Aβ deposition may act as a sink for trapping potentially harmful transition metal ions (particularly redox active metal ions), which in turn become a potent generator of both ROS and RNS that are flowing back to peripheral circulation [27, 107].Therefore, increased Aβ generation and ROS production comprise a 'vicious feedback cycle.' Because oxidative stress and Aβ production are proportionally linked to each other through an up-regulation of APP and BACE1 genes as described above, we then measured these two genes to examine the effect of our experimental diet on plaque formation (Fig.30&31). The results demonstrated that the increased expression of APP & BACE1 in the H group was induced by lipid peroxidation (MDA and ketone body), but they were not unregulated in the OPP supplement group and curcumin group. This result is also consistent with the amyloid plaque deposition and its burden from our histological work and enzyme linked immunoassay. The same changes with BACE1 as a result of increased lipid peroxidation product 4-hydroxynonenal (HNE) were reported by Gamba et al. [33], who found a significant correlation of BACE1 activity with oxidative markers in sporadic AD brain tissue [34]. Oxidative stress increases during normal aging and is believed to be an early event in AD pathology, so the measurement of the peripheral oxidant status might be an early biomarker correlated with the brain stress status [35].

Thus, we have observed the antioxidant effect of OPP both in periphery (plasma and liver) and brain. But this raises another question of whether polyphenols can enter the brain and directly impact βA. Polyphenols permeation through the BBB is dependent on the degree of lipophilicity of each compound and also depend on their interactions with efflux transporters, such as P-glycoprotein (PGP) and their stereochemistry [108, 109]. It has been reported that catechin and

epicatechin could cross a cellular model of BBB in a time-dependent and stereoselectivity manner[110]. Animal studies indicated that polyphenols are able to cross the BBB and to localize within the brain tissues independently of their route of administration. Janle et al. demonstrated that ^{14}C-labelled grape polyphenols showed accumulation from anterior to posterior slices of the brain following oral administration [111]. Except for BBB crossing, another mechanism is through neurotransmitter regulation. One study used the treatment of rats with polyphenol-rich *Ginkgo biloba* extract for 14 days and found that this resulted in significantly increased extracellular levels of dopamine and noradrenaline in the animals' prefrontal cortex. Of the three main *Ginkgo biloba* extract constituents, the polyphenol (flavonoid) fraction caused a significant (and most pronounced) increase in brain dopamine levels [112].

Although no studies to date have observed the ability of OPP to cross the BBB, it has been proven that when under the stress, microglial activation can impair BBB function by the release of various toxic molecules (ie.TNF-α). These neurotoxic molecules lead to a hyperpermeability condition of BBB associated with inflammation that is similar to what occurs in certain neurodegenerative disorders like AD. Therefore, one possibility is that OPP's antioxidant effect can be seen in the AD brain by reducing the flowing of free radicals from peripheral circulation toward brain and indirectly improving the high brain stress level (decreasing the lipid peroxidation, downregulating the amyloidgenic genes and decreasing amyloid accumulation).

Brain inflammation is another pathological scenario in AD[32]. The interactions between cytokines and components of the AD senile plaques have been reported to form a vicious circle similar to the ROS-induced plaque deposition [113]. Activated astrocytes and microglia are characteristically found in abundance near dead neurons and Aß plaques to produce several proinflammatory signal molecules, including cytokines, growth factors, complement molecules,

chemokines, and cell adhesion molecules [114]. Aβ protein of the plaques also potentiate the secretion of IL-6, IL-8 and TNF-α by IL-1β-activated astrocytoma cells and lipopolysaccharide-(LPS-) stimulated astrocytes [115]. In addition, it also has been reported that plasma cytokines are associated with AD progression [116]. Plasma cytokines are known to communicate with the brain and reflect central cytokine levels. The possible route involves cytokine activation of the endothelium signaling to macrophages in brain[117]. In our study there was an elevated level of the plasma IL-6 in animals with atherogenic diet, which might indicate a high inflammation level in brain as the amyloid plaque can serve as a generator of these cytokines or they can enter the brain from periphery due to a destructive BBB under the stress condition (Fig.29). Curcumin has been proven to inhibit the AD pathogenesis by its anti-inflammation as well as antioxidant effects, but direct effects of curcumin on the formation and destabilization of Aβ still remain unclear[64]. However, one possible mechanism could be its HDL-maintaining properties as was decribed by Fig. 11. It has been reported that people with high levels of HDL cholesterol are 60 percent less likely to develop AD after folloing 1,130 seniors with no history of cognitive decline and measuring their cholesterol levels every 18 months for four years. Those with the highest HDL counts, greater than 55 mg/dL, had a nearly 60 percent reduced risk of developing the disease compared to those whose levels were less than 39 mg/dL[118] . These data shed more light on the interactions between cholesterol and AD.

In addition to oxidative stress and inflammation, the role of cholesterol is further highlighted by the fact that abnormal intracellular cholesterol distribution is closely related to the Apolipoprotein E (ApoE). Astrocytes are the major source of ApoE followed by oligodendrycytes and microglia[119]. Neurons may express apoE under certain condition such as excitotoxic injury. When nerve injury happens in central nervous systems, the synthesis of apoE by glial cells

increased up to 150 fold [42]. Our result (Fig 32) shows a higher production of ApoE in H group which reflects the detrimental effect the oxidative stress in brain due to the high cholesterol diet, while OPP and curcumin can decrease the neuronal injury by their antioxidant and anti-inflammatory effects. ApoE has been reported as a contributor of the extracellular amyloid plaque deposition [120]. The precise mechanisms by which ApoE participates in AD pathogenesis remain largely undefined. Several hypotheses regarding its functions have been proposed which include mediating neuroinflammation, participating in the regulation of the cholinergic neurotransmitter system, neuronal signaling, and involving the integrity of the blood–brain barrier. However, the most prominent hypothesis for ApoE function is its key role as a mediator of Aβ metabolism. ApoE can bind to Aβ, affect its deposition and clearance, which is necessary in amyloid deposition. Furthermore, ApoE affects amyloid deposition in an allele-specific manner. However, the exact pathophysiologic process is yet to be elucidated [16]. So far only a limited body of studies were found to report the beneficial effect of polyphenols on expression of ApoE genotype in AD with dementia. It has been suggested in one study that frequent consumption of fruits and vegetables is associated with a decreased risk of all cause dementia (hazard ratio [HR] 0.72, 95% CI 0.53 to 0.97) especially amongst the APOE4 noncarriers [121]. The relationship between polyphenol intake and APOE genotype remains an area where further work is required for a better understanding of the underlying mechanisms of polyphenol supplements.

In the last section, data from a urinary metabolomic study provided supportive evidence of OPP on improving the effects of AD. Metabolome is a powerful tool used in the identification of the potential biomarkers of altered metabolism as result of disease processes and drug/nutrition intervention [122]. Today a simple, non -invasive and accurate method for detecting AD (prior to the onset of devastating symptoms) at its early stage is urgently needed. Identification of effective

biomarkers from urine samples could facilitate diagnosis and therapeutic trials. Meanwhile, the potential metabolite biomarkers that have been identified can provide further guidance toward pathway analysis involved in the pathology of AD, which may help in exploring the mechanism of the treatment by OPP and curcumin. In metabolomics, ^{1}H NMR spectroscopy is one of the main approaches to data acquisition. It provides quantitative information and is reproducible, hence suitable for multivariate analysis.

In our study, multivariate data analysis using SIMCA P+ software revealed no discrimination of urinary profiles among four group at baseline (Fig33); However, discrimination was revealed at week 12, at which time the control diet group was well separated from other three groups and curcumin group was also separated from the high cholesterol diet group and OPP supplement group. When we observed the loading plot, the regions of variables that are responsible for the separation of the control group were found at ppm 3.02-3.42, 2.5-2.6 and the regions of variable that separated the curcumin group were 7.2-7.4. For the high cholesterol diet group the metabolites were those with ppm of 3.8 and 4.05, meaning at the intermediate time point of the experiment, the urinary metabolomics profile of the animals had changed as response to diet (Fig.34). At the study's endpoint, the high cholesterol diet group was well separated from the other three groups (Fig. 35), which implies that the dietary effect of the OPP and curcumin resulted in the urinary metabolomics profiles of these animals becoming distinct from those without supplement despite three of the groups consuming a high cholesterol diet.

Next, a regression analysis was performed by the SIMCA software to evaluate the correlation between the AD pathology-related variable (water maze, amyloid β 42, lipid peroxidation and inflammation) and the urinary metabolomic profile. The spatial learning performance (EL) and the urinary metabolomic profiles were high correlated at the endpoint (R^2=0.7956) (Fig.36); there was

also a high correlation with the hippocampus amyloid β 42 level (R^2=0.7406) (Fig 37). Correlation between the urinary profile and lipid oxidation indicator [30] was slightly lower, R^2=0.6665, (Fig.38) and correlation with inflammation marker IL-6 was 0.6008 (Fig.39). The data suggests that the urinary metabolites change was strongly correlated with AD brain changes and there are some potential biomarkers that can be identified for the diagnosis of the disease. The urinary metabolite changes were also influenced by the oxidative stress and inflammation status of the body.

In order to identify the metabolites that are associated with the spectral discrimination of four different diet groups, NMR Suite Chenomx software was used to measure the concentration of each metabolite in the animals' urinary profiles. After gathering the group average concentration of each metabolite and comparing them throughout the four groups, there are more than 30 metabolites that showed a significant difference in concentration ($p<0.05$) (Table 4, Fig 40). All of the metabolites that were significant in their profile were then subjected to MetaboAnalyst 3.0, a web-based metabolomics data analysis tool for pathway analyses. Several significant pathways were detected including tryptophan metabolism, synthesis and degradation of ketone bodies, phenylalanine, tyrosine and tryptophan biosynthesis, and taurine and hypotaurine metabolism (Fig.41, Table 5). The topology analysis indicated that synthesis and degradation of ketone bodies and tryptophan metabolism were most impacted in this dietary study.

Studies have shown that high cholesterol and high fat administration lead to elevated rates of fat oxidation. Alteration in diet stimulates lipid oxidation and production of ketone bodies, including 3-hydroxybutyrate which is most abundant in serum and urine[123] .When the accumulation of cholesterol and phospholipids accelerates lipid oxidation, 3-hydroxybutyric acid (or beta-hydroxybutyrate), acetoacetate and other ketone bodies (i.e acetone) are raised in ketosis.

High levels of ketones are associated with atherosclerosis. One study found that a six month high-fat ketogenic diet produced significant increases in total cholesterol, LDL-cholesterol and atherogenic apoB–containing lipoproteins level in plasma, and there was a decrease in antiatherogenic HDL cholesterol. They noted that long term high ketone level adversely affects endothelial vascular function and promotes inflammation and formation of atherosclerotic lesions [124]. In addition, ketones, especially acetoacetate (AA), have been reported to increase cellular lipid peroxidation resulting from oxygen radical production that in turn led to elevated oxidative stress. The oxygen radicals generated by the ketone body acetoacetate can exert a cytotoxic effect by causing peroxidation of membrane phospholipids and the resulting accumulation of peroxidation products such as malondialdehyde [30]. These products have been known to cross-link membrane components and result in altered membrane permeability and ultimately, cellular dysfunction[125]. A recent study reported that ketoacidosis independently induced changes in pro-inflammatory cytokines, oxidative stress, and CVD as high levels of circulating IL-6 and TNF-α were elevated in hyperketonemic diabetics but not in normal diabetics patients[126]. Therefore, in our Chenomx data, a high level of ketones (3-hydroxybutyrate, acetoacetate) and ketone derivatives (α-oxoglutarate) in high cholesterol diet group can reflect high oxidative stress in the bodies of these rats (Fig.43). OPP and curcumin can help reduce plasma level of ketones via an antioxidant and antinflammation effect which were discussed in the MDA and IL-6 data above. Moreover, the cholesterol-lowering effect of curcumin may have led to a decrease in the β-hydroxybutyric acid level in the urine following its oral administration. These findings support those of another study by Li et al. [127], who showed that curcumin administration significantly reduced ketone body levels in mice fed a high cholesterol diet. In conclusion, supplementation

with OPP and curcumin reduces oxidation-induced ketone generation and attenuates the atherosclerosis events in rats on a high cholesterol diet.

Another pathway with high significance and impact in our rats' urinary profile is tryptophan metabolism. Some metabolites from its metabolism were significantly higher in the cholesterol fed animals as compared to the control group. Treatment with curcumin and OPP brought down the concentration of these metabolites significantly and closer to the control levels including 3 hydroxykynurenine (3HOK) and quinolinic acid [109]; significant effects on kynurenate, serotonin, and melatonin were only observed in the curcumin diet groups (Fig 42).

Tryptophan is an essential amino acid. It can enter a number of metabolic pathways: protein synthesis, the serotonin pathway, and the kynurenine pathway [128]. The tryptophan-kynurenine (TRY-KYN) pathway is the most tryptophan-consuming metabolic pathway. About 95% of the ingested tryptophan enters the kynurenine pathway, which is then followed by two steps: 1) formation of KYN from TRY and 2) post-KYN metabolism, in which kynurenine is further metabolized along the two distinct routes competing for kynurenine as a substrate, the KYN–kynurenic acid (KYNA) pathway and the KYN–nicotinamide adenine dinucleotide (NAD) pathway [129]. The KYN-KYNA pathway is regulated by kynurenine aminotransferases (KAT), the major biosynthetic enzymes of KYNA formation in the brain. Under these physiological conditions, most kynurenine in the brain is metabolized to KYNA; the KYN-NAD pathway is the competing pathway to the KYN-KYNA pathway. This pathway produces 3 HOK which is further metabolized to QA, the precursor of NAD. Because these metabolites (3 HOK and QA) are believed to possess a neuroactive and neurotoxic effect, the TRY-KYN-NAD pathway has been implicated in the pathological changes of the neurodegenerative diseases, such as Parkinson's disease (PD), Alzheimer's disease (AD), Huntington's disease (HD) etc., all of which are

characterized by neurotoxic processes [130]. Now there is an increasing body of evidence indicating that the TRY-KYN-NAD pathway is involved in the pathogenesis of AD[131]. Therefore, our urinary metabolomic data enable us to examine the effect of OPP and curcumin on the progression of AD using the alterations of these metabolites and the mechanisms that underlie the disease. As the diagram in Fig.47 shows, both OPP and curcumin decrease the urinary levels of 3HOK and QA, which are potent prooxidants in the brain. A great deal of evidence has shown that 3HOK is associated with the generation of the oxidative species superoxide (O^{2-}), hydroxyl radical ($H\cdot$) and hydrogen peroxide (H_2O_2), which frequently contribute to macromolecular damage within defective cells [132-134]. Moreover, QA, a downstream metabolite of 3 HOK, is also a potent neurotoxic element that has been shown to exhibit excitotoxic effects via N-methyl D-aspartate (NMDA) receptor agonism, as well as oxidative stress via lipid peroxidation [135]. QA is also strongly presented by the over-activated microglial[136]. Being potent antioxidants, OPP and curcumin can scavenge O^{2-} and OH• *in vitro*, as well as lipid hydroperoxyl free radicals. Polyphenols have also reported to inhibit nuclear factor κB signaling and thus suppress the overactivity of the microglial in a model of AD, and this activity is related to the activation of the SIRT-1[137]. Moreover, peripherally generated 3 HOK is able to cross the BBB because of its hydrophobic nature, increasing its bioavailability in the brain[136]. Therefore, both the peripheral and CNS-originated 3HOK can be reflected in the increasing amount of the urinary 3HOK level in the high cholesterol diet group without an antioxidant treatment.

Furthermore, it is very interesting that curcumin increased the KYNA and the metabolites involved in the serotonin pathway (serotonin, 5 hydroxytryptophan [5HT] and melatonin). Less than five percent of dietary tryptophan is converted to serotonin. Serotonin plays an important role in regulating various functions in the human body and serves as the precursor for melatonin

synthesis in pinealocytes [123]. Serotoninergic involvement in AD is evidenced by the observations of 5HT alteration in CSF, loss of 5HT synthesizing neurons and receptors, and the improvement of agitation and other behavioral symptoms of AD with serotonergic agents [26]. Our data show that curcumin supplements can increase the metabolism of serotonin and its downstream metabololite, melatonin, in circulation to deliver some AD improving effect. This result was supported by the other studies such as Wang et al., who demonstrated that curcumin antidepressant action is blocked by p-chlorophenylalanine, a tryptophan hydroxylase (TPH) inhibition. TPH is the key enzyme for down-stream production of serotonin from 5HT. Moreover, it has been demonstrated that the antidepressant action of curcumin involves the participation of 5-HT receptors [138]. In another study, the researchers treated the neuropathic mice with curcumin (45 mg/kg, twice per day for 3 weeks) and induced depressive-like behaviors via chemical depletion of brain serotonin. Intracerebroventricular injection of methysergide, a nonselective 5-HT receptor antagonist, separately counteracted the action of curcumin. Further, this anti-depression of curcumin was abrogated by repeated co-treatment with 5-HT1A receptor antagonist WAY-100635 [139]. Pharmacological studies suggest that the major antidepressant effects of curcumin are mediated through serotonergic transmission, most likely at 5-HT 1A/1B and 5-HT 2C subtypes. Curcumin can even attenuate stress-induced decreases in hippocampal 5-HT 1A mRNA levels [140].

KYNA is a NMDAR antagonist, and α7-nicotinic acetylcholine receptor (α7nAChR)-negative allosteric modulator. Early studies of KYNA demonstrated that it can be neuroprotective against neuronal damage caused by neurotoxic QA [109, 141]. Because the pathway of QA competed with KYNA in brain for the KYN substrate, one of the mechanisms forhow curcumin can increase KYNA might be related to the deactivation of the KYN-NAD pathway.

In addition to the metabolites and pathways discussed above, we also found other metabolites that may be involved in the AD pathology including tyrosine, homogentisate, allantoin, citrate, taurine, trimethylamine, and serine (Fig.44). Tyrosine is the precursor of several neurotransmitters, including L-dopa, dopamine, norepinephrine, and epinephrine. Tyrosine, through its effect on neurotransmitters, may affect several neurodegenerative and neuropsychiatric diseases, including Parkinson's disease, depression, and other mood disorders. The dopaminergic system may also be involved in the occurrence of cognitive decline and is predictive of rapidly progressive forms of AD. However, a clear picture of the role of the dopamine system in AD remains to be developed [142]. D-serine is another amino acid highly present in the brain and is derived from glycine. It is a neuromodulator and it is an endogenous coagonist of NMDA receptors. One study reported an abolishment of NMDA-elicited neurotoxicity after a nearly complete removal of D-serine. Therefore, endogenous serine is the dominant coagonist for NMDA receptor-elicited neurotoxicity, mediating all cell death elicited by NMDA receptor in organotypic slices. This further implicated endogenous serine as the mechanism of neuronal death in the nervous system[143]. Allantoin is a metabolite produced by the oxidation of uric acid in e purine metabolism in humans by various ROS. It has been reported that allantoin levels are increased in model rats with ischemic injury [142] and model mice with atherosclerosis[144], which are closely related to the occurrence of oxidative stress .Therefore, measurement of allantoin levels may be useful for quantifying amounts of oxidative stress. Homogentisate is also found to possess a prooxidant effect. When undergoing spontaneous oxidation into 1,4-benzoquinone-2-acetic acid (BQA), it is concomitant with the production of oxygen radicals such as superoxide anion ($O_2^{\bullet-}$), hydroxyl radical ($OH^{\bullet}$), and hydrogen peroxide (H_2O_2). Taurine is the most abundant free amino acid in humans, and it also has many potential health benefits because of its anti-oxidant and anti-

inflammatory properties. It has been found that taurine treatment can prevent the impairment of cognitive functions and improve the behavior activities associated with the generation of free radicals [145]. Citrate is a metabolite from the TCA cycle for energy production related to aging process. It has been reported that in both muscle and liver tissue, citrate synthase (CS) activity was increased in older mice, indicating increased mitochondrial activity or number [146]. In summary, alteration of the compounds found in the urinary metabolomic profiles of the AD-like animals reflect changes in small amino acids that participate in neurotransmitter modulations, the oxidative stress in the body and the aging-related energy production. OPP and curcumin can reduce the production of some of oxidative stress-related metabolites which might otherwise cross the BBB and attribute to progressive pathological changes in the brain.

Finally, in order to confirm the result obtained from the Chenomx, gene expression analysis was performed on the genes that regulate the TRY-KYN pathway and serotonin metabolism. The results showed a down-regulation of the KYN and KMO genes in the OPP group (Fig.46&47). This supports the effects of the antioxidant & anti-inflammatory propertyies of OPP, as it suggests that IFN-γ or TNF-α, alone or in combination, markedly increased transcripts of KYNU and KMO[147]. Curcumin groups showed a down-regulation in the HAAO and upregulation in the KAT as well as TPH genes (Fig.46&47). Compared to OPP, curcumin has a better bioavailability in the brain tissue. Because of curcumin's low molecular weight and polar structure, it can penetrate the blood-brain barrier effectively and directly impact on neurons. These interesting findings in the kynurenine pathway indicate the potential site of drug action, and presented the possibility of modifying the balance between the endogenous concentrations of QA and its antagonist, KYNA [131].

Taken together, our work has led us to the conclusion that oil palm phenolics (OPP) exhibit an AD related pathology- (cognitive decline, amyloid event and neuron death) improving effect on the atherogenic diet-induced AD rat model via their antioxidant and anti-inflammatory effect. Fig. 48 depicts the peripheral and CNS interaction in atherosclerosis and the main mechanisms of AD pathology in brain. Observations from this study can be further investigated using larger scale animal studies that may lead to a pilot human study. Our findings from the animals' urinary metabolomic profiles might provide a potential pharmaceutical / nutraceutical target for this future AD treatment.
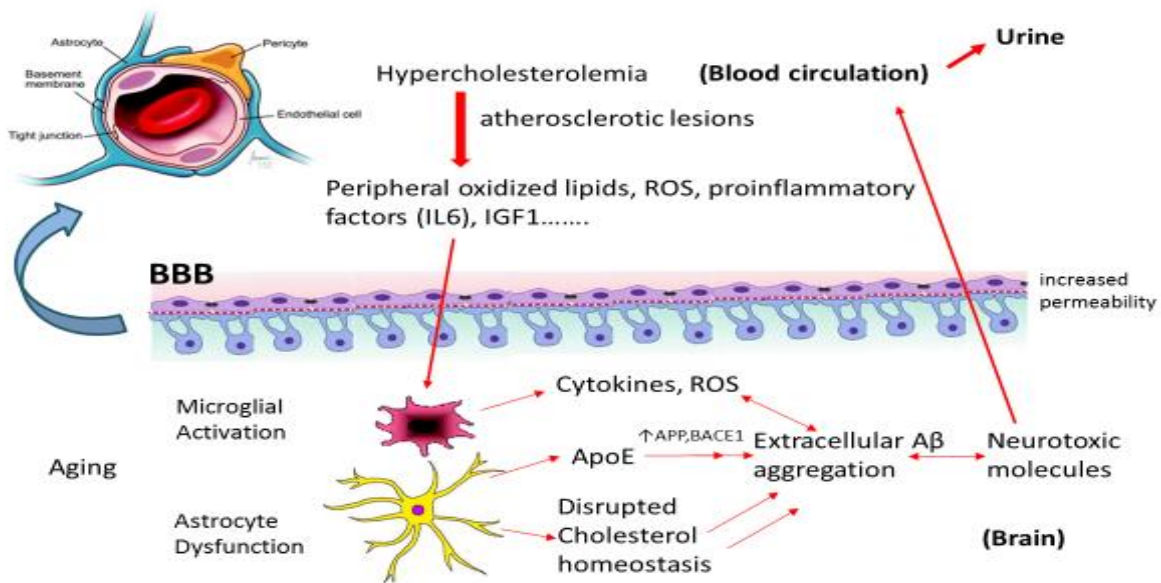
Fig.48 Schematic diagram outlining the peripheral & CNS interaction in atherosclerosis and AD pathology in brain. Briefly, the peripheral oxidized lipids and associated ROS and proinflammatory factors are generated in the atherosclerotic lesions under the hypercholesterolemia and they are permeable to the damaging BBB when the brain is under the stress. Brain microglial cells and astrocytes are further activated to release more cytokines, ROS and disrupt the intracellular/extracellular balance. ßamyloid 42 are abnormally produced and aggregated as a response or promoter of the oxidative stress and inflammation, which release more neurotoxic molecules that are accumulated in brain and meanwhile, exported back to the blood circulation. Some of these neurotoxic metabolites can be present in the urine and might serve as potential biomarkers for AD.

REFERENCES

1. Wilson, R.S., et al., The Natural History of Cognitive Decline in Alzheimer's Disease. Psychology and Aging, 2012. **27**(4): p. 1008-1017.

2. Aging, N.I.o., Alzheimer's Disease Fact Sheet. 2016: p. 1-8.

3. Honig, L.S., W. Kukull, and R. Mayeux, Atherosclerosis and AD - Analysis of data from the US National Alzheimer's Coordinating Center. Neurology, 2005. **64**(3): p. 494-500.

4. Risse, S.C., et al., Myoclonus, seizures, and paratonia in Alzheimer disease. Alzheimer Dis Assoc Disord, 1990. **4**(4): p. 217-25.

5. Hebert, L.E., et al., Alzheimer disease in the United States (2010-2050) estimated using the 2010 census. Neurology, 2013. **80**(19): p. 1778-1783.

6. Alzheimer's, A., 2016 Alzheimer's disease facts and figures. Alzheimers Dement, 2016. **12**(4): p. 459-509.

7. Bateman, R.J., et al., Clinical and Biomarker Changes in Dominantly Inherited Alzheimer's Disease. New England Journal of Medicine, 2012. **367**(9): p. 795-804.

8. Calhoun, M.E., et al., Amyloid plaque formation in APP transgenic mice is associated with neuron, synaptic bouton, and cholinergic fiber loss. European Journal of Neuroscience, 1998. **10**: p. 324-324.

9. Hartmann, T., et al., Distinct sites of intracellular production for Alzheimer's disease A beta 40/42 amyloid peptides. Nature Medicine, 1997. **3**(9): p. 1016-1020.

10. Freese, C., et al., A novel blood-brain barrier co-culture system for drug targeting of Alzheimer's disease: establishment by using acitretin as a model drug. PLoS One, 2014. **9**(3): p. e91003.

11.   Hardy, J. and D.J. Selkoe, Medicine - The amyloid hypothesis of Alzheimer's disease: Progress and problems on the road to therapeutics. Science, 2002. **297**(5580): p. 353-356.

12.   Constantinidis, J., Hypothesis regarding amyloid and zinc in the pathogenesis of Alzheimer disease: potential for preventive intervention. Alzheimer Dis Assoc Disord, 1991. **5**(1): p. 31-5.

13.   Walsh, D.M., et al., Naturally secreted oligomers of amyloid beta protein potently inhibit hippocampal long-term potentiation in vivo. Nature, 2002. **416**(6880): p. 535-539.

14.   Spillantini, M.G. and M. Goedert, Tau protein pathology in neurodegenerative diseases. Trends Neurosci, 1998. **21**(10): p. 428-33.

15.   Karran, E., M. Mercken, and B. De Strooper, The amyloid cascade hypothesis for Alzheimer's disease: an appraisal for the development of therapeutics. Nature Reviews Drug Discovery, 2011. **10**(9): p. 698-U1600.

16.   Gotz, J., et al., Formation of neurofibrillary tangles in P301l tau transgenic mice induced by Abeta 42 fibrils. Science, 2001. **293**(5534): p. 1491-5.

17.   Arbor, S.C., M. LaFontaine, and M. Cumbay, Amyloid-beta Alzheimer targets - protein processing, lipid rafts, and amyloid-beta pores. Yale J Biol Med, 2016. **89**(1): p. 5-21.

18.   Tanzi, R.E., The genetics of Alzheimer disease. Cold Spring Harb Perspect Med, 2012. **2**(10).

19.   Scheuner, D., et al., Secreted amyloid beta-protein similar to that in the senile plaques of Alzheimer's disease is increased in vivo by the presenilin 1 and 2 and APP mutations linked to familial Alzheimer's disease. Nature Medicine, 1996. **2**(8): p. 864-870.

20.   Holtzman, D.M., J. Herz, and G. Bu, Apolipoprotein E and apolipoprotein E receptors: normal biology and roles in Alzheimer disease. Cold Spring Harb Perspect Med, 2012. **2**(3): p. a006312.

21.   Van Cauwenberghe, C., C. Van Broeckhoven, and K. Sleegers, The genetic landscape of Alzheimer disease: clinical implications and perspectives. Genet Med, 2016. **18**(5): p. 421-30.

22.   Fan, J.L., et al., Transgenic Rabbits Overexpressing Human Hepatic Lipase Have Reduced Levels of High-Density-Lipoproteins and Intermediate Density Lipoproteins and Diminished Responses to Dietary-Cholesterol. Circulation, 1994. **90**(4): p. 289-289.

23.   Teixeira, J., et al., Alzheimer's disease and antioxidant therapy: how long how far? Curr Med Chem, 2013. **20**(24): p. 2939-52.

24.   Belanger, M., I. Allaman, and P.J. Magistretti, Brain energy metabolism: focus on astrocyte-neuron metabolic cooperation. Cell Metab, 2011. **14**(6): p. 724-38.

25.   Uttara, B., et al., Oxidative stress and neurodegenerative diseases: a review of upstream and downstream antioxidant therapeutic options. Curr Neuropharmacol, 2009. **7**(1): p. 65-74.

26.   Butterfield, D.A., A.M. Swomley, and R. Sultana, Amyloid beta-Peptide (1-42)-Induced Oxidative Stress in Alzheimer Disease: Importance in Disease Pathogenesis and Progression. Antioxidants & Redox Signaling, 2013. **19**(8): p. 823-835.

27.   Atwood, C.S., et al., Amyloid-beta: a chameleon walking in two worlds: a review of the trophic and toxic properties of amyloid-beta. Brain Research Reviews, 2003. **43**(1): p. 1-16.

28.   Rauk, A., Why is the amyloid beta peptide of Alzheimer's disease neurotoxic? Dalton Trans, 2008(10): p. 1273-82.

29.   Leuner, K., et al., Mitochondrial dysfunction: The first domino in brain aging and Alzheimer's disease? Antioxidants & Redox Signaling, 2007. **9**(10): p. 1659-1675.

30.   Collaboration, V., et al., Radio imaging of the very-high-energy gamma-ray emission region in the central engine of a radio galaxy. Science, 2009. **325**(5939): p. 444-8.

31.   Gamba, P., et al., Oxidized cholesterol as the driving force behind the development of Alzheimer's disease. Frontiers in Aging Neuroscience, 2015. **7**: p. 119.

32.   Rubio-Perez, J.M. and J.M. Morillas-Ruiz, A review: inflammatory process in Alzheimer's disease, role of cytokines. ScientificWorldJournal, 2012. **2012**: p. 756357.

33.   Wilkins, H.M., et al., Bioenergetic dysfunction and inflammation in Alzheimer's disease: a possible connection. Front Aging Neurosci, 2014. **6**: p. 311.

34.   Wang, W.Y., et al., Role of pro-inflammatory cytokines released from microglia in Alzheimer's disease. Ann Transl Med, 2015. **3**(10): p. 136.

35.   Minagar, A., et al., The role of macrophage/microglia and astrocytes in the pathogenesis of three neurologic disorders: HIV-associated dementia, Alzheimer disease, and multiple sclerosis. J Neurol Sci, 2002. **202**(1-2): p. 13-23.

36.   Mohandas, E., V. Rajmohan, and B. Raghunath, Neurobiology of Alzheimer's disease. Indian J Psychiatry, 2009. **51**(1): p. 55-61.

37.   Josefson, D., Statins may reduce risk of Alzheimer's disease. BMJ, 2000. **321**(7268): p. 1040.

38.   Ransmayr, G., [Cholesterol and statins in Alzheimer disease]. Wien Med Wochenschr, 2003. **153**(11-12): p. 258-9.

39.   Sharman, M.J., et al., The Guinea Pig as a Model for Sporadic Alzheimer's Disease (AD): The Impact of Cholesterol Intake on Expression of AD-Related Genes. PLoS One, 2013. **8**(6): p. e66235.

40.   Sparks, D.L., The early and ongoing experience with the cholesterol-fed rabbit as a model of Alzheimer's disease: the old, the new and the pilot. J Alzheimers Dis, 2008. **15**(4): p. 641-56.

41.   Adibhatla, R.M. and J.F. Hatcher, Altered lipid metabolism in brain injury and disorders. Subcell Biochem, 2008. **49**: p. 241-68.

42.   Zhang, J. and Q. Liu, Cholesterol metabolism and homeostasis in the brain. Protein Cell, 2015. **6**(4): p. 254-64.

43.   Kuo, Y.M., et al., Elevated low-density lipoprotein in Alzheimer's disease correlates with brain A beta 1-42 levels. Biochemical and Biophysical Research Communications, 1998. **252**(3): p. 711-715.

44.   Bhat, N.R., Linking cardiometabolic disorders to sporadic Alzheimer's disease: a perspective on potential mechanisms and mediators. J Neurochem, 2010. **115**(3): p. 551-62.

45.   Fu, A.L., et al., Alternative therapy of Alzheimer's disease via supplementation with choline acetyltransferase. Neurosci Lett, 2004. **368**(3): p. 258-62.

46.   Davies, P., Challenging the cholinergic hypothesis in Alzheimer disease. JAMA, 1999. **281**(15): p. 1433-4.

47.   Cummings, J.L., T. Morstorf, and K. Zhong, Alzheimer's disease drug-development pipeline: few candidates, frequent failures. Alzheimers Res Ther, 2014. **6**(4): p. 37.

48.   Bandyopadhyay, S., et al., Novel drug targets based on metallobiology of Alzheimer's disease. Expert Opin Ther Targets, 2010. **14**(11): p. 1177-97.

49.   Shi, L., et al., A novel dual GLP-1/GIP receptor agonist alleviates cognitive decline by re-sensitizing insulin signaling in the Alzheimer icv. STZ rat model. Behav Brain Res, 2017. **327**: p. 65-74.

50.   Keeney, J.T., et al., Cell cycle proteins in brain in mild cognitive impairment: insights into progression to Alzheimer disease. Neurotox Res, 2012. **22**(3): p. 220-30.

51.   Arshavsky, Y.I., Why Alzheimer's disease starts with a memory impairment: neurophysiological insight. J Alzheimers Dis, 2010. **20**(1): p. 5-16.

52.   Reisberg, B., et al., Mortality and temporal course of probable Alzheimer's disease: a 5-year prospective study. Int Psychogeriatr, 1996. **8**(2): p. 291-311.

53.   Grandy, J.K., Updated guidelines for the diagnosis of Alzheimer disease: a clinical review. JAAPA, 2012. **25**(4): p. 50-5.

54.   McLean, D., et al., Anti-amyloid-beta-mediated positron emission tomography imaging in Alzheimer's disease mouse brains. PLoS One, 2012. **7**(12): p. e51958.

55.   Hostetler, E.D., et al., [18F]Fluoroazabenzoxazoles as potential amyloid plaque PET tracers: synthesis and in vivo evaluation in rhesus monkey. Nucl Med Biol, 2011. **38**(8): p. 1193-203.

56.   Bei, L., et al., A test of lens opacity as an indicator of preclinical Alzheimer Disease. Exp Eye Res, 2015. **140**: p. 117-23.

57.   Ables, A.Z., Memantine (Namenda) for moderate to severe Alzheimer's disease. Am Fam Physician, 2004. **69**(6): p. 1491-2.

58.   Scarmeas, N., et al., Mediterranean diet, Alzheimer disease, and vascular mediation. Arch Neurol, 2006. **63**(12): p. 1709-17.

59.   Calon, F., Omega-3 polyunsaturated fatty acids in Alzheimer's disease: key questions and partial answers. Curr Alzheimer Res, 2011. **8**(5): p. 470-8.

60.   Shi, C., et al., Ginkgo biloba extract in Alzheimer's disease: from action mechanisms to medical practice. Int J Mol Sci, 2010. **11**(1): p. 107-23.

61.   Yang, X., et al., Coenzyme Q10 attenuates beta-amyloid pathology in the aged transgenic mice with Alzheimer presenilin 1 mutation. J Mol Neurosci, 2008. **34**(2): p. 165-71.

62.   Hugel, H.M., Brain Food for Alzheimer-Free Ageing: Focus on Herbal Medicines. Natural Compounds as Therapeutic Agents for Amyloidogenic Diseases, 2015. **863**: p. 95-116.

63.   Sambanthamurthi, R., et al., Oil palm vegetation liquor: a new source of phenolic bioactives. British Journal of Nutrition, 2011. **106**(11): p. 1655-1663.

64.   Sambanthamurthi, R., et al., Positive outcomes of oil palm phenolics on degenerative diseases in animal models. British Journal of Nutrition, 2011. **106**(11): p. 1664-1675.

65.   Leow, S.S., et al., Oil palm phenolics confer neuroprotective effects involving cognitive and motor functions in mice. Nutr Neurosci, 2013. **16**(5): p. 207-17.

66.   Crichton, G.E., M.F. Elias, and A. Alkerwi, Chocolate intake is associated with better cognitive function: The Maine-Syracuse Longitudinal Study. Appetite, 2016. **100**: p. 126-32.

67.   Lim, G.P., et al., The curry spice curcumin reduces oxidative damage and amyloid pathology in an Alzheimer transgenic mouse. Journal of Neuroscience, 2001. **21**(21): p. 8370-7.

68. Wang, P., et al., Increased chemopreventive effect by combining arctigenin, green tea polyphenol and curcumin in prostate and breast cancer cells. RSC Adv, 2014. **4**(66): p. 35242-35250.

69. Ganguli, M., et al., Apolipoprotein E polymorphism and Alzheimer disease: The Indo-US Cross-National Dementia Study. Arch Neurol, 2000. **57**(6): p. 824-30.

70. Ng, T.P., et al., Curry consumption and cognitive function in the elderly. Am J Epidemiol, 2006. **164**(9): p. 898-906.

71. MartinAragon, S., J.M. Benedi, and A.M. Villar, Modifications on antioxidant capacity and lipid peroxidation in mice under fraxetin treatment. Journal of Pharmacy and Pharmacology, 1997. **49**(1): p. 49-52.

72. Rajakrishnan, V., et al., Neuroprotective role of curcumin from Curcuma longa on ethanol-induced brain damage. Phytotherapy Research, 1999. **13**(7): p. 571-574.

73. Lim, G.P., et al., The curry spice curcumin reduces oxidative damage and amyloid pathology in an Alzheimer transgenic mouse. Journal of Neuroscience, 2001. **21**(21): p. 8370-8377.

74. Mishra, S. and K. Palanivelu, The effect of curcumin (turmeric) on Alzheimer's disease: An overview. Ann Indian Acad Neurol, 2008. **11**(1): p. 13-9.

75. Webber, K.M., et al., Estrogen bows to a new master: the role of gonadotropins in Alzheimer pathogenesis. Ann N Y Acad Sci, 2005. **1052**: p. 201-9.

76. Folch, J., M. Lees, and G.H. Sloane Stanley, A simple method for the isolation and purification of total lipides from animal tissues. J Biol Chem, 1957. **226**(1): p. 497-509.

77. Khazipov, R., et al., Atlas of the Postnatal Rat Brain in Stereotaxic Coordinates. Front Neuroanat, 2015. **9**: p. 161.

78.   Villegas, I., S. Sanchez-Fidalgo, and C.A. de la Lastra, Chemopreventive effect of dietary curcumin on inflammation-induced colorectal carcinogenesis in mice. Mol Nutr Food Res, 2011. **55**(2): p. 259-67.

79.   Henke, K., et al., Human hippocampus associates information in memory. Proc Natl Acad Sci U S A, 1999. **96**(10): p. 5884-9.

80.   Toriya, M., et al., Long-term infusion of brain-derived neurotrophic factor reduces food intake and body weight via a corticotrophin-releasing hormone pathway in the paraventricular nucleus of the hypothalamus. J Neuroendocrinol, 2010. **22**(9): p. 987-95.

81.   Muller, G.J., et al., Ischemia leads to apoptosis--and necrosis-like neuron death in the ischemic rat hippocampus. Brain Pathol, 2004. **14**(4): p. 415-24.

82.   Wan, W., et al., Abeta(1-42) oligomer-induced leakage in an in vitro blood-brain barrier model is associated with up-regulation of RAGE and metalloproteinases, and down-regulation of tight junction scaffold proteins. J Neurochem, 2015. **134**(2): p. 382-93.

83.   Butterfield, D.A., et al., Evidence that amyloid beta-peptide-induced lipid peroxidation and its sequelae in Alzheimer's disease brain contribute to neuronal death. Neurobiology of Aging, 2002. **23**(5): p. 655-664.

84.   Bedi, K.C., Jr., et al., Evidence for Intramyocardial Disruption of Lipid Metabolism and Increased Myocardial Ketone Utilization in Advanced Human Heart Failure. Circulation, 2016. **133**(8): p. 706-16.

85.   Dursun, E., et al., The interleukin 1 alpha, interleukin 1 beta, interleukin 6 and alpha-2-macroglobulin serum levels in patients with early or late onset Alzheimer's disease, mild cognitive impairment or Parkinson's disease. Journal of Neuroimmunology, 2015. **283**: p. 50-57.

86.   Kincses, Z.T., J. Toldi, and L. Vecsei, Kynurenines, neurodegeneration and Alzheimer's disease. J Cell Mol Med, 2010. **14**(8): p. 2045-54.

87.   Granholm, A.C., et al., Effects of a saturated fat and high cholesterol diet on memory and hippocampal morphology in the middle-aged rat. J Alzheimers Dis, 2008. **14**(2): p. 133-45.

88.   Sparks, D.L., et al., Induction of Alzheimer-Like Beta-Amyloid Immunoreactivity in the Brains of Rabbits with Dietary-Cholesterol. Experimental Neurology, 1994. **126**(1): p. 88-94.

89.   Fassbender, K., et al., Simvastatin strongly reduces levels of Alzheimer's disease beta-amyloid peptides A beta 42 and A beta 40 in vitro and in vivo. Proceedings of the National Academy of Sciences of the United States of America, 2001. **98**(10): p. 5856-5861.

90.   Dias, H.K., et al., LDL-lipids from patients with hypercholesterolaemia and Alzheimer's disease are inflammatory to microvascular endothelial cells: mitigation by statin intervention. Clin Sci (Lond), 2015. **129**(12): p. 1195-206.

91.   Boimel, M., et al., Statins reduce the neurofibrillary tangle burden in a mouse model of tauopathy. J Neuropathol Exp Neurol, 2009. **68**(3): p. 314-25.

92.   Assis, R.P., et al., Combined Effects of Curcumin and Lycopene or Bixin in Yoghurt on Inhibition of LDL Oxidation and Increases in HDL and Paraoxonase Levels in Streptozotocin-Diabetic Rats. Int J Mol Sci, 2017. **18**(4).

93.   Ganjali, S., et al., Effects of curcumin on HDL functionality. Pharmacol Res, 2017. **119**: p. 208-218.

94.   Shankar, G.M. and D.M. Walsh, Alzheimer's disease: synaptic dysfunction and Abeta. Mol Neurodegener, 2009. **4**: p. 48.

95.   Ahmed, M., et al., Structural conversion of neurotoxic amyloid-beta(1-42) oligomers to fibrils. Nature Structural & Molecular Biology, 2010. **17**(5): p. 561-U56.

96.   Naslund, J., et al., Relative Abundance of Alzheimer a-Beta Amyloid Peptide Variants in Alzheimer-Disease and Normal Aging. Proceedings of the National Academy of Sciences of the United States of America, 1994. **91**(18): p. 8378-8382.

97.   Borchelt, D.R., et al., Familial Alzheimer's disease-linked presenilin 1 variants elevate A beta 1-42/1-40 ratio in vitro and in vivo. Neuron, 1996. **17**(5): p. 1005-1013.

98.   Eckman, C.B., et al., A new pathogenic mutation in the APP gene (1716V) increases the relative proportion of A beta 42(43). Human Molecular Genetics, 1997. **6**(12): p. 2087-2089.

99.   Roher, A.E., et al., Beta-Amyloid-(1-42) Is a Major Component of Cerebrovascular Amyloid Deposits - Implications for the Pathology of Alzheimer-Disease. Proceedings of the National Academy of Sciences of the United States of America, 1993. **90**(22): p. 10836-10840.

100.   Lesne, S., et al., A specific amyloid-beta protein assembly in the brain impairs memory. Nature, 2006. **440**(7082): p. 352-357.

101.   Hamaguchi, T., et al., Phenolic compounds prevent Alzheimer's pathology through different effects on the amyloid-beta aggregation pathway. Am J Pathol, 2009. **175**(6): p. 2557-65.

102. Martins, I.J., et al., Apolipoprotein E, cholesterol metabolism, diabetes, and the convergence of risk factors for Alzheimer's disease and cardiovascular disease. Molecular Psychiatry, 2006. **11**(8): p. 721-736.

103. Keller, J.N., et al., Evidence of increased oxidative damage in subjects with mild cognitive impairment. Neurology, 2005. **64**(7): p. 1152-1156.

104. Markesbery, W.R., et al., Lipid peroxidation is an early event in the brain in amnestic mild cognitive impairment. Annals of Neurology, 2005. **58**(5): p. 730-735.

105. Ding, F., et al., Early decline in glucose transport and metabolism precedes shift to ketogenic system in female aging and Alzheimer's mouse brain: implication for bioenergetic intervention. PLoS One, 2013. **8**(11): p. e79977.

106. Siman, R., et al., Processing of the Beta-Amyloid Precursor - Multiple Proteases Generate and Degrade Potentially Amyloidogenic Fragments. Journal of Biological Chemistry, 1993. **268**(22): p. 16602-16609.

107. Atwood, C.S., et al., Neuroinflammatory responses in the Alzheimer's disease brain promote the oxidative post-translational modification of amyloid deposits. Alzheimer's Disease, 2001: p. 341-361.

108. Youdim, K.A., et al., Interaction between flavonoids and the blood-brain barrier: in vitro studies. Journal of Neurochemistry, 2003. **85**(1): p. 180-192.

109. Youdim, K.A., et al., Flavonoid permeability across an in situ model of the blood-brain barrier. Free Radic Biol Med, 2004. **36**(5): p. 592-604.

110. Vauzour, D., Dietary Polyphenols as Modulators of Brain Functions: Biological Actions and Molecular Mechanisms Underpinning Their Beneficial Effects. Oxidative Medicine and Cellular Longevity, 2012.

111. Janle, E.M., et al., Pharmacokinetics and Tissue Distribution of C-14-Labeled Grape Polyphenols in the Periphery and the Central Nervous System Following Oral Administration. Journal of Medicinal Food, 2010. **13**(4): p. 926-933.

112. Yoshitake, T., S. Yoshitake, and J. Kehr, The Ginkgo biloba extract EGb 761 (R) and its main constituent flavonoids and ginkgolides increase extracellular dopamine levels in the rat prefrontal cortex. British Journal of Pharmacology, 2010. **159**(3): p. 659-668.

113. Atwood, C.S., et al., Role of free radicals and metal ions in the pathogenesis of Alzheimer's disease. Metal Ions in Biological Systems, Vol 36, 1999. **36**: p. 309-364.

114. Tuppo, E.E. and H.R. Arias, The role of inflammation in Alzheimer's disease. Int J Biochem Cell Biol, 2005. **37**(2): p. 289-305.

115. Forloni, G., et al., Beta-amyloid fragment potentiates IL-6 and TNF-alpha secretion by LPS in astrocytes but not in microglia. Cytokine, 1997. **9**(10): p. 759-62.

116. Leung, R., et al., Inflammatory proteins in plasma are associated with severity of Alzheimer's disease. PLoS One, 2013. **8**(6): p. e64971.

117. Konsman, J.P., P. Parnet, and R. Dantzer, Cytokine-induced sickness behaviour: mechanisms and implications. Trends Neurosci, 2002. **25**(3): p. 154-9.

118. Reitz, C., et al., Association of higher levels of high-density lipoprotein cholesterol in elderly individuals and lower risk of late-onset Alzheimer disease. Arch Neurol, 2010. **67**(12): p. 1491-7.

119. Mahley, R.W., K.H. Weisgraber, and Y. Huang, Apolipoprotein E4: a causative factor and therapeutic target in neuropathology, including Alzheimer's disease. Proc Natl Acad Sci U S A, 2006. **103**(15): p. 5644-51.

120.   Kim, J., J.M. Basak, and D.M. Holtzman, The role of apolipoprotein E in Alzheimer's disease. Neuron, 2009. **63**(3): p. 287-303.

121.   Barberger-Gateau, P., et al., Dietary patterns and risk of dementia - The three-city cohort study. Neurology, 2007. **69**(20): p. 1921-1930.

122.   Peng, B., H. Li, and X.X. Peng, Functional metabolomics: from biomarker discovery to metabolome reprogramming. Protein & Cell, 2015. **6**(9): p. 628-637.

123.   Coleman, M.D. and S.M. Nickols-Richardson, Urinary ketones reflect serum ketone concentration but do not relate to weight loss in overweight premenopausal women following a low-carbohydrate/high-protein diet. Journal of the American Dietetic Association, 2005. **105**(4): p. 608-611.

124.   Kwiterovich, P.O., et al., Effect of a high-fat ketogenic diet on plasma levels of lipids, lipoproteins, and apolipoproteins in children. Jama-Journal of the American Medical Association, 2003. **290**(7): p. 912-920.

125.   Jain, S.K., R. McVie, and J.A. Bocchini, Jr., Hyperketonemia (ketosis), oxidative stress and type 1 diabetes. Pathophysiology, 2006. **13**(3): p. 163-70.

126.   Schernthaner, G.H. and G. Schernthaner, Insulin resistance and inflammation in the early phase of type 2 diabetes: potential for therapeutic intervention. Scand J Clin Lab Invest Suppl, 2005. **240**: p. 30-40.

127.   Prati, F., et al., Multitarget drug discovery for Alzheimer's disease: triazinones as BACE-1 and GSK-3beta inhibitors. Angew Chem Int Ed Engl, 2015. **54**(5): p. 1578-82.

128.   Oxenkrug, G.F., Tryptophan kynurenine metabolism as a common mediator of genetic and environmental impacts in major depressive disorder: the serotonin hypothesis revisited 40 years later. Isr J Psychiatry Relat Sci, 2010. **47**(1): p. 56-63.

129. Lovelace, M.D., et al., Recent evidence for an expanded role of the kynurenine pathway of tryptophan metabolism in neurological diseases. Neuropharmacology, 2017. **112**(Pt B): p. 373-388.

130. Bohar, Z., et al., Changing the face of kynurenines and neurotoxicity: therapeutic considerations. Int J Mol Sci, 2015. **16**(5): p. 9772-93.

131. Plangar, I., et al., Targeting the kynurenine pathway-related alterations in Alzheimer's disease: a future therapeutic strategy. J Alzheimers Dis, 2011. **24 Suppl 2**: p. 199-209.

132. Brown, O.R. and B. Draczynska-Lusiak, Oxygen activation and inactivation of quinolinate-producing and iron-requiring 3-hydroxyanthranilic acid oxidase: a role in hyperbaric oxygen-induced convulsions? Redox Rep, 1995. **1**(5): p. 383-5.

133. Klivenyi, P., J. Toldi, and L. Vecsei, Kynurenines in neurodegenerative disorders: therapeutic consideration. Adv Exp Med Biol, 2004. **541**: p. 169-83.

134. Guillemin, G.J. and B.J. Brew, Implications of the kynurenine pathway and quinolinic acid in Alzheimer's disease. Redox Rep, 2002. **7**(4): p. 199-206.

135. Lim, C.K., et al., Understanding the roles of the kynurenine pathway in multiple sclerosis progression. Int J Tryptophan Res, 2010. **3**: p. 157-67.

136. Nemeth, H., J. Toldi, and L. Vecsei, Role of kynurenines in the central and peripheral nervous systems. Curr Neurovasc Res, 2005. **2**(3): p. 249-60.

137. Maurya, P.K. and S.I. Rizvi, Protective role of tea catechins on erythrocytes subjected to oxidative stress during human aging. Nat Prod Res, 2009. **23**(12): p. 1072-9.

138. Wang, R., et al., Curcumin protects against glutamate excitotoxicity in rat cerebral cortical neurons by increasing brain-derived neurotrophic factor level and activating TrkB. Brain Res, 2008. **1210**: p. 84-91.

139. Zhao, X., et al., Chronic curcumin treatment normalizes depression-like behaviors in mice with mononeuropathy: involvement of supraspinal serotonergic system and GABAA receptor. Psychopharmacology (Berl), 2014. **231**(10): p. 2171-87.

140. Xu, Y., et al., Curcumin reverses impaired hippocampal neurogenesis and increases serotonin receptor 1A mRNA and brain-derived neurotrophic factor expression in chronically stressed rats. Brain Res, 2007. **1162**: p. 9-18.

141. Silva-Adaya, D., et al., Protective effect of L-kynurenine and probenecid on 6-hydroxydopamine-induced striatal toxicity in rats: implications of modulating kynurenate as a protective strategy. Neurotoxicol Teratol, 2011. **33**(2): p. 303-12.

142. Martorana, A. and G. Koch, "Is dopamine involved in Alzheimer's disease?". Frontiers in Aging Neuroscience, 2014. **6**.

143. Shleper, M., E. Kartvelishvily, and H. Wolosker, D-serine is the dominant endogenous coagonist for NMDA receptor neurotoxicity in organotypic hippocampal slices. Journal of Neuroscience, 2005. **25**(41): p. 9413-9417.

144. Leo, G.C. and A.L. Darrow, NMR-based metabolomics of urine for the atherosclerotic mouse model using apolipoprotein-E deficient mice. Magnetic Resonance in Chemistry, 2009. **47**: p. S20-S25.

145. Javed, H., et al., Taurine ameliorates neurobehavioral, neurochemical and immunohistochemical changes in sporadic dementia of Alzheimer's type (SDAT) caused by intracerebroventricular streptozotocin in rats. Neurological Sciences, 2013. **34**(12): p. 2181-2192.

146. Houtkooper, R.H., et al., The metabolic footprint of aging in mice. Scientific Reports, 2011. **1**.

147. Asp, L., et al., Effects of pro-inflammatory cytokines on expression of kynurenine pathway enzymes in human dermal fibroblasts. J Inflamm (Lond), 2011. **8**: p. 25.

ABSTRACT

THE *in vivo* EFFECT OF OIL PALM PHENOLICS (OPP) IN ATHEROGENIC DIET INDUCED RATS MODEL OF ALZHEIMER'S DISEASE (AD)

by

YAN WU

August 2017

Advisor: Dr. Smiti Gupta

Major: Nutrition and Food Science

Degree: Doctor of Philosophy

Alzheimer's disease (AD) is the most common cause of dementia in the aging population. It is characterized by cognitive decline and deposition of ß-amyloid plaques in the hippocampus. It has been shown that hypercholesterolemia induced by high cholesterol diet is associated with AD development. Increased level of oxidative stress has also been observed in AD patients. An important strategy to treat or delay the impairment is based on dietary modification, using food supplements. OPP, a water soluble fraction from oil palm fruit, rich in phenolics has been found to possess significant antioxidant activities. Its beneficial effects on cardiovascular diseases, diabetes and cancers have been previously reported. The current study was undertaken to investigate the effect of OPP in a rodent model for AD. Curcumin, a polyphenol extracted from the plant Curcuma longa, has shown its therapeutic benefits in Alzheimer's disease and was used as a positive control. Our results showed the dietary cholesterol induced hypercholesterolemia which increased AD-like pathological changes in aged rats including β-amyloid accumulation & cognitive decline. OPP & curcumin attenuate the process of AD for their antioxidant and anti-inflammatory effects by improving these pathological changes. Furthermore, OPP down-regulated amyloidogenic genes APP and ß

secretase (BACE1) expression as well as ApoE gene expression when the brain is in the presence of oxidative stress. In addition, metabolomic approach was also used to investigate the effect of OPP on metabolism changes due to the high cholesterol diet. Proton nuclear magnetic resonance (^{1}H NMR) spectra was used to acquire the spectrum of samples. Multivariate analysis software, SIMCA-P+, was applied to demonstrate the differences in urinary ^{1}H NMR profiles among the groups. Principal Component Analysis (PCA) score plots showed clear separation among all four groups indicating differences in their metabolomics profiles at the end point. OPLS regression analysis gave significant correlations between the urinary metabolomic profiles and escape latency using water maze (R^2=0.7956) and the β amyloid burden (R^2=0.7406). The metabolites responsible for the differences in the metabolomic profile among groups were then quantified using CHENOMX NMR metabolite database. Some metabolites from the tryptophan metabolism pathway were significantly altered in the cholesterol fed group (H) as compared to the treatment groups (HP, HC). Treatment with curcumin (HC) or OPP (HP) modulated the concentration of these metabolites closer to the control levels. This pathway has been shown to be perturbed in neurodegenerative diseases. Taken together, OPP exhibited a potential therapeutic effect in high cholesterol diet induced AD. Moreover, specific urinary metabolites may serve as non-invasive biomarkers for progression of neurodegenerative diseases including AD.

AUTOBIOGRAPHICAL STATEMENT

Yan Wu

EDUCATION:

PhD. in Nutrition and Food Science (Minor major in Statistics), Wayne State University, USA. (Aug. 2012-Aug. 2017)

M.Sc. in Food Science, University of Wyoming, USA. (Aug. 2009 - May 2012)

B.M in Traditional Chinese Medicine (Alternative and Complementary Medicine), Shanghai University of Traditional Chinese Medicine, China (Jan. 2001- Jan. 2006)

PROFESSIONAL APPOINTMENTS:

Teaching Assistant, Nutrition and Food Lab, Wayne State University, USA. (Aug. 2012 – Aug.2017)

Research Assistant, Food Lab, University of Wyoming, Laramie, USA. (Aug. 2009 – Aug. 2012)

Licensed practitioner in Traditional Chinese medicine, Shanghai ShuGuang Hospital, China (Jan. 2006 – May 2009)

PROFESSIONAL ASSOCIATIONS:

The Neo-life Student Research Award, PhenHRIG, Experiment of Biology, 2016;

Institute of Food Technology (IFT) "Feeding Tomorrow" graduate scholarship, 2015-2016;
PhD Achievement Award, Institute of Food Technology (IFT) -Great Lake Section,2015;
6th Graduate Exhibition "Presentation Award" 2ed place, Wayne State University, 2015;
Thomas C.Rumble Fellowship, Wayne State University, 2014-2015;
Graduate Professional Scholarship, Wayne State University, 2012-2013;
Outstanding community volunteer, Shanghai university of Chinese medicine,2005;
Undergaduate Award, Shanghai University of Chinese Medicine, 2003;

PUBLICATIONS AND PRESENTATIONS:

Wu,Y ., Srirajavatsavai V., Sambanthamurthi, R., & Gupta, S. V. (2016). The Effect of Oil Palm Phenolics (OPP) on Urinary Metabolomic Profile in Atherogenic Diet Induced Rat Model of Alzheimer's Disease (AD). . FASEB J. 30,692.21

Wu Y, Srirajavatsavai V, Monplaisir K, Gupta S. (2015) The invivo effect of oil palm phenolics (OPP) in atherogenic diet induced rat model of Alzheimer's Disease. Poster presentation and competition,Experiment of Biology, April, Boston, MA.

I Al-Wahsh, Wu Y, Liebman M. (2011) A comparison of two extraction methods for food oxalate assessment. Journal of Food Composition and Analysis. Journal of Food Research. 1(2):233.

Al-Wahsh I, Wu Y, Liebman M. (2011) Acute probiotic ingestion reduces gastrointestinal oxalate absorption in healthy subjects. Urological Research.40: 191-196